



Doctoral School of University of Alcalá

Hydrology and Water Resource Management

Doctoral Thesis

Novel Strategies for Solving Environmental Problems Through Microbial Electrochemistry

Thesis submitted for the title of Doctor from the University of Alcalá by:

Colin Daniel Wardman

Directed by:

Dr. Abraham Esteve Núñez

Department of Analytical Chemistry, Physical Chemistry, and Chemical Engineering

University of Alcalá, 2025



Escuela de Doctorado de la Universidad de Alcalá

Hidrología y Gestión de Recursos Hídricos

Tesis Doctoral

Nuevas estrategias para resolver problemas ambientales mediante electroquímica microbiana

Tesis presentada para la obtención del título de Doctor por la Universidad de Alcalá por:

Colin Daniel Wardman

Dirigido por:

Dr. Abraham Esteve Núñez

Departamento de Química Analítica, Química Física e Ingeniería Química
Universidad de Alcalá, 2025

"No captain can do very wrong if he places his ship alongside that of the enemy."
Horatio Nelson

To my wife, family, and comrades

Summary

Microbial electrochemical technologies (METs) have proven versatile and highly applicable in environmental sciences. These technologies are based on the ability of electroactive bacteria (EAB) to donate electrons extracellularly. This ability allows EABs to donate electrons to insoluble electroconductive materials. The first applications of METs were to generate electricity from organic matter, but in the last decades, advances have been developed in the field of biosensors, bioelectrosynthesis, sustainable desalination, and wastewater (WW) treatment.

The current thesis explores how METs can improve the ability to monitor biological processes, treat recalcitrant WW, and tailor microorganisms for specific bioelectrochemical applications. This thesis contains introductory material for the contextualizing 4 chapters of original research, followed by a general discussion and conclusions.

Understanding metabolic processes in subsurface environments is vital for understanding geochemical processes. Microbial respiration in the subsurface is known to correlate somewhat with the concentration of hydrogen produced, although metabolic rates are difficult to estimate. Microbial fuel cells have been shown to respond to the turnover of metabolically essential compounds like acetate. In Chapter 2, this thesis shows that microbial fuel cells (MFC) can determine the acetate turnover rate in water-logged sediments. Given the integral nature of acetate as a central intermediate in anaerobic fermentation, this MFC biosensor can determine the metabolic rates of sediment microbes independent of the terminal electron-accepting process.

For decades, water engineers have used anaerobic digesters to treat many waste effluents, from urban WW to food industry waste. While these systems can treat various waste streams and produce biogas as renewable energy, they need constant monitoring to maintain the stability of the bioreactors. Common indicators of reactor health status are time-consuming to analyze and are not suitable for protecting microorganisms from toxicants present in the effluent. In Chapter 3, a three-electrode microbial electrolysis cell (MEC) biosensor was used to monitor the health of an up-flow anaerobic sludge blanket anaerobic digester and to detect biocides to protect against potential damage to its biomass.

Electroactive-constructed wetlands, or METlands, have successfully treated many types of WW. They have been shown to treat urban and industrial WW, and even pharmaceuticals

recalcitrant to other treatments. The METland concept is also actually a type of fixed-bed biofilter. The METland concept can also be applied to biofilters. Chapter 4 shows how an electroactive biofilter can treat a recalcitrant hydrocarbon (HC) WW media simulating petroleum refinery WW. The biofilters utilize alternating aerobic and anaerobic beds to select microbial communities that could efficiently treat HC WW.

Over the years, MET research has focused primarily on physical reactor design and electrode materials science, although microorganisms are also key to the operation and efficiency of bioelectrochemical applications. Developing mature microbial communities that function well in electrochemical devices such as microbial desalination cells can take weeks or months. The ability to produce customized microbial communities for specific processes could greatly decrease startup time and increase efficiency. In Chapter 5, a novel combination of a three-electrode single chamber MEC is combined with a continuous culture device called a gradostat. The gradostat was used to adapt *Geobacter sulfurreducens* to quickly increasing saline concentrations. Furthermore, the integrated MECs allow for the study of *G. sulfurreducens*' ability to respire a graphite electrode at various salinities and the effects on planktonic cells.

The final section of this thesis has a general discussion, some main conclusions, and suggestions for future research in the framework of the investigated topic.

Resumen

Las tecnologías electroquímicas microbianas (MET) han demostrado ser versátiles y muy aplicables en las ciencias ambientales. Estas tecnologías se basan en la capacidad de las bacterias electroactivas (EAB) para donar electrones a nivel extracelular. Esta capacidad permite a las EAB donar electrones a materiales electroconductores insolubles. Las primeras aplicaciones de las MET fueron generar electricidad a partir de materia orgánica pero, en las últimas décadas, se han desarrollado avances en el cambo de los biosensores, la bioelectrosíntesis, la desalinización sostenible y el tratamiento de aguas residuales (WW).

La tesis actual explora como las MET pueden mejorar la capacidad de monitorear procesos biológicos, tratar WW recalcitrantes y adaptar microorganismos para aplicaciones bioelectroquímicas específicas. Esta tesis contiene material introductorio para contextualizar los 4 capítulos de investigación original, seguido de una discusión general y unas conclusiones finales.

Entender los procesos metabólicos en entornos subterráneos es vital para comprender los procesos geoquímicos. Es conocido que las respiraciones microbianas en el subsuelo tienen cierta correlación con la concentración de hidrógeno producido, si bien las tasas metabólicas son difíciles de estimar. Se ha demostrado que las celdas de combustible microbianas responden a la oxidación de compuestos metabólicamente esenciales como el acetato. En el Capítulo 2, esta tesis demuestra que las celdas de combustible microbianas (MFC) pueden determinar la tasa de oxidación de acetato en sedimentos anegados. Dada la naturaleza integral del acetato como intermediario central en la fermentación anaeróbica, este biosensor MFC puede determinar las tasas metabólicas de los microoorganismos del sedimento independientemente del proceso terminal de aceptación de electrones.

Durante décadas, los ingenieros de aguas ha utilizado digestores anaerobios para tratar muchos efluentes de residuos, desde aguas residuales urbanas hasta residuos de la industria alimentaria. Si bien estos sistemas pueden tratar varios corrientes de residuos y producir biogás como energía renovable, necesitan un monitoreo constante para mantener la estabilidad de los biorreactores. Los indicadores comunes sobre el estado de salud reactor requieren mucho tiempo de análisis y no resultan apropiados para proteger a los microorganismos de tóxicos presentes en los efluentes.. En el Capítulo 3, se utilizó un biosensor de celda de electrólisis microbiana (MEC) de tres electrodos para monitorear la salud de un digestor anaerobio de flujo ascendente y para detectar biocidas para proteger de posibles daños en su bioamasa.

ix

Los humedales construidos electroactivos, o METlands, han tratado con éxito muchos tipos de aguas residuales. Se ha demostrado que tratan aguas residuales urbanas e industriales, e incluso productos farmacéuticos recalcitrantes para otros tratamientos. El concepto METland también es en realidad un tipo de biofitro de lecho fijo. El Capítulo 4 muestra cómo un biofiltro electroactivo puede tratar un medio de aguas residuales de hidrocarburos (HC) recalcitrantes que simulan aguas residuales de refinerías de petróleo. Los biofiltros utilizan lechos aerobios y anaeróbicos alternados para seleccionar comunidades microbianas que podrían tratar de manera eficiente las aguas residuales de HC.

A lo largo de los años, la investigación en METs se ha centrado fundamentalmente, en el diseño físico del reactor y en la ciencia de los materiales de los electrodos, si bien los microbioorganismos son también claves para el funcionamiento y la eficiencia de las aplicaciones bioelectroquímicas. El desarrollo de comunidades microbianas maduras que funcionen bien en dispositivos electroquímicos como las celdas de desalinización microbiana puede llevar semanas o meses. La capacidad de producir comunidades microbianas personalizadas para procesos específicos podría aumentar en gran medida el tiempo de puesta en marcha y la eficiencia. En el Capítulo 5, se combina una novedosa combinación de una celda de electroquímica microbiana de tres electrodos con un dispositivo de cultivo continuo llamado gradostato. El gradostato se utilizó para adaptar *Geobacter sulfurreducens* a concentraciones salinas que cambián de forma dinámica. Además, las celdas de desalinización microbianas integradas permiten el estudio de la capacidad de *G. sulfurreducens* para respirar un electrodo de grafito a varias salinidades y los efectos sobre las células planctónicas.

La sección final de esta tesis tiene una discusión general, unas conclusiones principales y sugerencias para investigaciónes futura en el marco de la temática investigada.

Table of Contents

Chapter 1: Introduction and Objectives	1
Introduction	2
1 - Microbial Electrochemical Technologies	2
1.1 - Microbial Fuel Cells Biosensors	3
1.2 Three Electrode-Based Biosensors	6
2 - Hydrocarbon Wastewater Treatment	8
2.1 - Conventional Hydrocarbon Treatment	8
2.1.1 - Petroleum Wastewater Processing	8
2.1.2 - Aerobic Activated Sludge Systems	8
2.1.3 - Sequencing Batch Reactors	9
2.1.4 - Electrochemical Treatment	11
2.1.5 - Biofilm-Based Reactor	13
2.2 – Electroactive Biofilters: the METland Concept	15
3 - Adaptive Laboratory Evolution	17
Objectives	20
Chapter 2: Measuring Microbial Metabolism in Sediments	21
1 – Introduction	22
2 - Materials and Methods	25
2.1 – Sediments	25
2.2 - Sediment Fuel Cells and Incubation	25
2.3 - Microbial Metabolic Rates	26

2.4 - Confocal microscopy	27
3 - Results and Discussion	27
4 - Conclusions	32
Chapter 3: Monitoring Anaerobic Digestors with Biosensors	33
1 - Introduction	34
2 - Materials and Methods	36
2.1 - UASB Operation	36
2.2 - Bioelectrochemical sensor	38
2.3 – Analytics	38
3 - Results and Discussion	38
3.1 - Impact of Natural and Synthetic Biocides on UASB bioreacter performance	tor 38
3.2 - MEC Biosensor Monitoring Effluent COD	39
3.3 - Biocide Effect on the MEC Biosensor	40
4 - Conclusions	42
Chapter 4: Electrochemical Biofilters Treating Hydrocarbon	
Wastewater	44
1 - Introduction	45
2 - Materials and Methods	47
2.1 - Reactor Designs	47
2.1.1 - Anaerobic-Aerobic Hybrid Biofilter	47
2.1.2 - Multi-Phase Hybrid Bed Biofilter	48

2.1.3 - Hybrid E-sink Biofilter	49
2.2 - Reactor Operation	50
2.2.1 - Synthetic Wastewater	50
2.2.2 - Operational Modes	50
2.3 - Chemical Analysis	51
2.4 - Microbial Community Analysis	51
3 - Results & Discussion	52
3.1 - COD and Nitrogen Removal	52
3.1.1 - Hybrid E-sink Biofilter	52
3.1.2 - Anaerobic-Aerobic Hybrid Biofilter	54
3.1.3 - Multi-Phase Hybrid Bed Biofilter	55
3.2 - Microbial Community Analysis	57
3.2.1 - Aerobic Microbial Communities	60
3.2.1 - Anaerobic Microbial Communities	61
3 - Conclusions	62
Chapter 5: Novel Use of The Gradostat for the Adaptation of	
Microbes	64
1 – Introduction	65
2 - Materials and Methods	68
2.1 - Gradostat Design	68
2.2 - Test Conditions	69
2.2.1 - Electron Acceptor Gradient	69
2.2.2 - Salt Gradient with Electrochemical Cells	69
2 2 3 - Planktonic Test Reactor	69

2.3 - Sample Analysis	70
3 - Results & Discussion	70
3.1 - Fumarate Limitation	70
3.2 - In situ Biofilm Growth under a Saline Gradient	72
3.3 - Electrochemical Analysis of Cells in the Planktonic Phase	76
4 – Conclusions	79
Chapter 6: General Discussion, Conclusions, and Future Work	80
General Discussion	81
Final Conclusions	86
Future Work	87
References	89
List of Figures	108
Abbreviations	112

Chapter 1:

Introduction and Objectives

Introduction

1 - Microbial Electrochemical Technologies

Electrical current production from microbes is not a new concept. In 1911, Michael Potter demonstrated that bacteria could produce an electrical current (Potter, 1911). This professor from the University of Durham, unknowing to him at the time, had just discovered electroactive bacteria (EAB). Other people throughout the mid-20th century did experiments adjacent to EAB (van Hees, 1965). However, it wasn't until the 1980s that two groups of bacteria were discovered that would be the foundation of microbial electrochemical technologies.

Shewanella putrefaciens MR-1 was isolated from the anaerobic sediment of Oneida Lake, NY. The microbe was capable of reducing insoluble manganese. In the same year, another group of microbes was discovered that would fundamentally change the understanding of biogeochemistry and lead to the creation of a whole new field of microbiology. A strain of the genus *Geobacter* was isolated from the Potomac River and could reduce multiple insoluble metals, notably iron oxide (Lovley and Phillips, 1988). Many other EABs would be discovered in the *Geobacter* genus, including what would become the model organism for extracellular electron transfer (EET). In 1994, a novel species capable of very efficient reduction of ferric iron was discovered. This species, *Geobacter sulfurreducens*, is a gramnegative, rod-shaped, aerotolerant (Lin, Coppi and Lovley, 2004) anaerobic bacteria (Caccavo *et al.*, 1994). *G. sulfurreducens* is capable of reducing extracellular insoluble electron acceptors, including electrodes.

EET allows for the transfer of electrons to insoluble materials that cannot be transported into the periplasm or cell interior. *G. sulfurreducens* can make direct contact with metal oxides and electrodes (Fig. 1). They can generate electricity either through biofilm growth on an electrode (Daniel R. Bond and Lovley, 2003) or through planktonic cell electron discharge (Tejedor-Sanz, Ortiz and Esteve-Núñez, 2017). The critical component to *G. sulfurreducens*' electroactivity is the e-pili, made of the type iv pilin monomer protein, PilA (Reguera *et al.*, 2005). These pili can conduct electricity across long distances (Malvankar *et al.*, 2011). It has been shown that these pili are responsible for conducting electricity by deleting aromatic amino acids from the *pilA* gene and greatly reducing *G. sulfurreducens*' ability to generate current (Vargas, Nikhil S. Malvankar, *et al.*, 2013). Furthermore, deleting

pilA almost completely stops electroactivity compared to the wild-type (Reguera *et al.*, 2005).

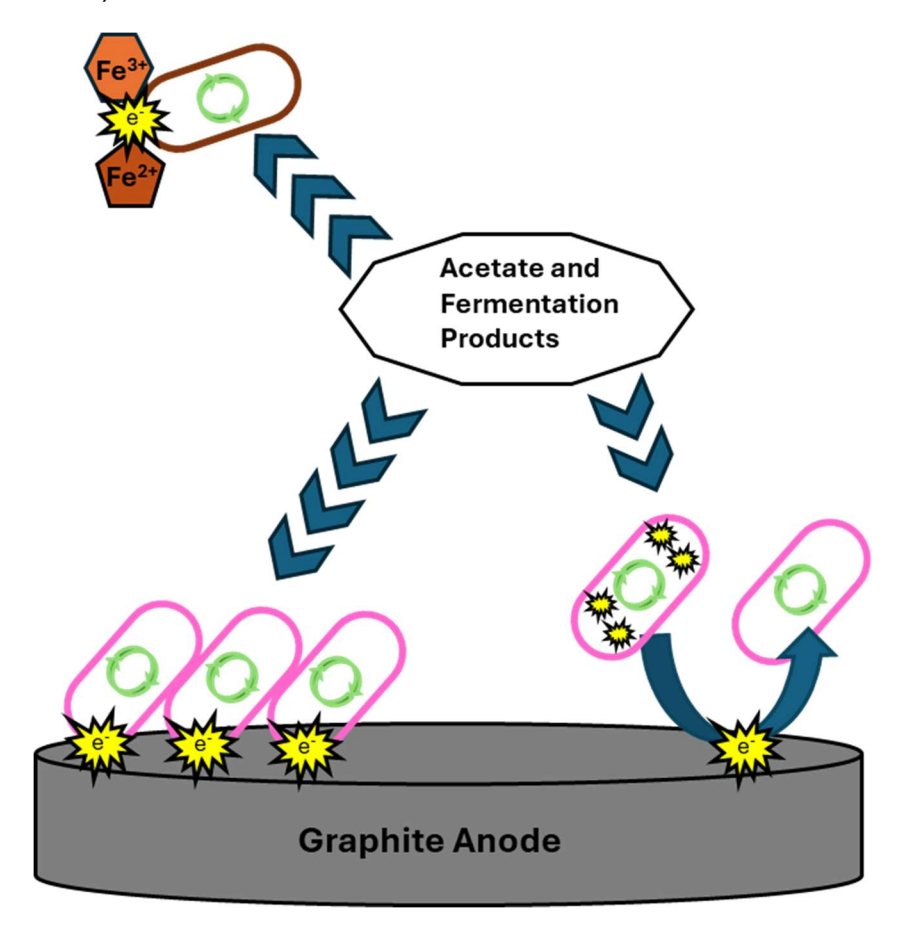


Figure 1: Diagram showing iron reduction, direct reduction of the electrode, and planktonic reduction of the electrode.

G. sulfurreducens and other EAB can interact with electrodes in multiple ways. These electrode interactions can be classified into polarized systems and nonpolarized systems. This thesis will examine both the nonpolarized and polarized interactions.

1.1 - Microbial Fuel Cells Biosensors

Though not credited with it at the time, Potter produced a primitive microbial fuel cell (Potter, 1911). Currently, Microbial Fuel Cells (MFCs) are composed of two electrodes connected by a resistor and separated by some form of ion exchange barrier. MFCs have a biological electrocatalyst at the anode of either a microbe or protein system. This work will focus on the microbial electrocatalyst. The MFC can operate at ambient temperatures and neutral pHs. Finally, MFCs use microbes to oxidize organic matter and generate electrical current at the anode (Fig. 2). The general goal of the MFC is to extract electricity from chemical energy (Logan et al., 2006).

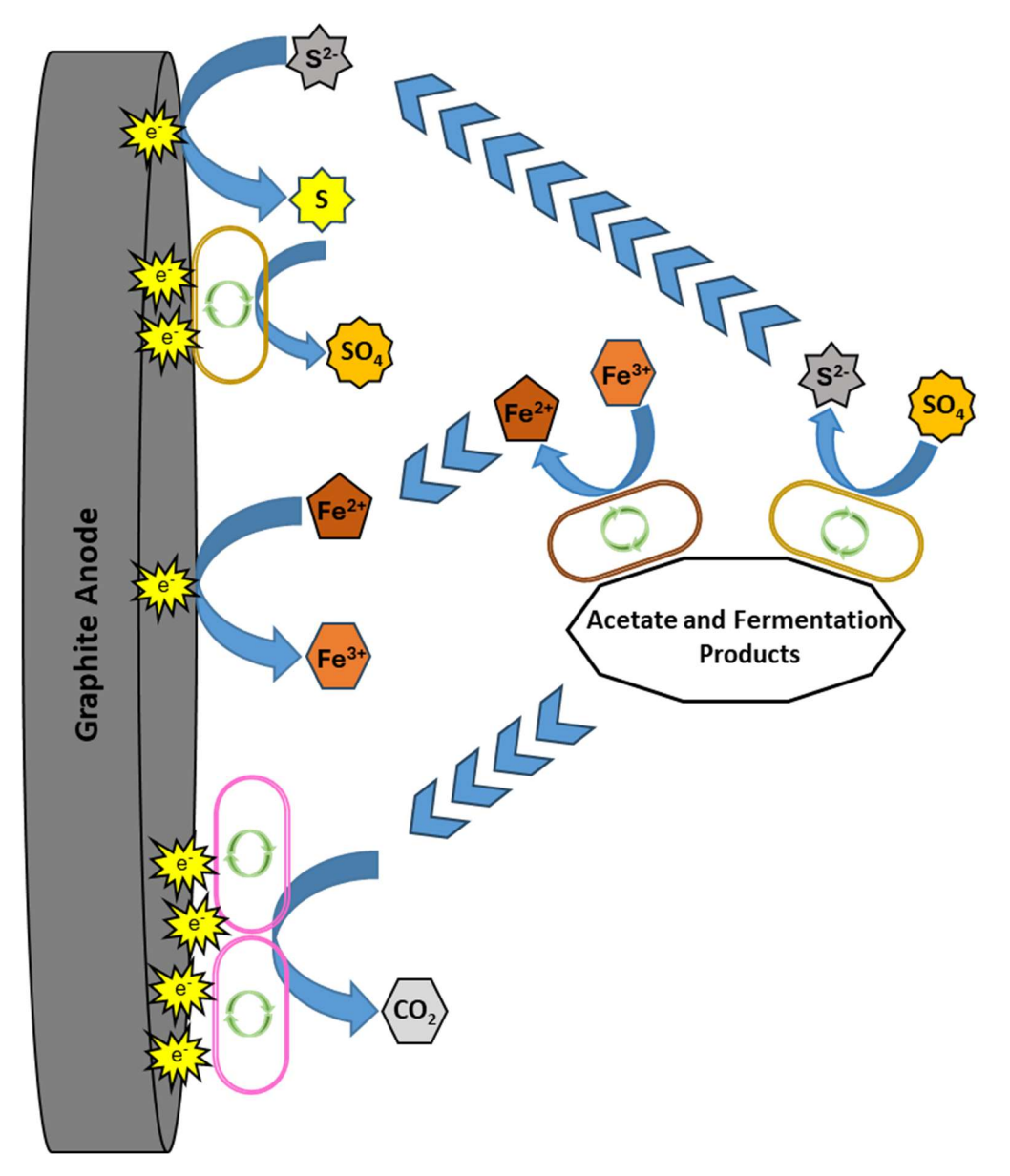


Figure 2: Microbial interactions with the anode of an MFC biosensor.

The first MFC to use *G. sulfurreducens* to generate electricity was a two-chamber fuel cell separated by a cation exchange membrane with a graphite anode and cathode. The electrodes were connected with a 500-ohm resistor. It took about 3 days for *G. sulfurreducens* to colonize the anode. The system's peak current generation was about 0.4 mA (Daniel R. Bond and Lovley, 2003). The current produced by MFCs has also been used as a signal to monitor specific parameters. MFCs have been shown to generate current proportional to available organic matter. Artificial WW has been used to directly correlate MFC current generation and biological oxygen demand (BOD). One system showed a strong correlation up to 300 mg/L of BOD (Do *et al.*, 2020). This biosensor used a two-chamber

Chapter 1: Introduction

design, which works well in a lab environment, but a single-chamber design works better for use in WW treatment or the field.

Using a single chamber MFC to understand BOD is a method that has been tested with more complex WWs. A 3D-printed MFC biosensor detected BOD levels with sterile artificial WW and raw urban WW (Salvian *et al.*, 2024). The MFC biosensors could detect BOD concentration within the usual error range in conventional BOD tests (Salvian *et al.*, 2024). Another study examined the long-term viability of using a single chamber MFC for sensing BOD using synthetic and natural WW. This study found that the biosensor was stable and produced reproducible signals for over 800 days (Spurr *et al.*, 2021).

In an MFC without an ion exchange membrane, *G. sulfurreducens* produced a current directly proportional to the acetate concentration available (Tront *et al.*, 2008). What is interesting about this lab-based experiment is that the setup did not use a two-chamber system or a conventional one-chamber system like the above studies. The anode was placed at the bottom of a column, with the cathode at the top, separated by glass beads, and connected with a 100-ohm resistor. This configuration is very similar to sediment fuel cells that can be used in natural environments.

Bodies of water are often characterized by an oxygenated water column above an organic matter-rich anaerobic sediment. The redox differential between the two can be used to generate electricity (Bose *et al.*, 2018). The sediment acts as an unlimited source of electron donors, and the oxygenated section of the water column is a limitless source of electron acceptors, separated by a sediment/water interface. These conditions and spatial separation create the perfect conditions for utilizing an MFC. The sediment microbial fuel cell (S-MFC) can harvest electrons from anaerobic sediment to generate power (Fig. 3). One can generate electricity in the environment independent of terminal electronaccepting processes by placing a graphite anode in the sediment, connected through a resistor, to a cathode in the water column. These S-MFCs work in the marine environment

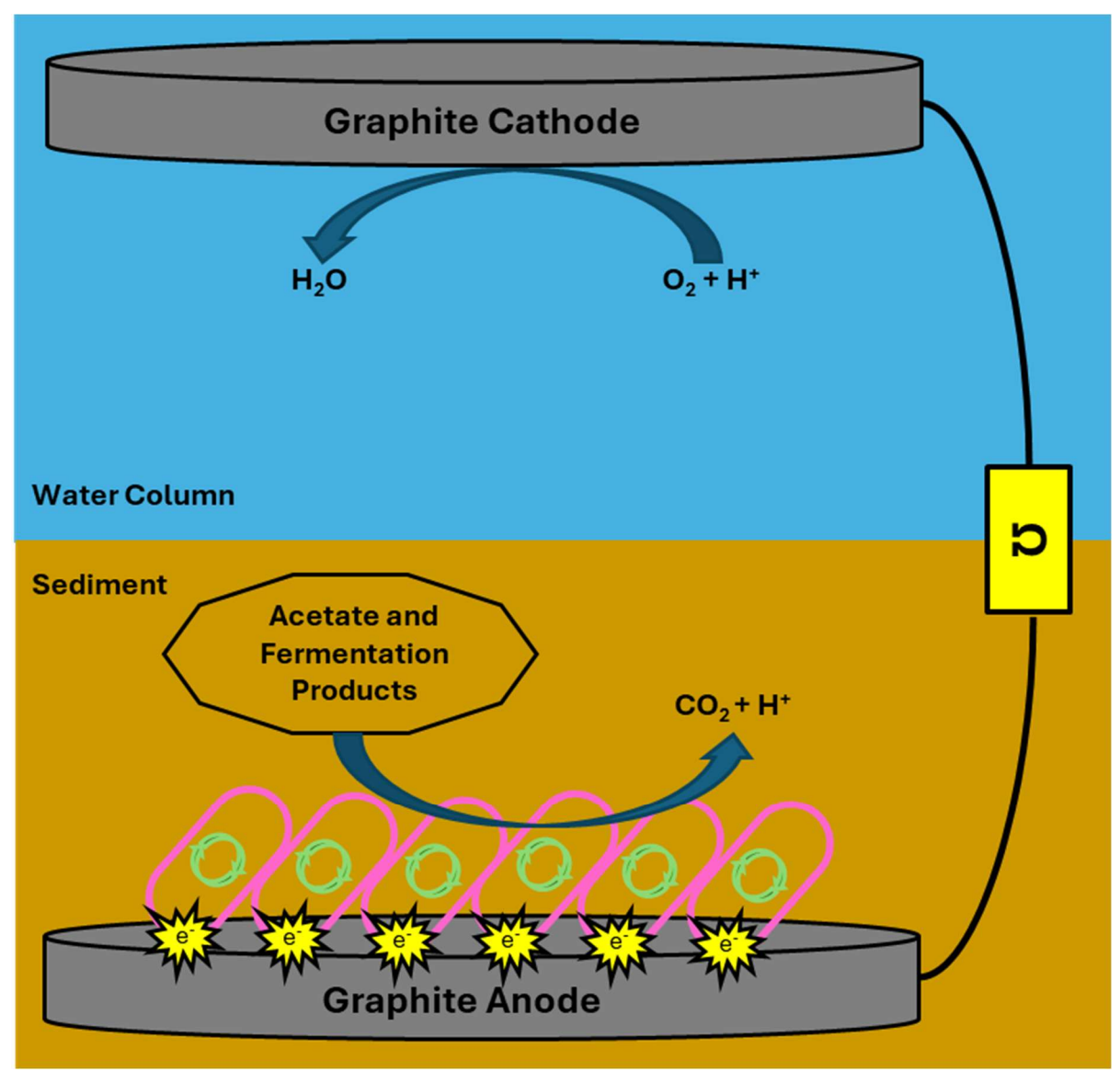


Figure 3: Diagram of the mechanisms and function of a sediment microbial fuel cell.

(Tender *et al.*, 2002), in iron-reducing sediment (Williams *et al.*, 2010), and in methanogenic sediments (Seok *et al.*, 2008).

Part of this thesis will explore how S-MFC can operate as biosensors for metabolic rates in marine sediment, iron-reducing sediment, and methanogenic sediment. Chapter 1 will explore the connection between current production and metabolic rate by using acetate turnover as a proxy for metabolic rate.

1.2 Three Electrode-Based Biosensors

The microbial electrolysis cell (MEC) is an externally polarized system. Its simplest form has a working electrode, a counter electrode, and a reference electron in a single chamber. The working electrode is poised at a specific voltage as compared to the reference

Chapter 1: Introduction

electrode by a potentiostat. The working electrode is where the reaction to be studied takes place. In this case, an anodic reaction is where electrons are donated to the working electrode or anode. The counter electrode is where a reverse reaction occurs. For example, organic matter at the working electrode is oxidized at a graphite electrode with the production of CO₂, and at the platinized counter electrode, protons are combined to make hydrogen (Call and Logan, 2008). Like the MEC above, three-electrode systems have been used as biosensors for organic matter concentration (Fig. 4).

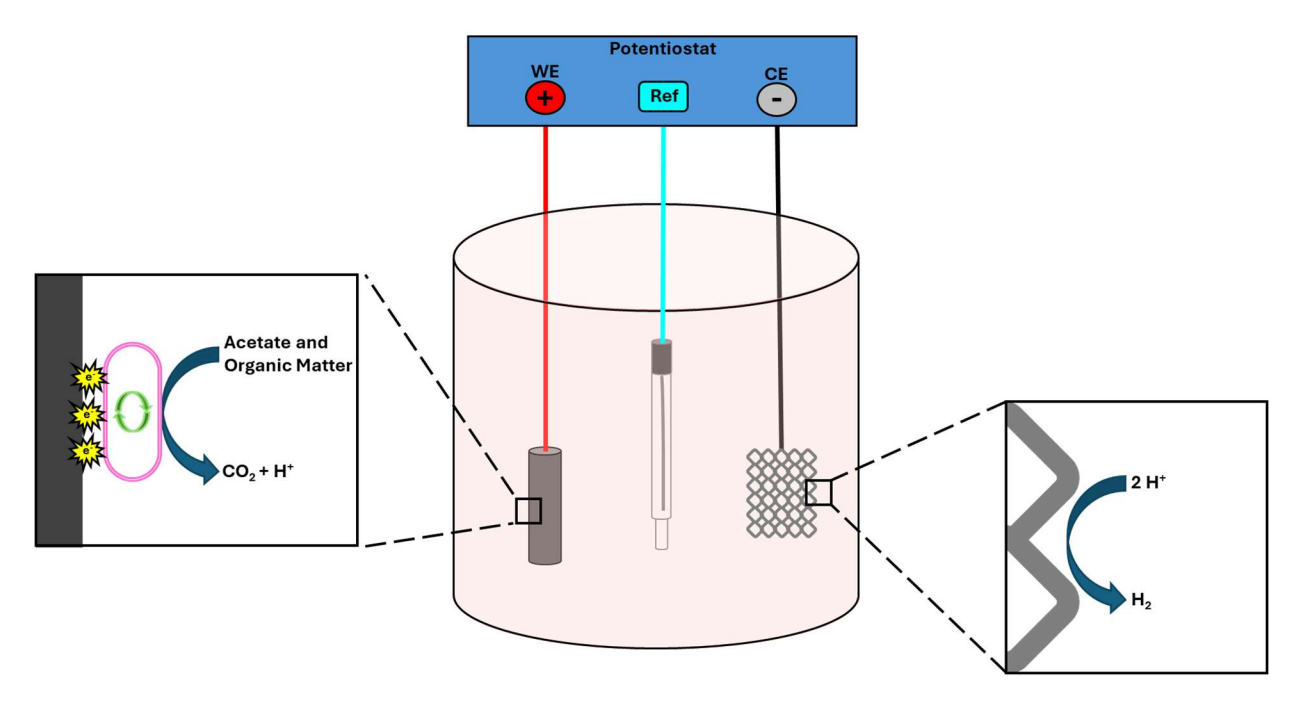


Figure 4: Diagram of the three electrode biosensors with the working electrode (Red), counter electrode (Black), and reference electrode (Blue). Highlighted are interactions that are possible at the WE and CE surfaces.

It was possible to detect the organic matter concentration of a media using a three-electrode system. Estevez-Canales et al. showed a strong correlation between current production and organic matter concentration. It was possible to correlate acetate concentration to the current generated using small-scale (75 μ L) reactors attached to screen-printed electrodes. There was a positive correlation between current production (μ A) and acetate concentration (mM) with a high degree of confidence (R²= 0.988) (Estevez-Canales *et al.*, 2015). This correlation shows how a three-electrode system can sense organic matter in solution.

Three-electrode systems have also been used to detect toxic compounds (Wu et al., 2023). Escherichia coli was immobilized on a three-electrode system. The system produced a 90-110 μ A/cm2 current in regular operation. It was shown that with the introduction of formaldehyde, the current density would quickly drop to 40-60 μ A/cm² (Uria et al., 2020).

They successfully showed that a three-electrode system could detect compounds toxic to the immobilized E. coli.

Chapter 3 of this thesis tests the ability of an MEC-based biosensor to monitor COD concentration and respond to biocides that would interrupt the ability of microbes to respire a working electrode.

2 - Hydrocarbon Wastewater Treatment

2.1 - Conventional Hydrocarbon Treatment

In 2023, the world produced 101.8 million barrels per day (U.S. Energy Information Administration, 2023). Millions of liters of water are contaminated yearly in crude oil extraction and processing. Produced water is a term for water that is both a tool and byproduct of oil and gas extraction. Produced water is often heavily contaminated with hydrocarbons, organic matter, and nitrogen compounds. Though produced water can be hard to treat due to high concentrations of phenols, salts, and other toxic compounds, it is not the only wastewater produced in oil extraction and refinement. For every barrel refined in a petrochemical plant, 246-341 liters of water are used (Alva-Argáez, Kokossis and Smith, 2007). That means the contaminated wastewater produced is between 0.4 and 1.6 times the refined oil (Coelho *et al.*, 2006). The need for cheap, efficient technology to clean wastewater has never been more critical. This technology is even more important in water-starved regions where many top oil producers are located (Fakhru'l-Razi *et al.*, 2009).

2.1.1 - Petroleum Wastewater Processing

Before produce water (PW) or petroleum refinery wastewater (PRW) can be treated biologically, it must undergo physicochemical processes. Here, heterogeneous and non-soluble wastewater fractions must be removed, like suspended solids, polar oils and particles (Renault *et al.*, 2009). This separation is achieved through oil-water separation, equalization, coagulation, flocculation, and floatation (Diya'uddeen *et al.*, 2011). These steps are essential to maintaining the efficiency and viability of the microbes in biological treatment.

2.1.2 - Aerobic Activated Sludge Systems

Aerobic activated sludge systems (AAS) rely on biologically active sludge, an amalgam of suspended solids and microbes that often form granules, to remove organic matter and nitrogen from wastewater. The primary treatment occurs in a biological reactor or aeration tank containing an influent and activated sludge mixture. The output of "mixed liquor," the term for the combination of sludge and effluent, enters a settling tank where the sludge

separates from effluent. The sludge is used to seed the influent waste stream or is rejected to a sludge digester (Haandel and Lubbe, 2012). These systems have been applied to treating PW and PRW in multiple forms (Kuyukina, Krivoruchko and Ivshina, 2020).

Different groups have had differing levels of success with treating PW and PRW with conventional AAS. Tellez et al. studied the use of AAS on PW generated in New Mexico. The water was pretreated with gas/oil separation tanks. The main biological reactor was a 4530-liter aeration tank. This system could remove 92 % of the COD at a rate of 165 g/m³*day (Tellez, Nirmalakhandan and Gardea-Torresdey, 2002). Santo et al. used a lab-scale version of an AAS. This AAS consisted of a 6-liter biological reactor fed with PRW from a refinery wastewater treatment plant. The maximum COD removal was 95% at a rate of 456 g/m³*day (Santo et al., 2013). Though this is a much greater rate than Tellez et al., it was achieved at a lab scale, in a controlled environment, versus full-scale application.

Conventional AAS has a set of disadvantages. The requirement of a final settling tank or clarifier tends to hamper upstream processes. This requirement forces the biomass concentration in the aeration tank to be maintained at low levels to reduce loading rates in the clarifier. Furthermore, this increases the size of the aeration tank. In high-flow events, such as rain, sludge/suspended solids can be released into the effluent stream (Haandel and Lubbe, 2012). These problems, along with high initial investment and operational costs for aeration, further disadvantage AAS.

2.1.3 - Sequencing Batch Reactors

Sequencing batch reactors (SBR) are a type of activated sludge treatment often employed in residential and industrial WW treatment. These reactors differ from a standard activated sludge reactor by not needing a clarifier or settling tank. The sequencing part of the SBR refers to a group of successive steps carried out in the reactor vessel (Chen *et al.*, 2019) (Fig. 5). First, the filling step allows for the introduction of WW into the reactor, which is mechanically mixed with the sludge present in the reactor. Second is the reacting step, where air is introduced into the system through pumps to help the activated sludge oxidize the available organic matter. Third, the sludge is allowed to settle. Fourth, the treated wastewater is decanted. Finally, the system may idle depending on the amount/need for water to be treated (Jafarinejad, 2017). The SRB has differing effectiveness levels for treating PW and PRW.

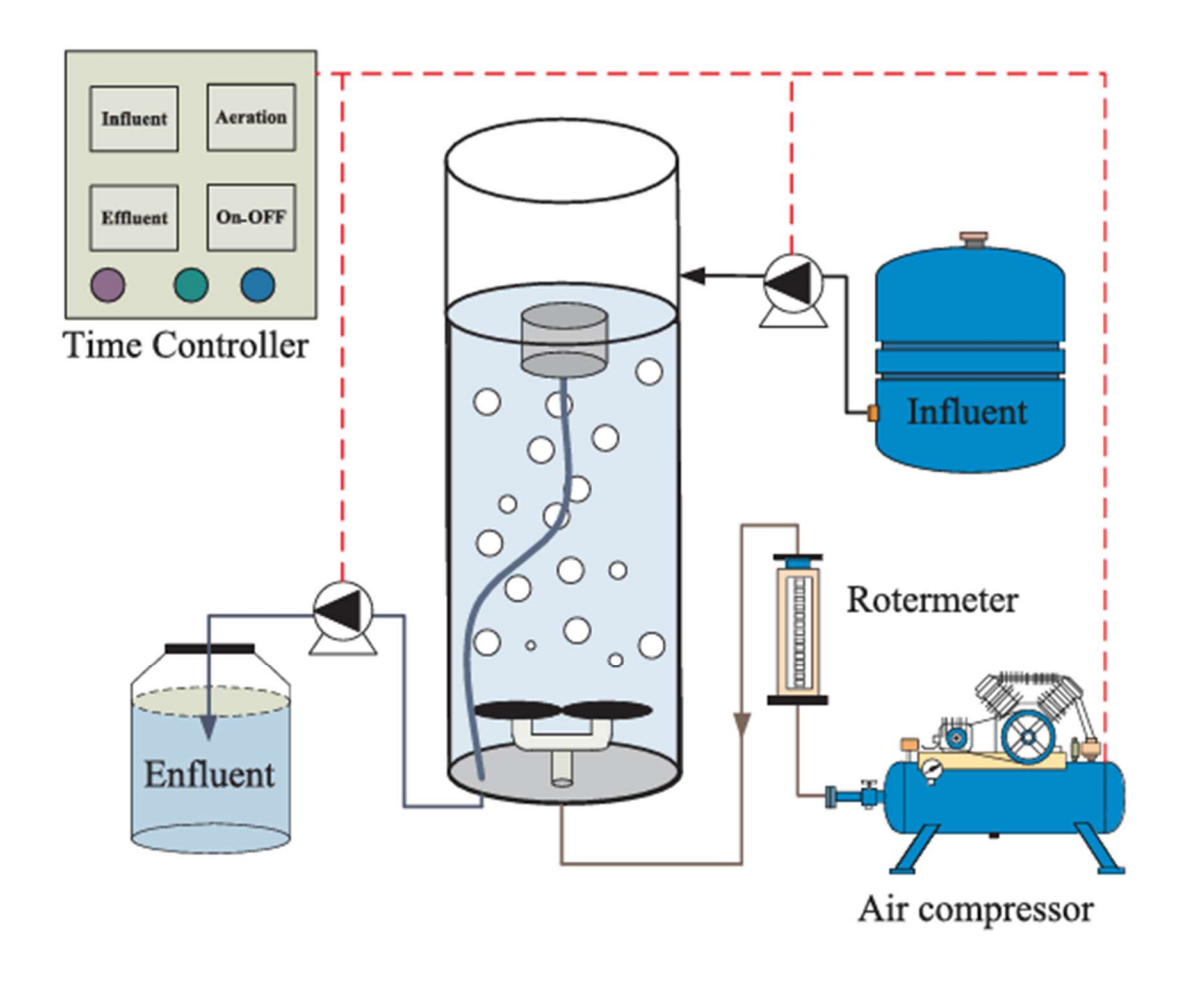


Figure 5: Diagram of reactor used by Chen et al. 2019

The efficacy of the SBR can vary greatly depending on the wastewater source and operation. Thakur et al. tested the effectiveness of the SBR on PRW. The water treated had a COD of about 350 mg/L. They achieved an 80% COD removal with an HRT of about 20 hours. With a reactor volume of 5 liters, they removed 337 g/m³*day of COD.(Thakur, Srivastava and Mall, 2014) Freire used the SBR to treat PW. This waste stream had an average COD of 2,000 mg/L^-1. The system could remove between 30-50% of the COD. This efficiency corresponds to removing COD at 1090 g/m3*day (Freire, Cammarota and Sant'Anna, 2001). Though the SBR can effectively treat some of the contamination in PRW, they must be combined with further treatments for complete remediation.

Furthermore, SBRs have some significant drawbacks. Since the SRB uses a single vessel for all the steps in the treatment process, storage tanks or installing multiple SRBs is required. SRB also requires higher aeration capacity (Haandel and Lubbe, 2012). These two aspects lead to increased installation and operational costs.

Furthermore, like conventional AAS, they depend on the quality of their waste streams. High levels of phenol can limit the ability of the sludge to settle (Leong *et al.*, 2011), and increases in salinity can cause an overall loss of biomass (Baldoni-Andrey *et al.*, 2006). Both of these lead to a greatly diminished treatment efficacy.

2.1.4 - Electrochemical Treatment

Electrochemical technologies, namely electrocoagulation and electrooxidation, have recently been applied to PRW treatment. Electrooxidation can remove contaminants through two methods: 1) the direct electrolysis of pollutants by the electrode surface and 2) the generation of an intermediate compound at the electrode that can degrade the pollutant (Panizza and Cerisola, 2009). With electrocoagulation, pollutants are destabilized by metal hydroxides generated by a sacrificial anode (Wang et al., 2016; Shokri and Sanavi Fard, 2022). This process has an advantage over chemical coagulation due to the lack of secondary contaminants and less sludge production (An et al., 2017). Both of these electrochemical processes have been applied to the treatment of PRW.

An electrooxidation apparatus requires two electrodes: an anode and a cathode. A power supply powers these electrodes and generates oxidized agents to degrade contaminants like hydrocarbons to water and carbon dioxide (Crini and Lichtfouse, 2019) (Fig. 6). Electrooxidation was successfully performed by Yavuz et al. using a boron-doped diamond anode. The boron-doped diamond anode could eliminate 98% of the COD in 75 min at a rate of 10874 g/m³*day (Yavuz, Koparal and Öğütveren, 2010). This efficacy and rate are very impressive for PRW treatment, but it is not a viable option for full-scale implementation due to the cost of the anode. The results are quite different when a more conventional anode material is used that can scale up. Santos et al. used a dimensionally stable anode of Ti/Ru. They only succeeded in removing 57% of the COD in 70 hours at a rate of 62 COD g/m³*day (Santos et al., 2006). This lack of removal could be due to the poisoning of the anode by chemical species like sulfate in the PRW.

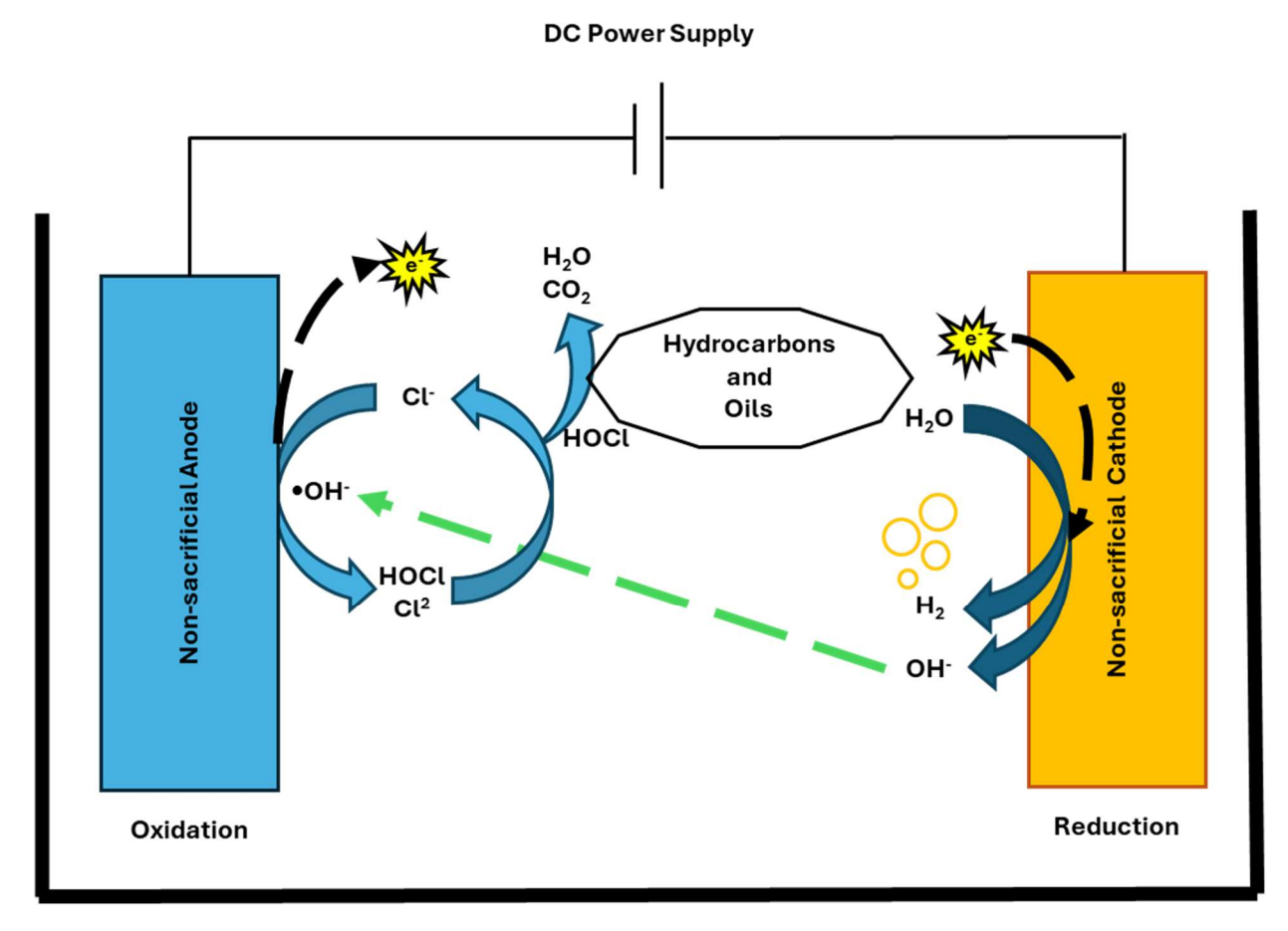


Figure 6: Diagram of an electrooxidation cell.

Electrocoagulation does not suffer from these limitations because the sacrificial electrodes are made of low-cost material like iron or aluminum that does not poison (Fig. 7). El-Naas et al. used aluminum and iron electrodes to remove COD from PRW. The highest COD removal efficiency was using Al electrodes at 63% at a rate of 9011 g/m³*day (El-Naas et al., 2009). This rate seems very high compared to other biotic treatments but has more to do with the high sulfate concentration in this particular PRW. So, the high COD removal is more related to eliminating sulfate than organic matter or oils. Sekman et al. used aluminum electrodes to treat mixed wastewater from maritime vessels and ports (bilge water, contaminated ballast water, and waste oil). This leads to a mixture with a large proportion of oil, either emulsified or with a very small droplet size. This heterogeneity is ideal for electrocoagulation and is reflected in their COD removal efficiency of 93% and a rate of 105090 g/m³*day (Sekman et al., 2011).

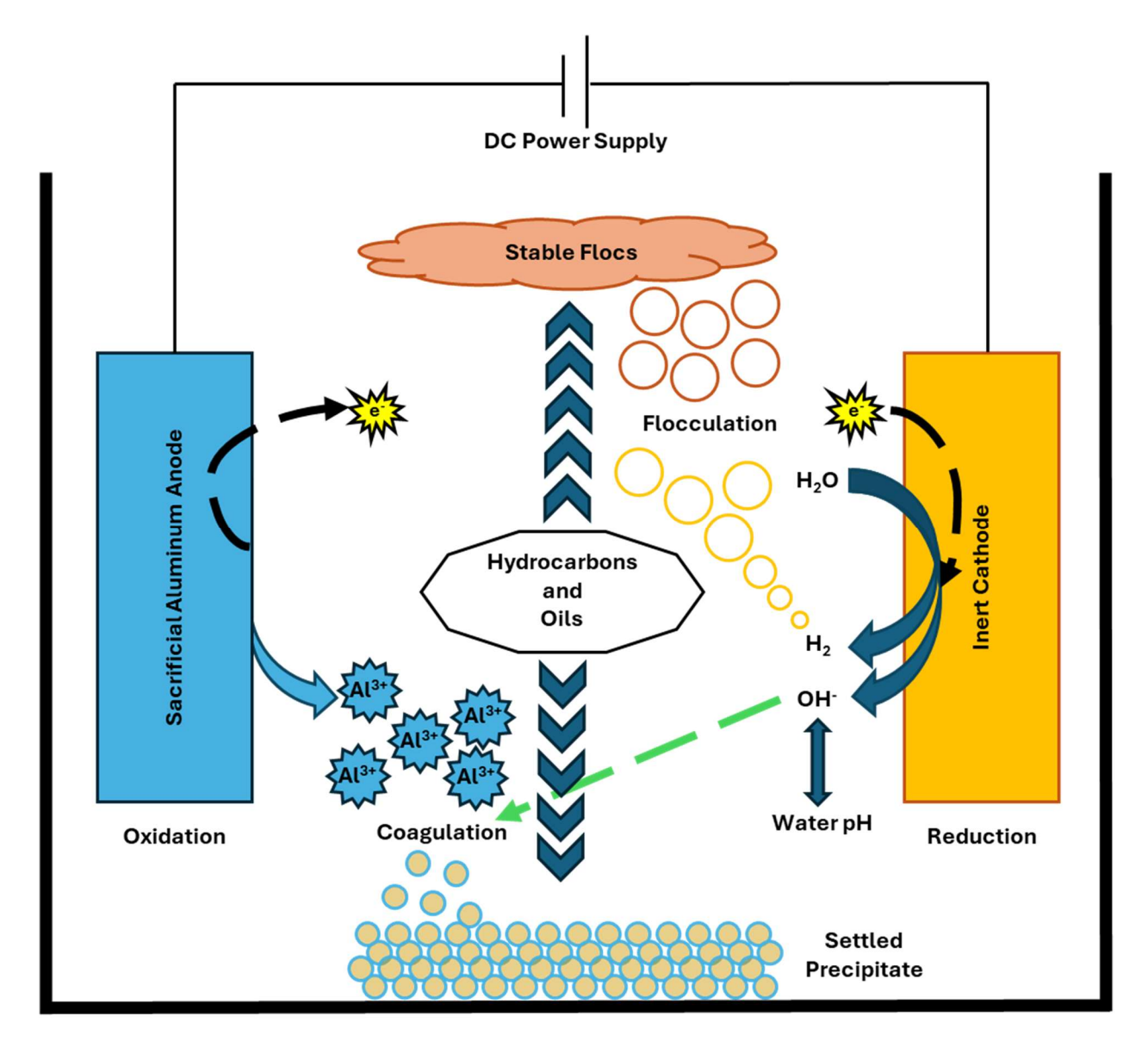


Figure 7: Diagram of the mechanism for electrocoagulation.

2.1.5 - Biofilm-Based Reactors

Biofilm-based reactors (BBR), unlike the AASs, use biofilms attached to a support material like gravel or a plastic matrix. These support materials can include but are not limited to gravel, sand, plants, and plastic structures specifically designed for the purpose. Examples of BBR include constructed wetlands (Lu *et al.*, 2022), fluidized bed bioreactors (Alwared and Jaber, 2020), and fixed bed bioreactors (Molaei *et al.*, 2022). These systems have some advantages over the previously mentioned techniques. These systems often use less energy because they may not require an external oxygen source. In the case of the constructed wetland (CW), pumping may not even require energy if the system is gravity-fed. Comparing a surface flow wetland to an SBR, the former uses less than 0.1 (kW*h)/m³

Chapter 1: Introduction

versus the latter using 1.13 (kW*h)/m³ (Kadlec and Wallace, 2001). Furthermore, fixed bed reactors and constructed wetlands are often made from low-cost materials like gravel. Though the space requirements for CW and fixed bed biofilters may be much larger than those for more energy-intensive processes, this size can be advantageous because it can accept a much larger volume of wastewater.

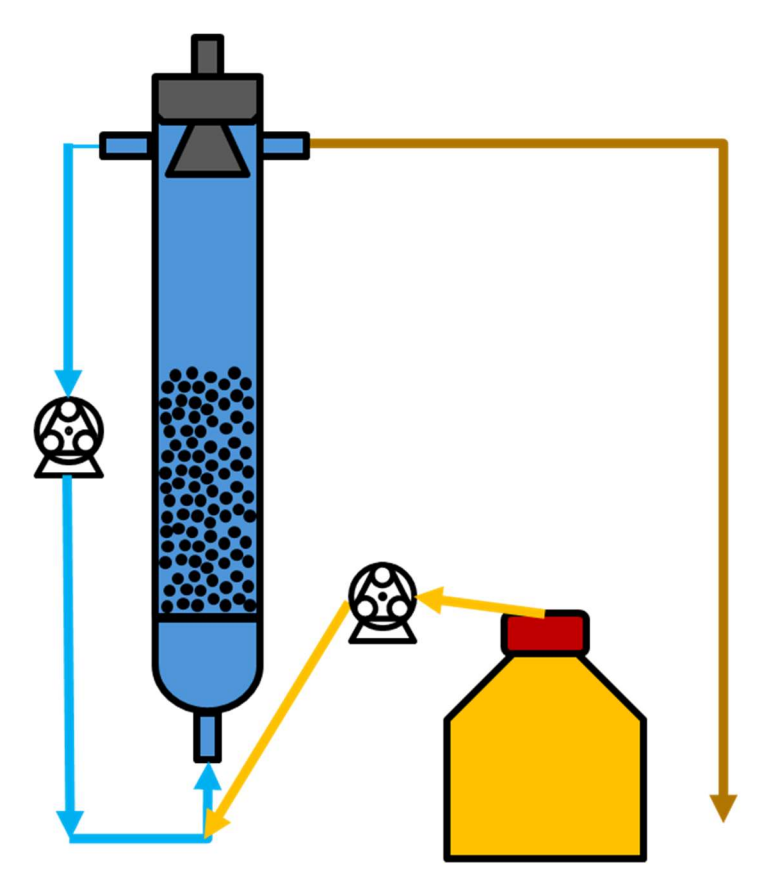


Figure 8: Diagram of a fluidized bed reactor.

Fluidized bed bioreactors (FBR) and moving bed reactors(Yan, Feng and Liu, 2024) act under the same principle of increasing mass transfer by fluidizing the bed or biofilm support particle through gas or liquid movement (Asensio, Llorente, Sánchez-Gómez, et al., 2021) (Fig. 8). These have been successfully applied to multiple different types of wastewater treatment. Schneider et al. used an FBR to treat PRW. The FBR had an average removal efficiency of 76 % for COD at a rate of 142 g/m3*day. (Schneider, Cerqueira and Dezotti, 2011). While these can be very efficient, they require much energy to constantly pump air or wastewater to maintain a fluidized bed. One way to avoid this energy expenditure is to use a

fixed-bed reactor. Patel et al. used an anaerobic up-flow fixed bed reactor to treat PRW at 37 °C. The system has a COD removal efficiency of 95% at a rate of 20615 g COD g/m³*day (Patel and Madamwar, 2002). Compared to other systems that have been reviewed, this system runs at a very high rate. While having espoused the virtue of the fixed bed for excellent energy efficiency, this system used high temperatures to achieve the rates above. This temperature will negatively impact the system's energy efficiency and may cause energy usage similar to SBR and other energy-intensive treatments.

The type of system that consumes the least energy is the CW. Though the elimination rates in these systems are often lower, they can achieve this, in some cases, without using any energy. Czudar et al. studied free surface water CW for the treatment of PRW. The system is a 15,500 m³ treatment CW fed 225 m³ of wastewater daily. The system can eliminate 54%

of the available COD at a rate of 0.98 g/m³*day (Czudar *et al.*, 2011). Though this removal efficiency varies by season, it is consistently below the discharge limit set for the area. Another example of using CWs is Mustapha et al. used a vertical subsurface flow CW to treat PRW. They could remove 60% of the COD at 20 g/m³*day. (Mustapha, van Bruggen and Lens, 2015).

2.2 - Electroactive Biofilters: the METland Concept

The BBR had the highest potential for a low-energy, low-cost treatment solution out of the above systems. As discussed in the first section, METs can be used for various applications. Another way they can be used is as an electrochemical snorkel (MES). If electrical current production is not the goal of the microbial electrochemical device, then those electrons can be used for other purposes. Instead, using an MES, one can take the electrons produced by the oxidation of organic matter and transfer them directly to oxygen (Erable, Etcheverry and Bergel, 2011). The MES acts as if the resistor was removed from a S-MFC. Instead of harvesting electrons, electrons can be used more efficiently from the oxidation of organic matter. This same concept can be applied to nitrate, nitrite, sulfates, and thiosulfates. This direct transfer of electrons allows for an anodic reaction in sediment or an electroconductive bed and an abiotic cathodic reaction with oxygen in the upper water column or air (Hoareau, Erable and Bergel, 2019). This concept can be further applied to the bed of a CW or a biofilter.

By using the basic concept of the CW and replacing the inert bed material with electroconductive material, it is possible to make an applied MES that can treat many different waste streams (Wang et al., 2020). The combination of a MET and a constructed wetland is called the METland (Esteve-Núñez, 2025). When flooded, the METland produces a naturally occurring redox gradient, promoting COD and nitrogen removal at greater efficiencies than conventional flooded bed material (Aguirre-Sierra, Bacchetti-De Gregoris, A. Berná, et al., 2016). Furthermore, the METland has shown itself robust even under aerobic conditions. In an aerated downflow state, the METland has improved nitrification and COD removal (Aguirre-Sierra et al., 2020). This efficiency comes from the electroconductive bed's ability to allow electrons to flow through the bed to where they are needed. Through the bed, electrons can pass from anodic regions, areas predominated by oxidative reactions, to cathodic regions, with predominantly reductive reactions. This electron flow creates a redox gradient along the bed. This profile has been measured across the bed (Ramírez-Vargas et al., 2018, 2019; Prado de Nicolás, Berenguer and Esteve-Núñez, 2022; Wei, 2024). The sustainability of the system was demonstrated by multi-criteria evaluation, sensitivity analysis, and life cycle assessment (Peñacoba-Antona et al., 2021; Peñacoba-Antona, Gómez-Delgado and Esteve-Núñez, 2021) and has been

Chapter 1: Introduction

validated at northern and southern latitudes in Europe (Peñacoba-Antona *et al.*, 2022a). The METland can function at full scale to treat urban and industrial WW (Mosquera-Romero *et al.*, 2023) and can deal with emerging contaminants (Jiménez-Conde, 2024). Furthermore, these unique abilities have allowed the treatment of many different types of difficult WWs.

The METland concept has evolved to generate a number of novel electroactive biofilters. These electroactive biofilters use the abilities inherent in the METland to produce biofilters that can treat previously recalcitrant WWs (Fig. 9). The electroactive biofilter was tested using emerging contaminants from the medical and pharmaceutical industries. The electroactive biofilter detoxified 80% of the complex mixture of 13 pharmaceuticals, removed 90 % of the COD, and nitrified 70% of the N-NH4 (Pun, Boltes, Letón, Esteve-Nuñez, et al., 2019). The electroactive biofilter has also been shown to treat a complex mixture of pharmaceutical and herbicide enantiomers. The chirality of these contaminants provides them with unique toxicities and can require different degradation pathways based on the enantiomer. The electroactive biofilter treated 80% of the pharmaceuticals and 50-75% of the herbicides tested. Furthermore, the electroactive biofilter changed the chirality of some of the chemicals, reducing ecotoxicity (Pun et al., 2025). Another complex pollutant the electroactive biofilter could treat was surfactant-polluted WW. The electroactive biofilter could remove 98% and 96% surfactants from real and synthetic WWs. The electroactive biofilter did this because it creates a unique environment that allows very specialized communities of microbes to form. The community that formed in the electroactive biofilter treating surfactant WW was a more specialized community of surfactant degrading and electroactive microbes than a conventional gravel filter (Noriega Primo, López-Heras and Esteve-Núñez, 2024).

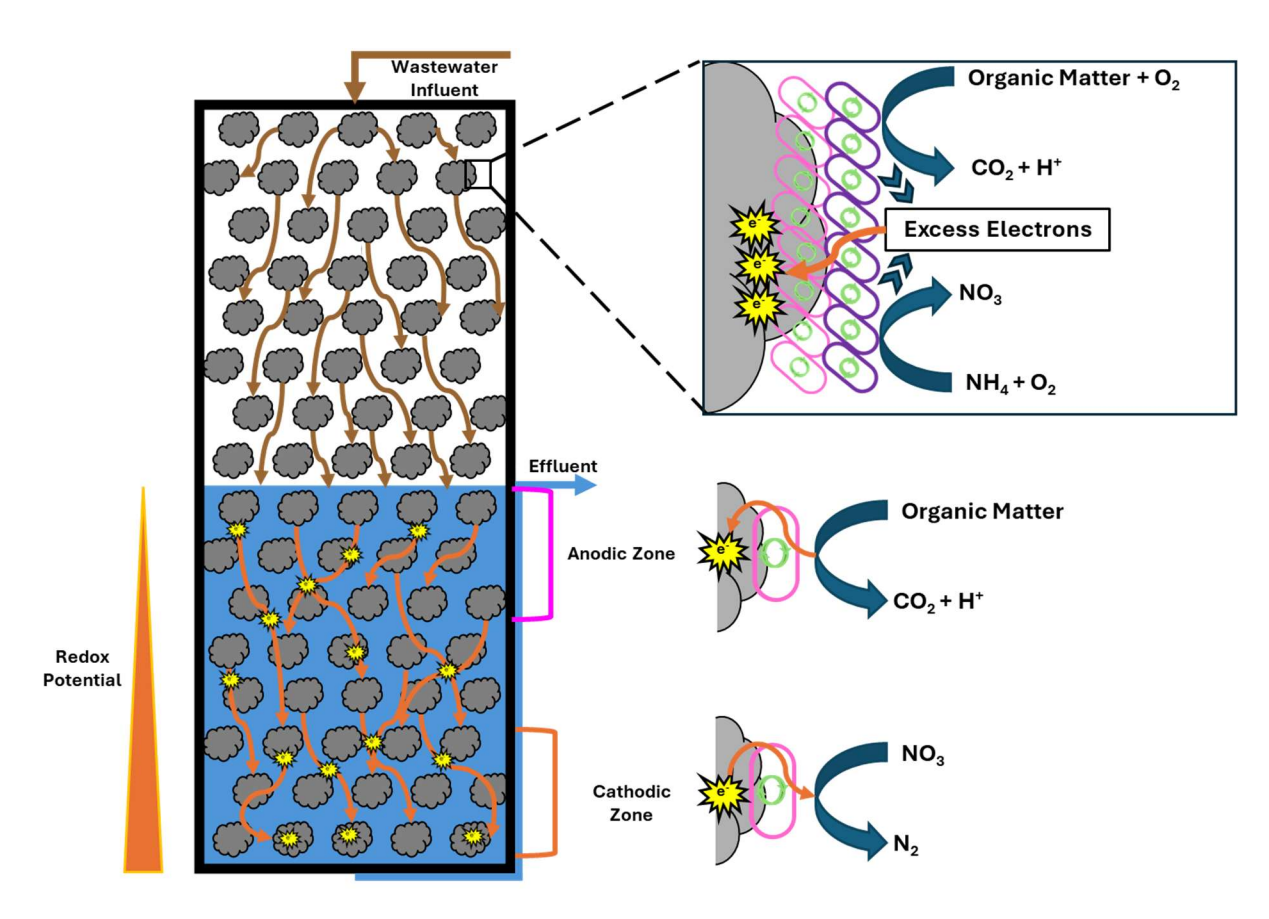


Figure 9: Diagram of proposed mechanisms for aerobic and anaerobic METfilers.

Chapter 4 applies the robust treatment concept of the METland to 3 novel biofilter designs. These electroactive biofilters can treat recalcitrant HC WW media by alternating aerobic and anaerobic electroconductive bed sections while selecting for a specialized community able to degrade HCs.

3 - Adaptive Laboratory Evolution

Adaptive laboratory evolution (ALE) is a type of directed evolution that seeks to improve bacterial strains by artificial mutation or by natural selection by imposed selective pressures in the laboratory. Studies about the controlled evolution of bacteria are seen as far back as the mid-20th century (Novick and Szilard, 1950). In these experiments, a simple method was used, exposing bacterial strains or species to a selective pressure for sufficient time for the desired phenotype to appear. This evolution can happen unconsciously in the way cell cultures are maintained. By using the growth, transfer, and freezing method, standard laboratory practices select subpopulations in a pure culture that grow best in a media of choice and can survive the freezing process. Since this process

can happen by coincidence, with the intention of a researcher, it can produce very resilient results.

ALE does not rely solely on random mutagenesis or directed mutation. No *a priori* knowledge or gene target is required to produce a phenotype of interest. Even if one knows a target gene or operon, engineered strains often have unintended consequences due to the incredible complexity of cellular genetic control. ALE targets maintaining any genomewide mutations that could benefit the desired phenotype in response to the applied selective pressure (Shepelin *et al.*, 2018). ALE aims to improve fitness, but fitness can change depending on desired results. Suppose cells are maintained at exponential growth without nutrient limitation. In that case, the ability to grow or the growth rate defines what cells are qualitatively fit or quantitatively more or less fit (Fig. 10). From an experimental design point of view, this leads to a few major categories of ALE applications.

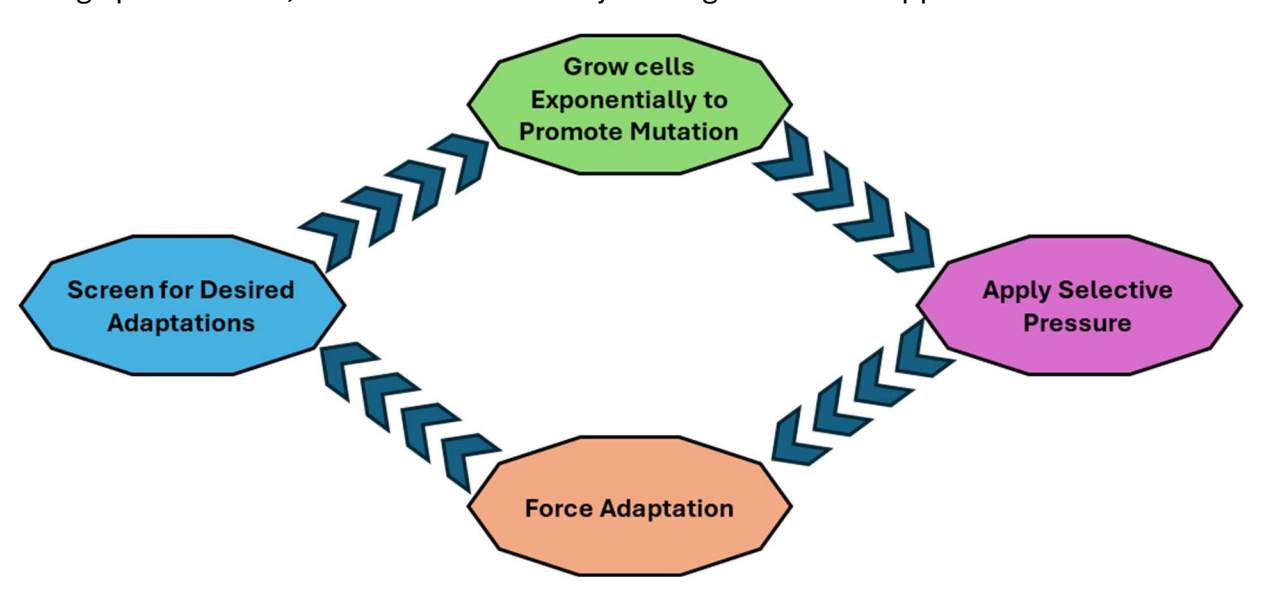


Figure 10: Diagram of the workflow for adaptive laboratory evolution.

There are 5 typical applications of ALE. The first is growth rate optimization. This optimization is often applied to biotechnologically or industrial-relevant strains to improve growth time (Pfeifer *et al.*, 2017). The second application is to increase yield. In this case, a push-pull between the resources required for growth and metabolite production can be hard to overcome. This push-pull can be overcome using a higher mutation induction through mutagenic chemicals and by screening mutants for the desired phenotype in devices similar to where the strain will be applied, like a chemostat (Ingelman *et al.*, 2024). The third application is substrate utilization, where substrate uptake can be increased(Espinosa *et al.*, 2020) or decreased (Zhang *et al.*, 2018) depending on the desired application. The fourth is to help understand the basic science of evolution. An example is studying the response to genetic disruption over generations to gain insight into

metabolic networks (McCloskey *et al.*, 2018). The final application of ALE is increased tolerance to cell stress, which is of particular concern to this thesis.

Cell stress can take many forms, but invariably inhibiting the cell's ability to function efficiently. ALE has been used to study many different stressors like pH (Salas-Navarrete et al., 2022), nutritional stressors (LaPanse, Krishnan and Posewitz, 2021), temperature (Deatherage et al., 2017), inhibitors (Wang et al., 2018), and UV irradiation (Ramos et al., 2016). This thesis will deal mainly with how microbes can be adapted to osmotic stress conditions. Osmotic stress is created when the gradient of solutes is not even across a membrane. ALE has been used to increase the performance of wine yeast Saccharomyces cerevisiae by adapting them to hyperosmotic KCl solutions (Tilloy and Ortiz-julien, 2014). Another group adapted a strain of Rhodotirula to hyperosmotic conditions and increased their tolerance to methanol for use with crude glycerol (Wei et al., 2024). Another group used semi-continuous growth conditions to boast fatty acid productivity while adapting a microalga to saline conditions (Sandberg et al., 2019). Many ALE strategies use batch culturing or a continuous culture system like a chemostat. However, unlike the chemostat, another continuous culture device can apply more than one level of selective pressure or a gradient of selective pressures.

In nature, there are many environments where microbes inhabit that are not stable. Take the estuary, from the fresh water of a river to the salt water of a bay or ocean. There is a constantly changing gradient of salinity as one moves from one to the other. To replicate this in a laboratory, it is necessary to section off each specific salinity into a reactor that flows into another reactor. This segregation inevitably creates interconnected reactors that produce a salinity gradient analogous to that estuary. This first system was passive, with diffusion creating a gradient across different cells (Cooper and Copeland, 1973). This passive system was improved upon using bidirectional pumping between sealed chemostats. This improved device was called a gradostat (Lovitt and J. W. . Wimpenny, 1981). The gradostat was designed to simulate a structured ecosystem like the one described above but in a controlled way that allows one to choose specific parameters like the solute, the concentration of said solute, dilution rates, and hydraulic retention time. This controllability allows for a system that is more suitable for specific microbial experiments and ALE. Since the 1990s, this device has mostly been used as a mathematical model (Jager et al., 1987)(Gaki et al., 2009). In chapter 5 of this thesis, a gradostat is combined with a single chamber MEC. This combination is done to explore the ability of the system to perform ALE and microbial electrochemistry on G. sulfurreducens.

Objectives

This thesis aims to understand better how to apply METs to solve complex global environmental problems. The focus is on biosensing, WW treatment, and adapting microbes to microbial electrochemical devices.

- **Objective 1:** To Understand the connection between the current generated with an S-MFC and the metabolism in water-logged sediments.
- **Objective 2:** Determine if a three-electrode electrochemical biosensor can be used to determine the health of an anaerobic digester and detect biocides to protect it.
- **Objective 3:** By applying the METland concept to biofilters, use alternating aerobic and anaerobic bed sections in a single biofilter to treat hydrocarbon-contaminated water and select for a robust microbial community to treat that water.
- **Objective 4:** To build a gradostat capable of growing *G. sulfurreducens* and studying how salinity affects *G. sulfurreducens*' ability to respire an electrode by combining the gradostat with the MEC concept.

Chapter 2:

Measuring Microbial Metabolism in Sediments

Bioelectrochemical strategies for Measuring Microbial Metabolism of Sediments and Waterlogged Soils

1 - Introduction

Understanding anaerobic metabolism is very important for understanding the biogeochemistry of all freshwater and saltwater sediments and water-logged soils (Yavitt, Lang and Wieder, 1987; Canfield *et al.*, 1993; Lovley and Chapelle, 1995; Liesack, Schnell and Revsbech, 2000),. It is possible to determine the terminal electron-accepting process in sediments by measuring hydrogen concentrations (Lovley and Goodwin, 1988; Lovley, Chapelle and Woodward, 1994; Chapelle *et al.*, 1997). Unfortunately, measuring the metabolic rates of microbes in anaerobic sediments is much more difficult.

The difficulty of measuring anaerobic microbial metabolism comes from the time-consuming nature of the process and the technical expertise required to accomplish it. Typically, the process requires incubating sediment samples and monitoring metabolic products like CO₂. The analysis of metabolic products requires sophisticated methods and equipment. The choice of techniques or equipment can affect the observed metabolic rates (Chapelle and Lovley, 1990; Phelps *et al.*, 1994)All these factors make determining anaerobic microbial metabolism very expensive and challenging to study over long periods. Studies detailing the long-term effects of a contamination event or the rate of bioremediation of a known contaminated site quickly become cost-prohibitive.

Microbial fuel cells (MFCs) showed early promise in determining organic matter concentrations from microbially generated current (Daniel R Bond and Lovley, 2003). In specific applications like wastewater or the presence of particular substances, the MFCs have shown a strong correlation between current density and microbially available organic matter (Zhang and Angelidaki, 2011; Do *et al.*, 2020). These studies were performed at the lab scale with solutes in the range of millimolar concentrations. This substrate level is well outside of what is seen in natural sediments and water-logged soils; therefore, these estimates may not be appropriate for environmental application.

In artificial environments like wastewater, MFCs have shown much success in determining chemical characteristics like BOD (Salvian *et al.*, 2024). Furthermore, introducing an unlimited electron acceptor in the form of an electrode has been shown to increase the

Chapter 2: Measuring Microbial Metabolism in Sediments

bioremediation of polluted sediments (Tucci *et al.*, 2021). Thus, the current produced by an MFC is stimulated by the metabolism of the surrounding sediments. In sediments, the amount of organic matter like amino acids, sugars, and acetate is generally low, regardless of the metabolic rates of the microbes therein. The organic matter turnover rates are vital to the microbes' metabolic rates, not the organic matter concentration.

An example of this is hydrogen concentration in flooded soils and sediments. Sediments with vastly different hydrogen production rates have very similar overall hydrogen concentrations if the hydrogen oxidizing community uses the same terminal electron acceptor. The hydrogen concentration will be maintained in these sediments, independent of the hydrogen production rate, to keep hydrogen oxidation favorable for the predominant electron acceptor that can generate the most energy. This constraint by redox potentials means if there is a sudden increase in the hydrogen production rate, there will be an equal increase in the quantity of microbes that perform the oxidization and an increase in the reduction of whatever terminal electron-accepting process is dominant in that environment (Lovley and Goodwin, 1988). This process is similar to other electron donors.

The anode of an MFC, in the sediment environment, acts like any other natural terminal electron acceptor, such as inorganic carbon, sulfate, or iron-oxides. It has been observed that the anode of a sediment MFC can play an active role in the breakdown of different recalcitrant chemicals. This effect on recalcitrant chemicals shows that in electron-acceptor-limited environments, the anode can stimulate microbial metabolism (Garbini, Barra Caracciolo and Grenni, 2023). So, in normal subsurface environments, the MFC's current should directly correlate with the metabolic rate of microorganisms in the surrounding sediment. Acetate is the most common and important intermediate in sediments for respiration (Lovley and Chapelle, 1995). When an MFC anode is placed in anaerobic sediments, most organisms that colonize it oxidize acetate. While other organic matter and hydrogen may contribute to the current generation of the MFC, these should only play a minor role compared to acetate. Therefore, the current generation of an MFC should show a strong correlation to the turnover rate of acetate independent of the dominant terminal electron-accepting process of the sediment.

Chapter 2: Measuring Microbial Metabolism in Sediments

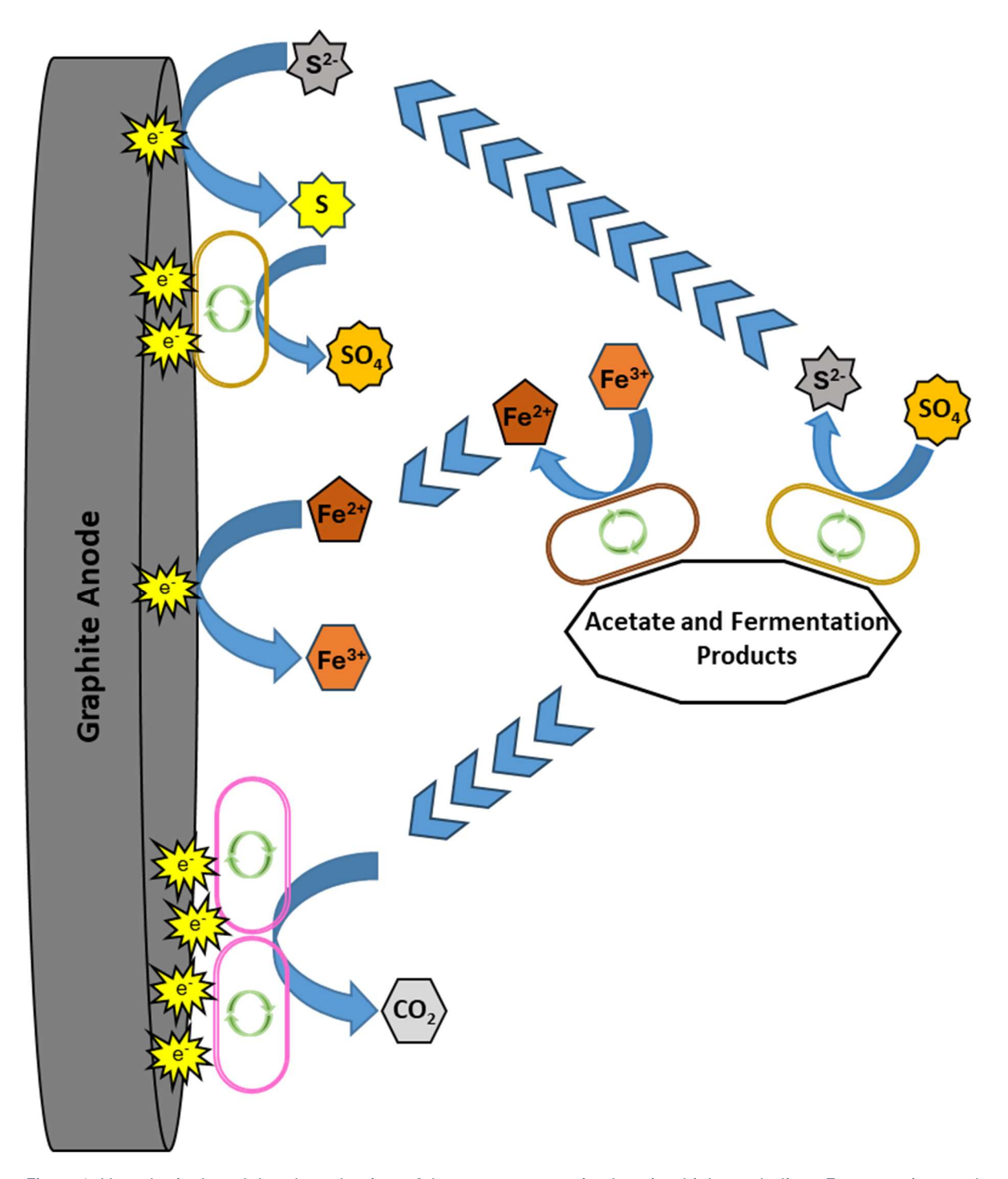


Figure 1: Hypothetical model and mechanism of the current generation by microbial metabolism. Fermentation products and acetate will produce the majority of the current. Reactions distal to the electrode may also contribute to the current by producing Fe(II), sulfide, and subsequent abiotic oxidation at the anode.

The microbes that colonize the anode are not the only contributors to the current generation. The anode can abiotically oxidize reduced terminal electron acceptor and contribute to current generation. These reduced terminal electron acceptors do not need to be produced at the electrode but can be generated at some distance from the anode.

Compounds like ferrous iron and sulfide can be abiotically oxidized at the anode. Furthermore, the sulfide oxidation at the anode can produce elemental sulfur. This sulfur can be an electron donor for microbes like *Desulfobulbus* (Holmes, Bond and Lovley, 2004) and *Desulfuromonas* (Zhang et al., 2014).

MFCs have been deployed in the field in sediments and have generated detectable current densities using graphite anodes of 0.05 – 0.2 mA/m² (Williams *et al.*, 2010). Poised MECs were also placed in arctic peat soils, and currents were detectable.

This study shows that an MFC, consisting of a graphite anode connected to a graphite cathode through a resister, can monitor the microbial metabolism of iron-reducing, sulfate-reducing, and methane-producing sediments. By using a 2-14C-acetate tracer, it was demonstrated that acetate turnover rates in sediment are directly correlated to the current density in an MFC independent of the terminal electron-accepting processes.

2 - Materials and Methods

2.1 - Sediments

Three different sediments were used in this study to show that the rate of microbial metabolism detected with an MFC was independent of the dominant terminal electron-accepting process. The first sediment was dominated by Fe(III) reduction. These samples were taken from Rifle, CO, as previously described (Anderson *et al.*, 2003; Williams *et al.*, 2010). These samples were excavated and shipped to the University of Massachusetts, where they were stored at 15° C (Barlett *et al.*, 2012). The second sediment was dominated by sulfate reduction and came from a marine environment. The sediment was taken from a site in Nantucket, MA, at low tide in a salt marsh. The sampling process was previously described (Broadaway and Hannigan, 2012). In brief, samples were taken from a 2-25 cm depth, sealed in containers without headspace, and stored at 15° C. The third sediment was methanogenic freshwater sediment from Puffers Pond, Amherst, MA. Samples were taken from a 5-25 cm depth with 0.1-0.25 m of water above the sediments. Sampling proceeded similarly to the Nantucket samples, which were sealed in containers and stored at 15° C.

2.2 - Sediment Fuel Cells and Incubation

The sediment fuel cells were constructed using PVC pipes with butyl stoppers in the bottom. Due to the limited availability of Fe (III) reducing sediment, a 7.6 cm diameter pipe was used, while the methanogenic and sulfate-reducing sediment used a 10.2 cm diameter. Sediments were homogenized under a constant stream of nitrogen gas. This

homogenized sediment was then used to fill the PVC to a height of 23 cm. The sediment column was then submerged under 23 cm of water from the site of origin. Triplicate sampling ports of 10.5 mm diameter were present and aligned to the same height as the anodes of the system. These ports were also sealed with butyl stoppers. Each cylinder had two anode and cathode pairs. The anodes were placed at 8 or 16 cm from the bottom of the sediment column (Fig. 2A). The anodes were constructed from a polystyrene tube, with one end housing the anode. The anode was made of a graphite cylinder housed inside the tube such that only a circular face of 28.26 mm^2 was exposed to the sediment. The anode was connected to a carbon bottle brush cathode with marine-grade insulated wire through a 560Ω resistor. The cathode was suspended in the water above the sediment.

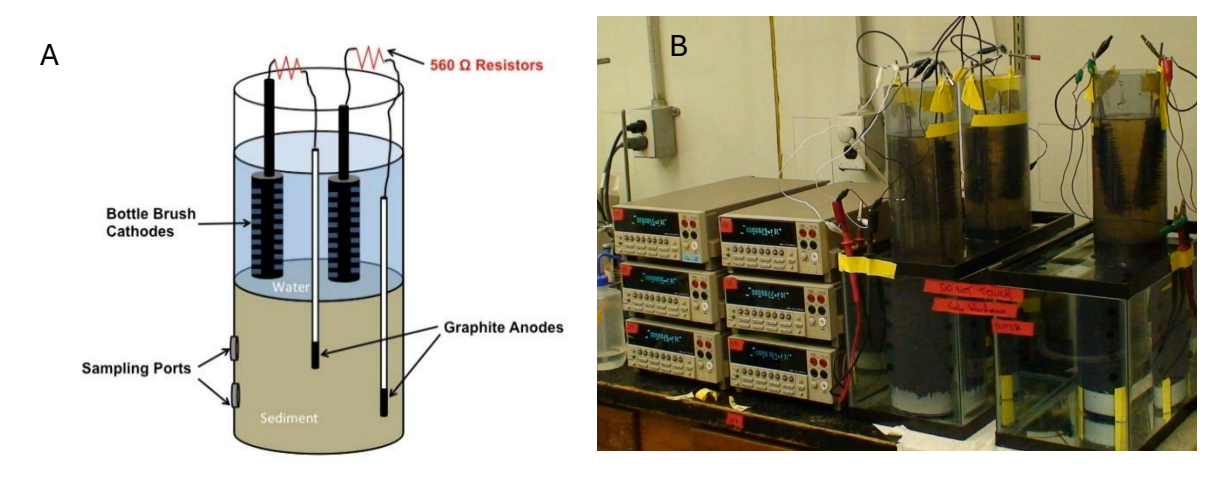


Figure 2: A) Diagram of the sediment cylinder. B) Sediment cylinders in aquaria with current monitoring equipment.

Three cylinders were incubated per temperature tested (4° C, 20° C, and 37° C). These temperatures were chosen to represent a broad array of naturally occurring conditions and control the metabolism of the microbes. The cylinders were placed in aquaria filled with water above the sediment level of the cylinders to isolate the anodes from oxygen further and increase the stability of the temperature of the sediments and anodes (Fig. 2B). Ideally, each temperature would have triplicate cylinders with duplicate sediment fuel cells. Still, some electrodes had to be excluded due to faults in the construction. These faults were caused by water infiltration, causing shorts, which prevented current production or cracks, allowing for uncontrolled anode colonization. These faults led to 3-6 reliable signals per temperature tested. Methanogenic sediment current production was measured hourly by a Keithley 2700 or a 2000 Digital Multimeter (Cleveland, OH). The other sediments' current was measured daily with a UEI DM284 Digital Multimeter (Beaverton, OR).

2.3 - Microbial Metabolic Rates

Given acetate's importance in electron flow in anaerobic sediments, acetate turnover rate was chosen as the best proxy for microbial metabolic rate. To be able to correlate current production to acetate turnover rate, a steady-state current density was required. The sediment columns were sampled after the current density was steady for 4-10 days. Three 3 cm cores were removed through the sampling ports around each anode and placed in an anoxic 60 ml serum bottle. Each core was weighed, and the six bottles from each cylinder were placed in a water bath that matched the incubation temperature of the cylinder. Each core was injected with 0.1 ml of anoxic 2-C¹⁴-acetate (American Radiolabeled Chemicals Inc. St Louis, MO). The specific activity of the isotope was 45 mCi/mmol, which provided 1.2-1.7 uCi and 15 μ M acetate per injection.

To detect $^{14}\text{CO}_2$ and $^{14}\text{CH}_4$, a gas chromatograph (GC-8A, Shimadzu, Kyoto, Japan) was connected to a GC-RAM radioactivity detector (LabLogic, Broomhill, UK). Over 8 – 24 hours, 0.5 ml of headspace was injected to detect $^{14}\text{CO}_2$ and $^{14}\text{CH}_4$ as previously described (Hayes, Nevin and Lovley, 1999). The acetate turnover rate was determined from the initial $^{14}\text{CO}_2$ and $^{14}\text{CH}_4$ production slope vs time.

2.4 - Confocal microscopy

Anodes were imaged with a confocal laser scanning microscope (Leica, Solms, Germany). Cells were stained with LIVE/DEAD BacLight (Molecular Porbes, Eugene, OR). Live cells were stained with green SYTO 9, and dead/compromised cells were stained with red propidium iodide. All image analysis was done with Leica LAS software (Leica Solms, Germany).

3 - Results and Discussion

To understand the connection between the current generated by sediment in an MFC and microbial metabolic rates, an electron donor that is ubiquitous and independent of the terminal electron-accepting process was required. Acetate is central to the degradation of organic matter anaerobically, so it is a key intermediate whether the environment is dominated by Fe(III) reduction, sulfate reduction, or methanogenesis (Lovley and Chapelle, 1995). Given its central role in anaerobic metabolism, acetate and the rate of its mineralization to CO_2 and CH_4 would directly represent the combined rates of all anaerobic fermentation. Therefore, acetate would be a suitable proxy to correlate to current production.

This study hypothesized that current (I) would directly correlate to acetate turnover (V_a):

EQ. 1
$$I = Z \times V_a$$

Factors outside the current production and acetate turnover need to be represented in EQ. 1; therefore, the variably Z is added. Z represents the complex interactions and processes in the sediment and microbes that control the current generation. As long as Z is constant, as these contributing factors do not vary greatly over the set conditions tested herein, there will be a strong correlation between current and acetate turnover rates.

Acetate turnover (V_a), or the mineralization of acetate by microbes, is estimated from the turnover of radiolabeled acetate (k) and acetate concentration (A):

EQ. 2
$$V_a = k \times A$$

The sediments used herein had acetate concentrations lower than the limits of HPLC (10 μ M), so V_a could not be calculated. This lack of native acetate concentration added another unknown to EQ. 1:

EQ. 3
$$I = Z \times k \times A$$

Given the stability of sediments and the slow turnover rate of organic matter therein, acetate concentrations can be expected to remain constant. This concentration may change depending on the sediment's predominate terminal electron accepting process, but in each case, it should be constant across the tested conditions. Therefore, A, like Z, can be considered a constant, and there should be a strong and direct correlation between I and k:

EQ. 4
$$I = (ZA) \times k$$

Depending on the sediment type, ZA may change, but the correlation will remain constant. All the sediment studied here showed a strong and direct correlation between current density and the mineralization of 2-C¹⁴-acetate (Fig. 4-6). With all the sediments, temperature was an effective control for producing differing metabolic rates. Furthermore, one cracked anode was used to demonstrate evident biofilm growth (Fig. 3).

Chapter 2: Measuring Microbial Metabolism in Sediments

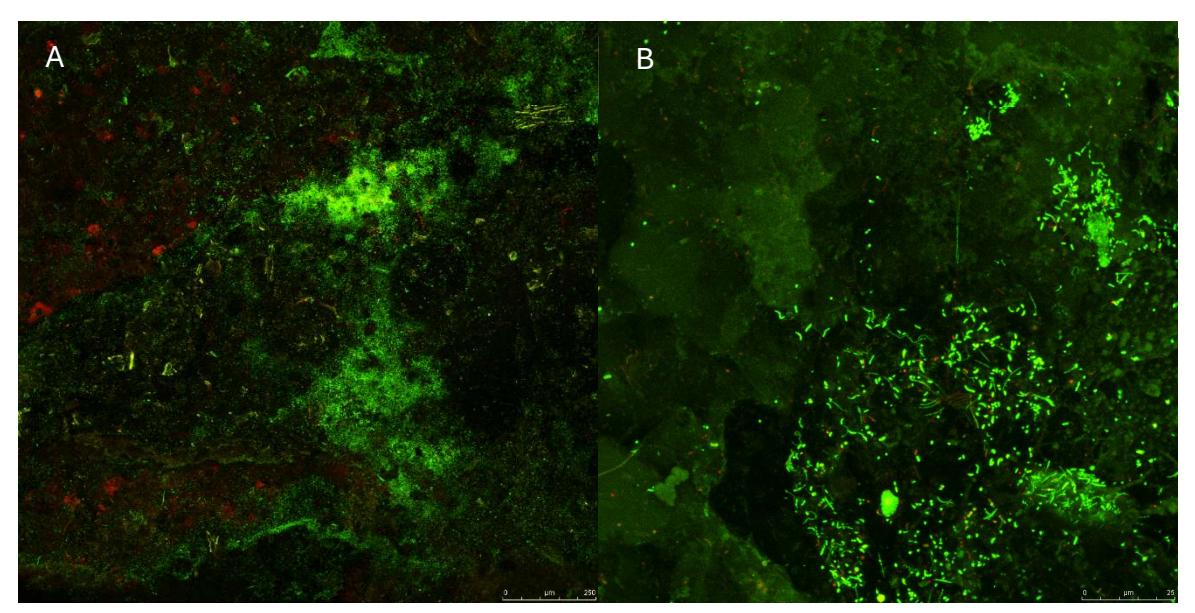


Figure 3: Confocal laser scanning micrographs of a methanogenic sediment anode. Live cells are in green, and dead/compromised cells are in red. A) Total magnification is 100X. B) Total magnification is 1000X.

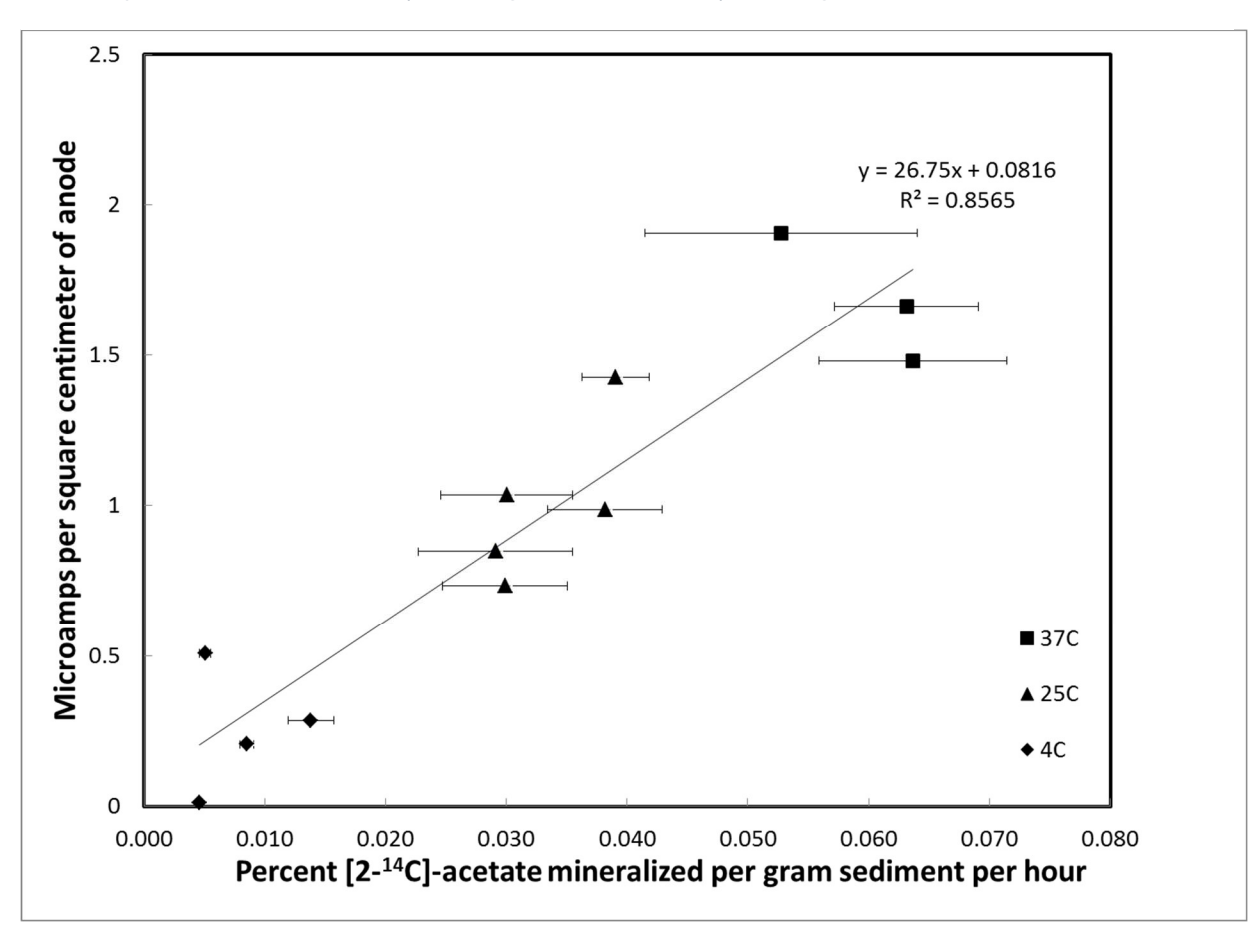


Figure 4: Direct correlation between current production and acetate mineralization in methanogenic sediments incubated at different temperatures (4° C, 25° C, 37° C) (R^2 =0.8565). Error bars are the standard deviation of the triplicate cores tested for acetate turnover rate.

Chapter 2: Measuring Microbial Metabolism in Sediments

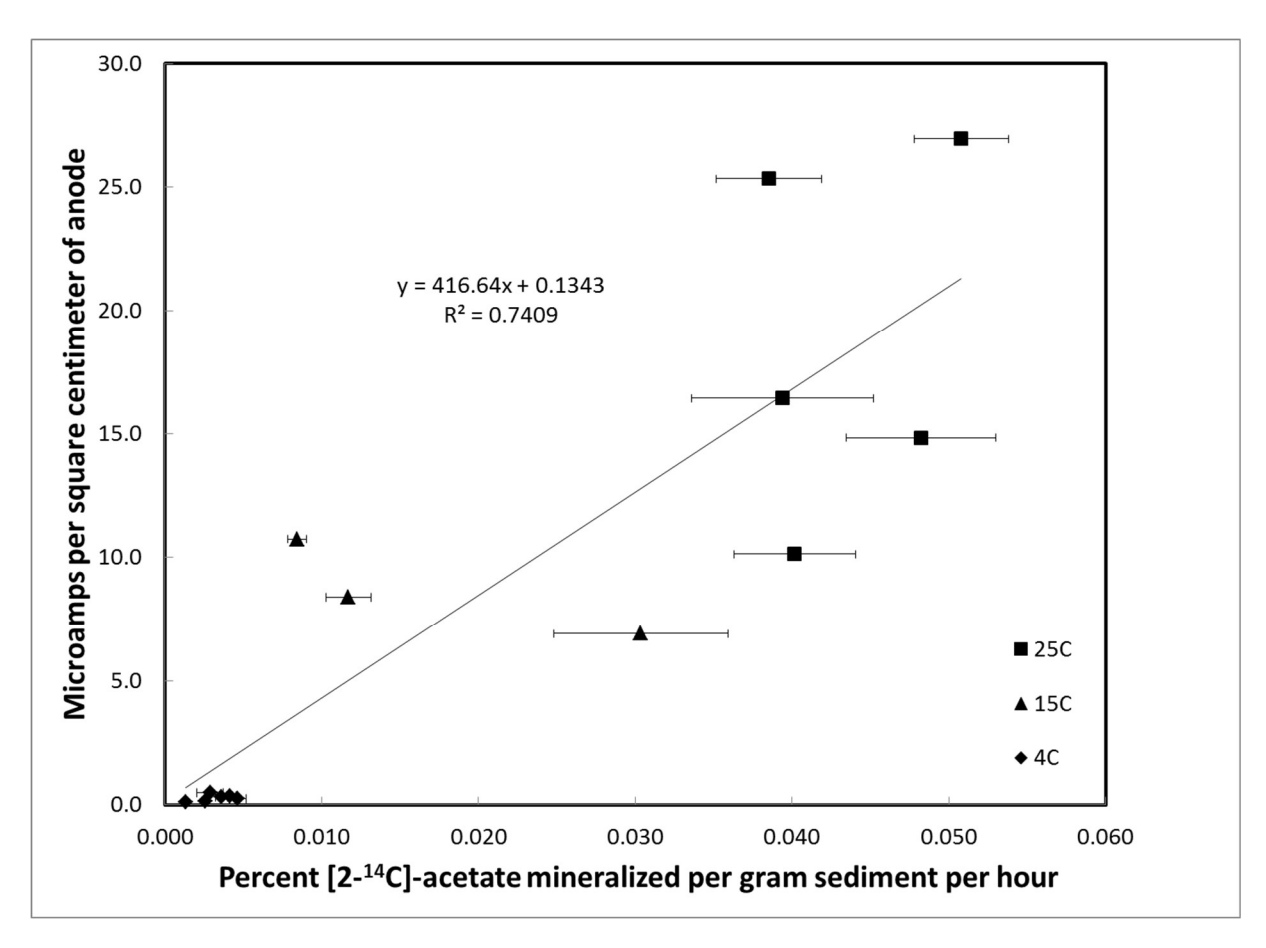


Figure 5: Direct correlation between current production and acetate mineralization in sulfate-reducing sediments incubated at different temperatures (4° C, 15° C, 25° C) (R^2 =0.7409). Error bars are the standard deviation of the triplicate cores tested for acetate turnover rate.

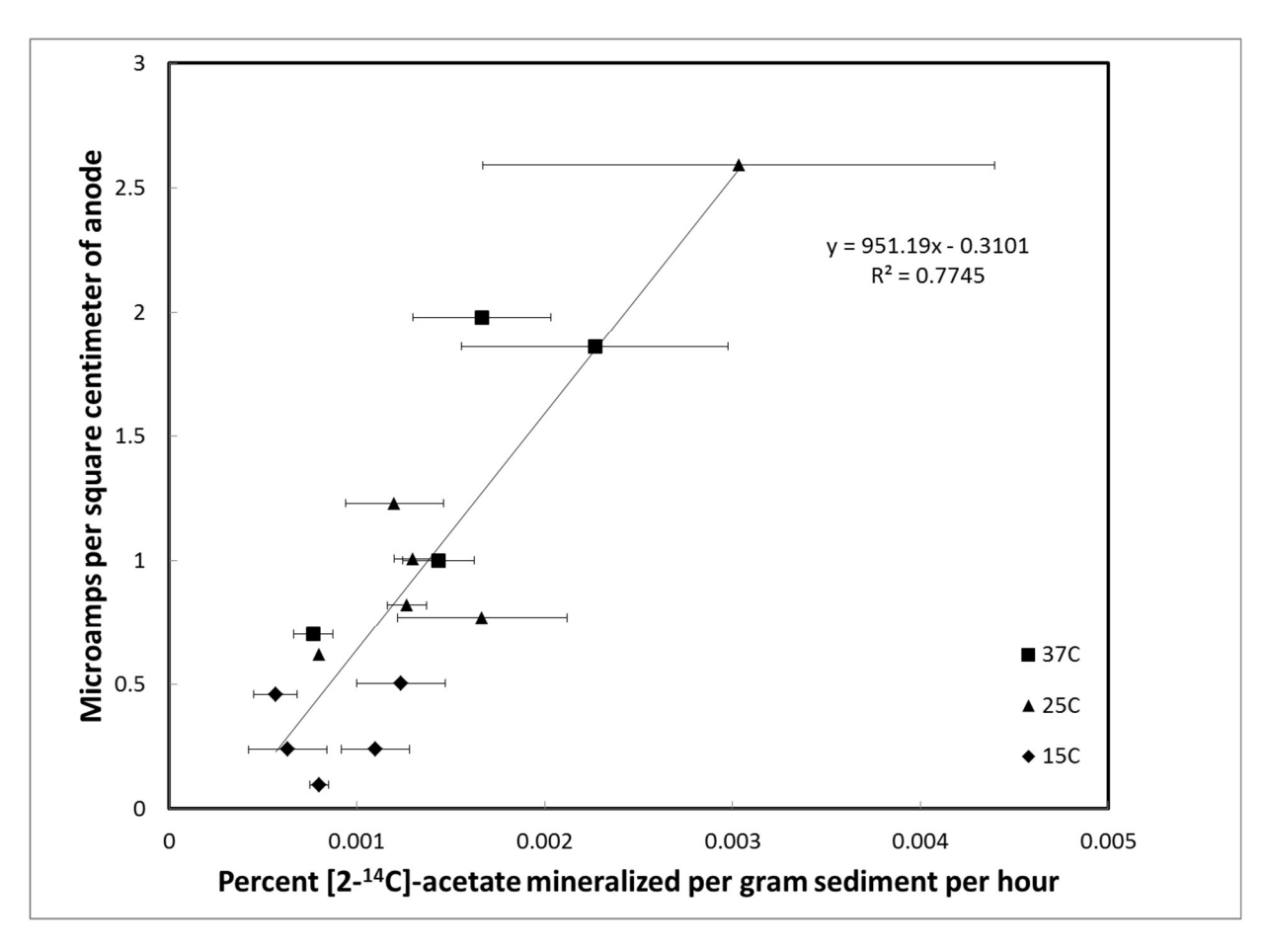


Figure 6: Direct correlation between current production and acetate mineralization in iron-reducing sediments incubated at different temperatures (15°C, 25°C, 37°C) (R²=0.7745). Error bars are the standard deviation of the triplicate cores tested for acetate turnover rate.

The Fe(III) reducing sediment has the lowest overall metabolic rates (Fig. 6) due to its lower organic matter content than the methanogenic and sulfate-reducing sediment. Given this lower organic matter content, the Fe(III) reducing sediment produced a current density similar to that of the methanogenic sediment (Fig. 4). Conversely, the sulfate-reducing sediment had a more similar metabolic rate to the methanogenic sediment but had a 15-fold higher current density (Fig. 5). This higher current density means that the ZA for the sulfate-reducing sediment was much higher than the methanogenic sediment. Generally, methanogenic sediments have higher acetate concentrations than sulfate-reducing sediments (Lovley and Phillips, 1987). This difference in acetate availability is because sulfate reducers attenuate acetate more than methanogens (Lovley and Klug, 1983, 1986). This attenuation means that something other than the availability of acetate affects the current density difference between the sulfate-reducing sediment and the methanogenic sediment.

The answer may lie in the difference in the terminal electron-accepting process. Both processes will produce acetate, hydrogen, and other fermentation byproducts proximal to

the anode surface, but one can create a product that can generate current abiotically. Distal from the anodes, fermentation produces methane and sulfide. Methane is unreactive, and while there are methane-oxidizing bacteria, it is unlikely to contribute to the current generation. Conversely, sulfide can be abiotically oxidized on the anode and generate current (Tender *et al.*, 2002) (Gong *et al.*, 2013). When the anode oxidizes sulfide, it produces elemental sulfur, which can, in turn, be oxidized to sulfate, producing more current (Holmes, Bond and Lovley, 2004; Zhang *et al.*, 2014). Therefore, sulfur-reducing sediment processes that are not directly related to the anode spatially can greatly increase the current density (Fig. 1).

A similar phenomenon is plausible in the iron-reducing sediment. At similar rates, the current density of the iron-reducing sediment is over twice that of the methanogenic sediment. Fe(II) is generated throughout the sediment, and like sulfide, it can abiotically donate electrons to the anode. Therefore, microbial activity distant from the anode can increase the current density (Fig. 1).

The terminal electron-accepting processes are fundamental to microbial fuel cells' current production. For this reason, it will be necessary to calibrate each system to each type of terminal electron-accepting process. However, by combining this technology with hydrogen concentration, it should be possible to make a device capable of quantifying the microbial metabolism of sediments and the terminal electron-accepting process.

4 - Conclusions

These results demonstrate that an MFC can determine the metabolic rate of a sediment independent of the terminal electron-accepting process dominant in that sediment. This novel technology can allow *in situ* monitoring of flooded soils and sediments over long periods and in remote areas. Furthermore, it can be done without a poised electrode, which decreases the cost of implementation to just the material cost of the system, which is negligible, and data logging equipment. This technology can be used beyond scientific pursuits to protect environments from containment plumes, oil leakage, or spillage.

Chapter 3:

Monitoring Anaerobic Digestors with Biosensors

Use of Electrochemical Biosensors for Monitoring Effluent Quality and Preventing Anaerobic Digestor Collapse

1 - Introduction

In 2022, the world produced 185M tonnes of beer from barley. Spain is the tenth-largest beer producer in the world (United Nations, 2024). For each tonne of beer, between 4.7 to 20 tonnes of water is required for production. Of the water used, about 3-10 tonnes becomes wastewater (WW) that needs to be treated (Abbasi and Abbasi, 2012). WW is generated from bottle washing, cleaning fermentation tanks, and packaging (Arantes *et al.*, 2017). This WW is generally very high in organic matter, represented by chemical oxygen demand (COD). The COD in the WW is mainly comprised of ethanol, sugar, and starch left over from the brewing process. There are also phosphorus, nitrogen, and volatile fatty acids (VFAs) (Simate *et al.*, 2011). Given that between half a billion and almost two billion tonnes of brewery WW are produced annually, brewery wastewater is a vital waste stream that needs to be addressed. Though relatively old technology, up-flow anaerobic sludge blanket (UASB) anaerobic digesters are ideal for dealing with this WW and are commonly used to treat brewery WW.

Developed in the 1970s, the UASB has grown in popularity recently (Mainardis, Buttazzoni and Goi, 2020). The UASB depends not on flocks but on granulated sludge, which is denser and tends to settle at a higher rate (Chen et al., 2021). The UASB can handle large COD loads but has some drawbacks. UASB's long start-up time and the slow formation of granules are some of its biggest problems (Rajagopal et al., 2019). Pre-seeding the UASB with already granulated biomass has shown that it can greatly decrease start-up times (Rajagopal et al., 2019). The main advantage of the UASB is the production of biogas for energy recovery, which allows for a sustainable solution to the treatment of brewery wastewater (Passos et al., 2020). Though the initial investment of time and budget is one disadvantage, once the UASB is operative, it is a very stable and reliable system for treating brewery WW and generating biogas. This system can catastrophically fail when overloaded or exposed to toxic chemicals.

Though very efficient, the UASB's stability is paramount. Many different factors can contribute to instability or failure. The major stability indicators are biogas production, pH, VFAs, and COD removal rates (Wu et al., 2019). Monitoring these indicators can be time-

Chapter 3: Monitoring Anaerobic Digestors with Biosensors

consuming and not have the required fidelity to determine whether the UASB will collapse or is in the process. pH is essential when considering the health of UASB (Tomei and Garrido, 2024). There may be stable pH in the reactor and influent, but there could still be a problem in the UASB. The COD removal rate is another good indicator of the health of the UASB, but it is slow to react to an imminent problem (Wu et al., 2019). The COD removal rate can show the problem clearly (Li et al., 2018) but may show the problem days after the initial event, which causes instability. Novel technology based on METs can resist many of these problems and produce stable systems that can treat WW under stress.

METs have already been applied to treating brewery WW compared to conventional anaerobic digestion (Asensio, Llorente, Fernández, et al., 2021). A microbial electrochemical fluidized bed reactor (ME-FBR) and an anaerobic fluidized bed reactor (AFBR) were tested. The two reactors were tested for resilience to organic matter overloading, the presence of a biocide, starvation, and operation at low temperatures. In all cases, the ME-FBR outperformed the AFBR. In this case, it is interesting that the ME-FBR maintained its COD and total nitrogen removal rates in the presence of a biocide (Asensio, Llorente, Fernández, et al., 2021). This stability shows that METs can function in the brewery WW environment and when exposed to biocide. METs may also be used to detect biocides in the brewing process.

Sterilization is a constant part of the brewing process. The fermentation vessels, cans or bottles, tubes, and hoses must be sterilely maintained. This process uses many different biocides, lubricants, and physical processes like heat or UV. Chemical additions like biocides can cause major problems for the stability of the UASB. Using microbial-based biosensors is a novel way to detect these agents and protect the stability of the UASB. The microbial-based biosensor has a unique ability to monitor the health of the microbes in the UASB. The biosensor is based on a three-electrode microbial electrolysis cell (MEC). The biosensor has a working electrode or anode where microbes can grow using the anode as an electron acceptor. Then, a reference electrode was used to control the poise of the working electrode and, finally, a counter electrode or cathode to close the circuit (Fig. 1).

Chapter 3: Monitoring Anaerobic Digestors with Biosensors

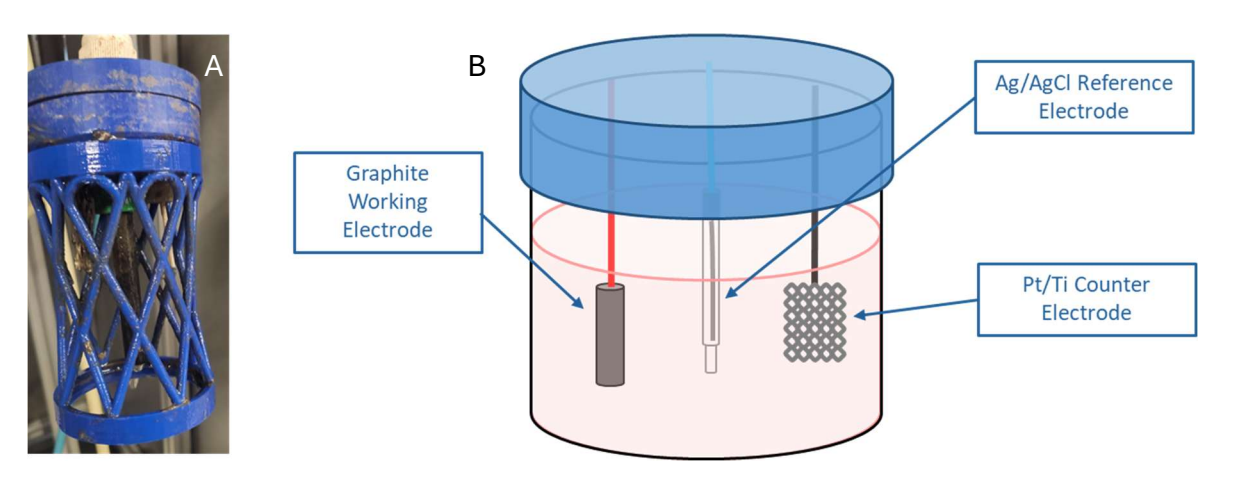


Figure 1: A) The three-electrode biosensor used in the study. B) Biosensor diagram, poised at 0.2 V versus Ag/AgCl

Previously, biosensors using a two-electrode microbial fuel cell configuration (MFC) have been used to monitor organic matter concentrations in wastewater (Di Lorenzo *et al.*, 2009; Salvian *et al.*, 2024). It has been shown that the cell voltage of biosensors integrated into constructed wetlands closely correlates to COD concentration (Corbella *et al.*, 2019a). This correlation allows the biosensor to monitor the health and efficiency of the wetland. When COD increases, it produces a signal within the biosensor informing operators of a problem with the wetland.

An MEC-based biosensor was previously used to monitor VFAs in the effluent of an anaerobic digestor (Li *et al.*, 2018). The systems have been reliably shown to detect the concentration of organic matter (Estevez-Canales *et al.*, 2015). Differentiating concentrations or turnover rates of organic matter through monitoring the rate of use of a terminal electron acceptor, in this case, the anode of the system correlates directly with the microbial metabolism of the biofilm on the anode (Estevez-Canales *et al.*, 2018). So, any inhibition of that metabolism could be a sign of the presence of a toxin.

Many examples of microbial electrochemical biosensors are being used to detect organic matter concentration, which can be used as a proxy for the health of the UASB and other wastewater treatment processes. This study shows that a three-electrode biosensor can detect changes in the COD concentration of the effluent of UASBs and possibly detect biocides that may cause a UASB to collapse.

2 - Materials and Methods

2.1 - UASB Operation

Two identical UASB reactors were used in a temperature-controlled cabinet at 35°C. The total volume of the UASBs was 1.3 liters. Recirculating flow was maintained such that 50%

of the UASB volume was occupied by fluidized granular sludge. All UASB were inoculated with 40 g/L total solids, equaling about 340 grams of sludge. They were fed at an organic loading rate (OLR) of 0.75 g/(L*Day) and a hydraulic retention time of 24 hours or a 54 mL/hour flow rate. The WW would average 750 mg/L COD, 15-20 mg/L total nitrogen, 3-5 mg/L total phosphorus, and influent would be maintained at a pH of 7.5 by a pH dosing pump (Blue Labs, London, UK). Many different biocides were tested, but this study focuses on three biocides to concentrate on the biosensor study. In testing the three biocides, one UASB was used as a control while the other was exposed to said biocide. The biocides herein will be referred to as biocide 1, 2, or 3 due to nondisclosure agreements (NDA). The manufacturer and product names are confidential. The reactors were fed with real WW from a brewing facility. This WW is the same as would feed an anaerobic digester from a larger commercial brewery. Granular sludge was used from a full-scale anaerobic digester. Overall, the testing conditions and operating parameters are summarized in Figure 2.

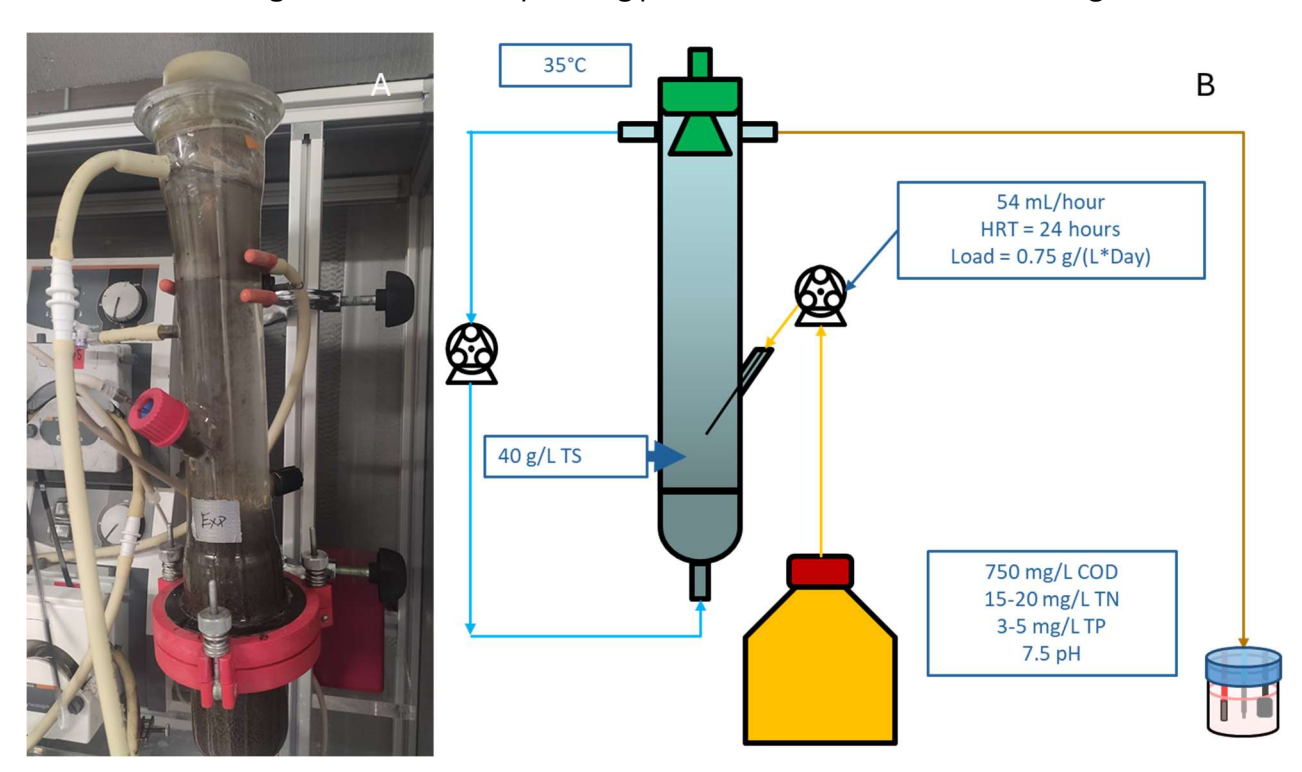


Figure 2: A) photo of the lab scale UASB in the temperature control cabinet. B) Diagrams of the UASB and biosensor with the conditions and operating parameters of the UASB.

After inoculation, the UASBs were run until a steady-state COD removal (12-15 mg COD*D day -1*mg TS⁻¹) rate was reached, which took 5-12 days. After reaching the steady state, the experimental UASB was exposed to the biocide being tested by adding it to the WW feedstock. Biocide 1 used fatty acid soap as the active ingredient, whereas 2 and 3 used an alkyl diamine based surfactant. The biocides were administered at 0.022% or 1.1 ml per 5

liters of WW. Samples were taken daily to determine the COD removal rates. The control was not subjected to biocide but fed the same WW as the experimental UASB.

2.2 - Bioelectrochemical sensor

The biosensor used was a commercial unit provided by Nanoelectra SL (Madrid, Spain) (Fig. 1A). The biosensor operated as a MEC and consisted of a graphite working electrode, a gel-based Ag/AgCl reference electrode, and a platinized titanium counter electrode (Fig. B). The biosensors were poised at 0.2 V vs the Ag/AgCl reference using a Nev 4 potentiostat (Nanoelectra SL, Madrid, Spain). The working electrode was allowed to colonize from the effluent of the UASB for 3 months before testing began. The biosensor was housed in a 400 ml cylindrical container directly fed by the effluent of the UASB.

2.3 - Analytics

COD was determined by photometric analysis (Hach LCI cuvette tests and Hach DR 3900 spectrophotometer). The media's conductivity was measured as previously described (Borjas et al., 2015). Total nitrogen, phosphorus, and VFAs were also measured using photometric analysis (Hach LCI cuvette tests and Hach DR 3900 spectrophotometer).

3 - Results and Discussion

3.1 - Impact of Natural and Synthetic Biocides on UASB bioreactor performance

The first biocides tested were natural and synthetic biocide. The natural biocide was soap-based, but the synthetic was surfactant-based. First, the biocides were run separately vs a control. After the initial tests, the two biocides were rerun in parallel to confirm their activity. Over all of the tests, the total nitrogen, total phosphorus, and total volatile fatty acids did not fluctuate in any significant manner. Biocide 1 was a natural product and did not negatively affect the ability of the UASB to remove COD (Fig. 3)

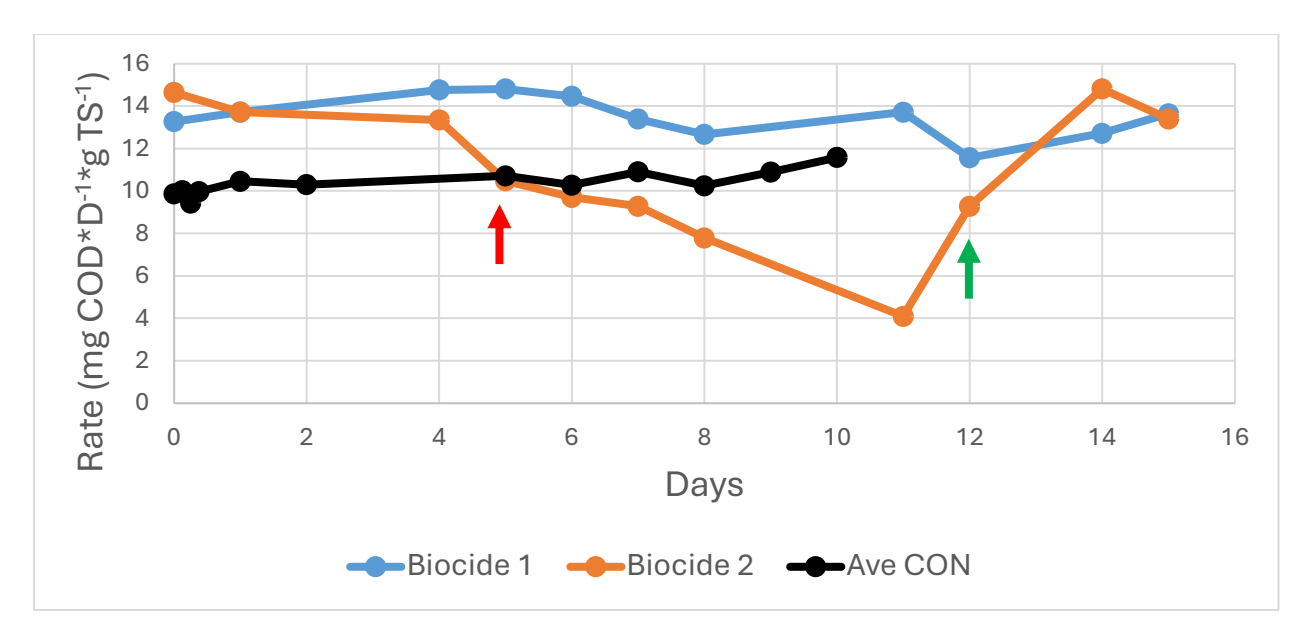


Figure 3: The removal rate of COD of anaerobic digestors over time after exposure to biocides. The red arrow denotes when the reactor started to have complications from the biocide. The green arrow denotes the cessation of biocides on day 12. Control represents an average of the multiple control UASBs during the biocides' initial round of testing, which did not operate for longer than ten days.

Over 15 days, the UASB exposed to biocide 1 had a removal rate averaging 14 mg COD*day⁻¹*mg TS⁻¹ (±0.3) as compared to the averaged biocide-free control of 10 mg COD*day⁻¹*mg TS⁻¹ (±0.3). Thus, biocide 1 did not affect the UASB's ability to remove COD. In contrast, biocide 2 had a definite negative impact on the ability of the UASB to remove COD. The UASB showed a lower removal rate per biomass unit and a loss of over half of the total granulated sludge. There was no apparent effect on the specific removal rate until after day 4. At this point, the COD removal rate drops precipitously. The overall loss of COD removal rate was 10 mg COD*day -1*mg TS⁻¹. The biocide exposure was stopped on the twelfth day (Fig. 3, green arrow), and the UASB recovered by the 14th day. Though the COD rate appears to recover on the day of biocide cessation, full recovery is not achieved until the biocide is completely washed out of the reactor.

The UASB can be very stable when operated under strict and specific conditions. Variables like OLR can be very high but must be changed slowly over time. Events that can cause severe damage and even collapse are sudden changes in pH (Tomei and Garrido, 2024). or salinity (Muñoz Sierra et al., 2019). Surfactants have been shown to have a similar effect as salinity. The surfactant can inhibit methane production and fundamentally disrupt granular sludge structure (Pérez-Armendáriz et al., 2010). Though biocide 2 was detected through monitoring COD removal rate, it was not detected until after it had damaged more than half of the sludge. Therefore, a faster detection method is needed.

3.2 - MEC Biosensor Monitoring Effluent COD

A MEC biosensor was installed in the UASB's effluent to monitor variations in the current in the absence or presence of a toxic compound (Fig. 2). It was observed that, in the absence of biocide, COD values followed the same trends as the current produced in the biosensor (Fig. 4)

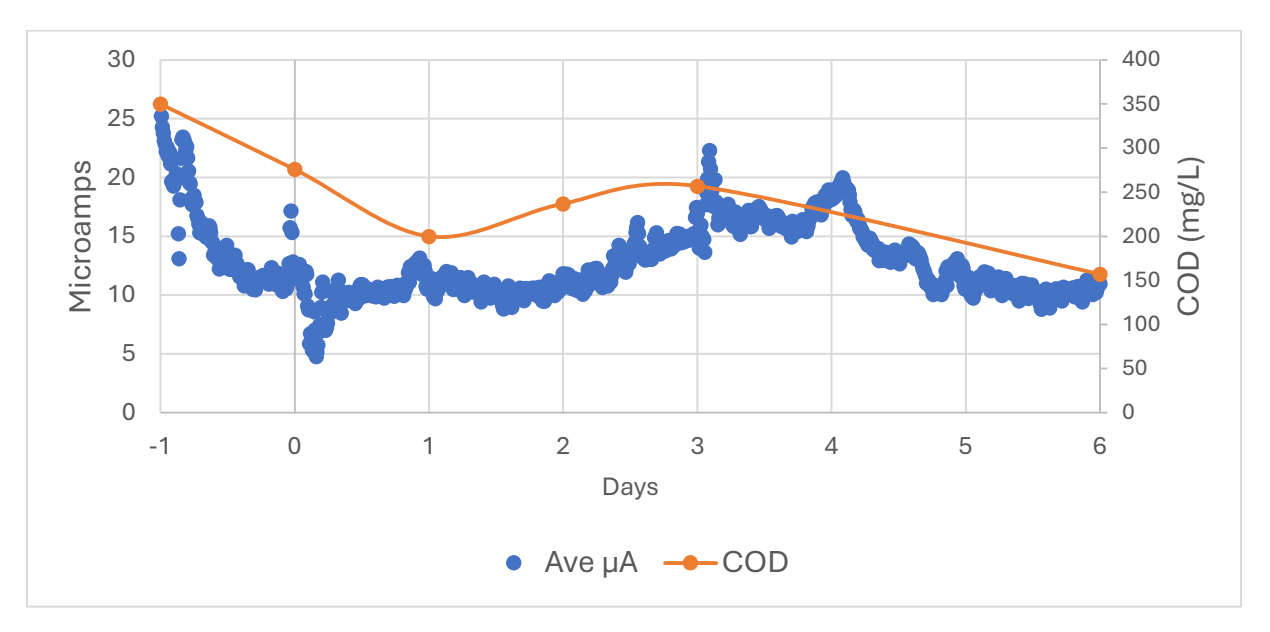


Figure 4: Average current produced (10 seconds) by the biosensor on the left axis (blue line). COD concentration on the right axis (orange line).

As the COD decreases, so does the current, and vice versa. The current and COD have a positive correlation with a correlation coefficient of 0.85 and an R² of 0.72. These correlations are not as strong as in previous laboratory studies (Di Lorenzo *et al.*, 2009; Salvian *et al.*, 2024). However, they are not greatly different from more realistic or pilot-scale applications (Corbella *et al.*, 2019a). The installation of the biosensors in this study was purposefully done in such a way as to mimic a more industrial application to determine their efficacy for potential commercial use. This application and low COD concentrations(Gao *et al.*, 2021) may have also affected the signal's noise level. Furthermore, these biosensors were located in the USAB effluent, where most of the biodegradable pollutants had already been metabolized. Therefore, the available organic matter may have been more recalcitrant than in previous studies, which could further explain noise in the signal and the decrease in correlation statistics (You *et al.*, 2015).

3.3 - Biocide Effect on the MEC Biosensor

A third biocide was applied to test the biosensor's ability to detect a surfactant-based toxin. Biocide 3 was used in the same manner as the first two biocides. Biocide 3 showed negative effects after 5 days of exposure (Fig. 4).

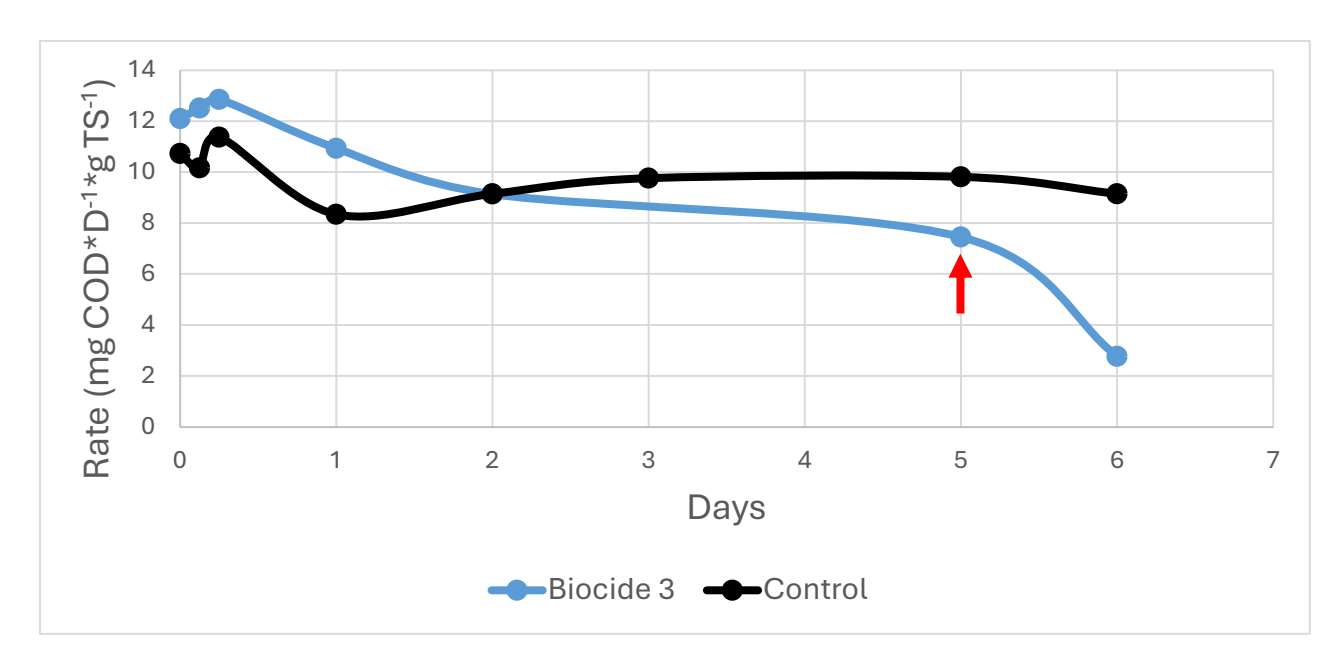


Figure 5: Shows the change in COD removal rate after being exposed to Biocide 3 at day zero. The red arrow denotes where the biocide started negatively affecting the reactor's COD removal rate.

On the 7th or 8th day of exposure, the sludge in the UASB had liquefied entirely. By the time the problem was detected, it may have been too late to stop the collapse of the UASB. The biosensor can indirectly monitor the health of the microbes in the UASB. The current produced by the biosensor acts as a signal indicating the presence of toxic pollutants in the UASB (Fig. 5).

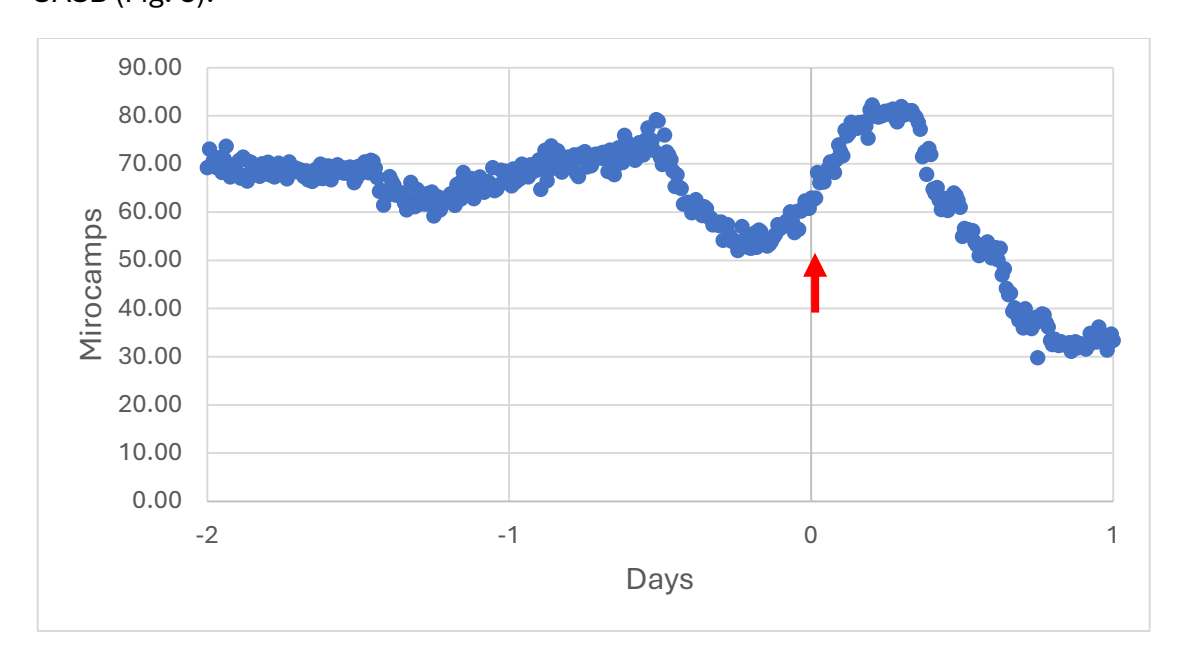


Figure 6: Exposure to the biocide started at day 0 (Red Arrow). Shortly after, the current dropped precipitously.

Figure 6 shows the biosensor's signal in microamps. Day 0 is the starting day of the exposure for UASB to biocide 3. Before exposure, the electrical current production averaged 66 microamps (±5.7*10⁻⁶). The UASB had a hydraulic retention time of 24 hours. This retention time would lead to a delay in the biocide's ability to affect the biosensor. Therefore, it would take time for the concentration of biocide in the effluent to reach a point where it affected the biosensor or approached the levels in the influent. Indeed, after about 6 hours, the current dropped rapidly. In less than 24 hours, it had fallen by over half to 31 microamps.

As mentioned previously, the COD concentration in the effluent was low (c.a. 210 mg/L), which can reduce the current and increase the noise or fluctuation of the signal. While the disturbance at the time of biocide exposure is more prominent than others seen in the chronoamperometry (CA) presented, it has less than half of the magnitude seen in the signal loss after biocide exposure. Furthermore, unlike the previous response seen without biocide present (Fig. 4) there is not an increase in current production when there is an increase in COD in the effluent (Fig. 5). As the specific removal rate decreases, it causes an increase in the available COD or organic matter to the biosensor. Therefore, one would expect the current production or signal to increase as the COD concentration increases. However, this is not what is happening to the current or signal. Instead, there is a decrease in current, revealing the biocide's negative impact on the biosensor's electroactive biofilm.

Previous MFC-based biosensors have shown decreases proportional to damage when dealing with alum-based flocculation (Li *et al.*, 2016). Biofilm-based biosensors, whether MFC or MEC, are sensitive to surfactants. While surfactants at low concentrations can increase current production by increasing the bioavailability of organic matter, as concentrations rise, they can have inhibitory effects (Pérez-Armendáriz *et al.*, 2010). In the cited case, the surfactant-based biocide had a clear negative impact on the granular sludge and a sufficient effect on the biosensor for it to be detected quickly.

4 - Conclusions

The literature has shown that MFC and MEC biosensors can detect changes in COD and BOD. COD is a key indicator of a UASB's health. This study has shown that the MEC biosensor can be used to determine changes in COD concentration when treating brewery wastewater in a UASB. These changes can be used to evaluate the performance of UASB in real time. Furthermore, the biocides tested had differing effects on the ability of UASB to remove COD. The natural biocide had no impact on the operation or ability to remove the COD of the UASB. The synthetic and surfactant-based biocides had negatively affected the COD removal rate. The effects of biocide 2 and 3 took days to manifest using conventional

Chapter 3: Monitoring Anaerobic Digestors with Biosensors

UASB monitoring techniques. Both biocides did not affect other indicators like pH or VFAs. The biosensor detected the presence of the biocide much more quickly than conventional methods but may need further testing given the frequency of signal disturbances. The noise generated in the signal could be due to a lack of sufficient isolation of the biosensor, the low concentration of organic matter, or the recalcitrant nature of the organic matter in the treated brewery wastewater.

Further tests should be conducted to corroborate these results and give a more robust definition of what level of disturbance qualifies as an event to take mitigating action without prior knowledge of said event. Furthermore, placing a biosensor in the influent line may reduce the USAB's exposure time to the toxic effects of a biocide by earlier detection. The influent biosensor would also allow for monitoring of the influent COD and OLR, which can affect the USAB's health. This combination of biosensors could act as an early warning system to bypass contaminated WW and monitor the digestor's performance. These biosensors by Nanoelctra SL could be used to determine a UASB's performance and help prevent damage to the system.

Chapter 4:

Electrochemical Biofilters Treating Hydrocarbon Wastewater

Designing hybrid configurations in electrochemical biofilters for treating hydrocarbon-contaminated water

1 - Introduction

Hydrocarbon (HC) contaminated wastewater (WW) is a constant byproduct of oil production, refinement, and industrial activities such as machining, automotive production, and repair. From 2008 to 2018, global oil consumption increased by 13.3 million barrels daily, leading to a daily output of 94.7 million barrels (BP, 2019). Produced water (PW) is often heavily contaminated with hydrocarbons, organic matter, and nitrogen compounds. Though produced water can be hard to treat due to high concentrations of phenols, salts, and other toxic compounds, it is not the only wastewater produced in oil extraction and refinement. For every barrel refined in a petrochemical plant, 246-341 liters of water is used (Alva-Argáez, Kokossis and Smith, 2007). That means the contaminated wastewater produced is between 0.4 and 1.6 times the oil refined (Coelho et al., 2006). The need for cheap, efficient technology to clean wastewater has never been more critical. Water consumption is even more vital in water-starved regions where many top oil producers are located (Fakhru'l-Razi et al., 2009). The focus here is on treating HC-contaminated WW by biological activity, specifically COD removal and nitrification.

Physiological processes are required before the biological treatment of the PW or petroleum refinery wastewater (PRW). Here, heterogeneous and non-soluble wastewater fractions must be removed, like suspended solids, polar oils, and particles (Renault et al., 2009). This separation is achieved through oil-water separation, equalization, coagulation, flocculation, and floatation (Diya'uddeen *et al.*, 2011). These steps are essential to maintain the efficiency and viability of the microbes in biological treatment.

After primary treatment, soluble contaminates, like emulsified oils and alkanes, must be removed, and several different conventional wastewater treatment solutions can be used. Aerobic activated sludge (AAS) systems use large aeration tanks to mix incoming wastewater with a granulated activated sludge that can biologically remove HC contaminants. Sludge separates from the treated WW in clarifiers (Haandel and Lubbe, 2012). Like the AAS, the sequencing batch reactor (SBR) utilizes activated sludge but

completes the process of WW influent treatment by activated sludge, clarification, and decantation in a single reactor. The SBR has the advantage over AAS because it completes the entire treatment in a single reactor (Jafarinejad, 2017). However effective, these processes are highly intensive for energy, chemical usage, and reactor maintenance costs (Kadlec and Wallace, 2001). These costs can be mitigated using less compact and less cost-intensive systems like biofilm-based reactors.

Unlike the AAS and SBR, the biofilm-based reactor (BBR) uses biofilms attached to a matrix that allows WW to flow through it. The high surface area of the matrix provides for a large amount of contact between the biofilm and the WW. In this way, the biofilm's microbes can treat the WW through organic matter or HC removal. Examples of BBRs used to treat HC WW include treatment wetlands (Czudar *et al.*, 2011), fluidized bed bioreactors (Schneider, Cerqueira and Dezotti, 2011), moving-bed biofilm reactors (Yan, Feng and Liu, 2024), and fixed bed reactors (Patel and Madamwar, 2002).

In recent years, a novel strategy called electrobioremediation has emerged in the field of environmental bioremediation (Wang *et al.*, 2020). The newborn concept uses electrochemistry to stimulate the activity of electroactive bacteria (EAB) for cleaning up polluted environments like water, soil, and sediments (Tucci *et al.*, 2021). Among the different technologies tested in the last decade, the only one that reached full scale was METland technology (Aguirre-Sierra, Bacchetti-De Gregoris, Antonio Berná, *et al.*, 2016; Esteve-Núñez, 2025), a hybrid context after merging treatment wetlands with *snorkel* electrochemical configuration (Erable, Etcheverry and Bergel, 2011). Thus, a new type of electrochemical fixed bed reactor made of a single electroconductive network was proven to boost electroactive bacteria for degrading organic pollutants from urban wastewater both under anoxic (Aguirre *et al.*, 2016) and passive-aerated conditions (Aguirre *et al.*, 2020). The sustainability of the system was demonstrated by multi-criteria evaluation, sensitivity analysis, and life cycle assessment (Peñacoba-Antona *et al.*, 2021; Peñacoba-Antona, Gómez-Delgado and Esteve-Núñez, 2021) and full scale was validated in both different Mediterranean and Northern European latitudes (Peñacoba-Antona *et al.*, 2022a).

The rationale of microbial electrochemical-assisted treatment wetlands, or METlands, is mainly based on boosting conductive-mediated interspecies electron transfer (Rotaru, Yee and Musat, 2021) and letting electrons flow from anodic regions (oxidative reactions) to the cathodic areas (reductive reactions). Such electron flow was demonstrated by monitoring the electric potential profile along the bed (Ramírez-Vargas et al., 2018; Prado de Nicolás, Berenguer and Esteve-Núñez, 2022; Wei, 2024), including the impact on METland's performance. Indeed, new strategies for controlling such electron flow were also reported, including the electron sink concept (Prado et al., 2020). Beyond organic pollutants from

urban wastewater, the METland has also shown the ability to remove more recalcitrant contaminants like pharmaceuticals (Pun, Boltes, Letón, Esteve-Nuñez, *et al.*, 2019; Pun *et al.*, 2025) and surfactants(Noriega Primo, López-Heras and Esteve-Núñez, 2024).

The METland concept has since been effectively applied at full scale to treat urban and industrial wastewater (Mosquera-Romero *et al.*, 2023) at differing latitudes, showing the strength and versatility of this treatment process. This ability can break down compounds as complex as pharmaceuticals could be applied to other complex compounds, like HC-contaminated WW. In the current study, the electroremediating ability of the METland inspired the design of a novel configuration for electroactive biofilters to clean up synthetic hydrocarbon waste streams mimicking those from an oil refinery.

2 - Materials and Methods

2.1 - Reactor Designs

All the reactors are based around a PVC cylinder with a 12 cm diameter and a total height of 41 cm. The biofilter comprises a bed with a 2-3 mm granularity provided by METfilter S.L. (Spain). All electroconductive material used in these reactors has been described previously (Aguirre-Sierra, Bacchetti-De Gregoris, Antonio Berná, et al., 2016).

2.1.1 - Anaerobic-Aerobic Hybrid Biofilter

The Anaerobic-Aerobic Hybrid (AAH) Biofilter consists of two bed types: anaerobic and aerobic. The AAH biofilter has a carbon fiber tube in the center of the PVC reactor cylinder. The central carbon fiber tube (5 cm x 50 cm) was packed with electroconductive bed material (1 L). The central tube is saturated to create an anaerobic environment. The space between the central tube and the PCV reactor housing is similarly packed but is unsaturated to create an aerobic bed (4L). The flow of WW starts at the bottom of the anaerobic bed. It overflows the tube to be evenly distributed through a perforated distribution plate (Fig. 1). The WW flows through the aerobic bed to exit the reactor through a perforated plate. The main PVC housing has a diameter of 12 cm, and the central carbon fiber tube has a diameter of 5 cm. The overall length of the PVC housing is 41cm, and the central tube is 50 cm.

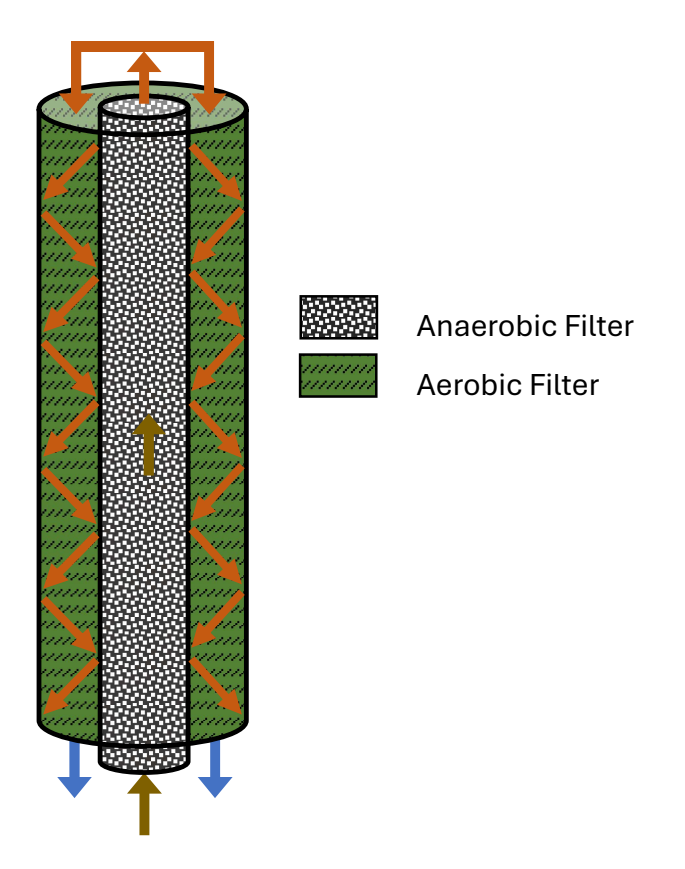


Figure 1: Schematic of the Anaerobic-Aerobic Hybrid Reactor showing the differing anaerobic and aerobic areas and route of media flow.

2.1.2 - Multi-Phase Hybrid Bed Biofilter

The Multi-Phase Hybrid Bed (MPHB) biofilter has a centrally located carbon fiber tube with the same dimensions as the AAH (5 cm x 50 cm). The flow of water follows the same schematic as the AAH. WW enters the central tube through the bottom, overflows the top to a distribution plate, and enters the surrounding bed. The difference in operation comes about halfway through the aerobic bed. The MPHB has a saturated bed section about halfway through the surrounding bed. This saturation created three bed sections: an anaerobic upflow section (1L), an aerobic downflow section (1.7 L), and a final anaerobic downflow section (1.8 L) (Fig. 3). There is a port for pumped aeration in the aerobic section.

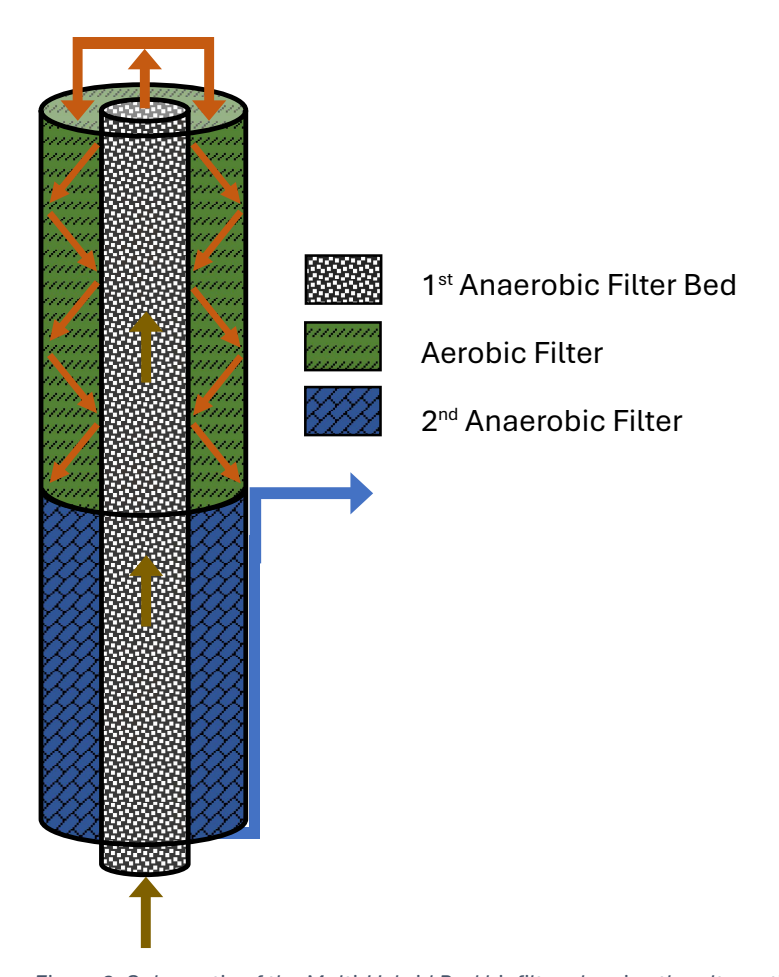


Figure 2: Schematic of the Multi-Hybrid Bed biofilter showing the alternating anaerobic, aerobic, and anaerobic areas and route of media flow.

2.1.3 - Hybrid E-sink Biofilter

The Hybrid E-sink Biofilter (HEB) was run downflow (Aguirre-Sierra *et al.*, 2020) with a total volume of 4.2 L of electroconductive material. The reactor was divided into two regions. The first, from the point of influent, was passively aerated (2.2 L). The second region was flooded and anaerobic (2.0 L). In the center of the bed was a 3 cm diameter by 50 cm carbon fiber tube (Fig. 3). This tube acted as an e-sink, and it was built (Prado *et al.*, 2020) to specifications similar to those of (Prado *et al.*, 2020). In brief, the bottom half (25 cm) of the e-sink had ion exchange membranes for the free flow of ions from the bed to the interior of the e-sink. The top half of the e-sink was perforated with 2 mm holes to allow for the exchange of gases with the aerobic bed. The bottom of the e-sink was sealed with a butyl stopper, and the bottom half was filled with MilliQ water (Millipore Sigma, USA). Air was supplied to the interior reservoir of the e-sink through an aquarium-style air stone and air pump. When used, an extra supply of pumped aeration was added through a PPE Luer-lock fitting in the side of the reactor just above the waterline. Again, an ordinary aquarium air pump was used.

Chapter 4: Electrochemical Biofilters Treating Hydrocarbon Wastewater

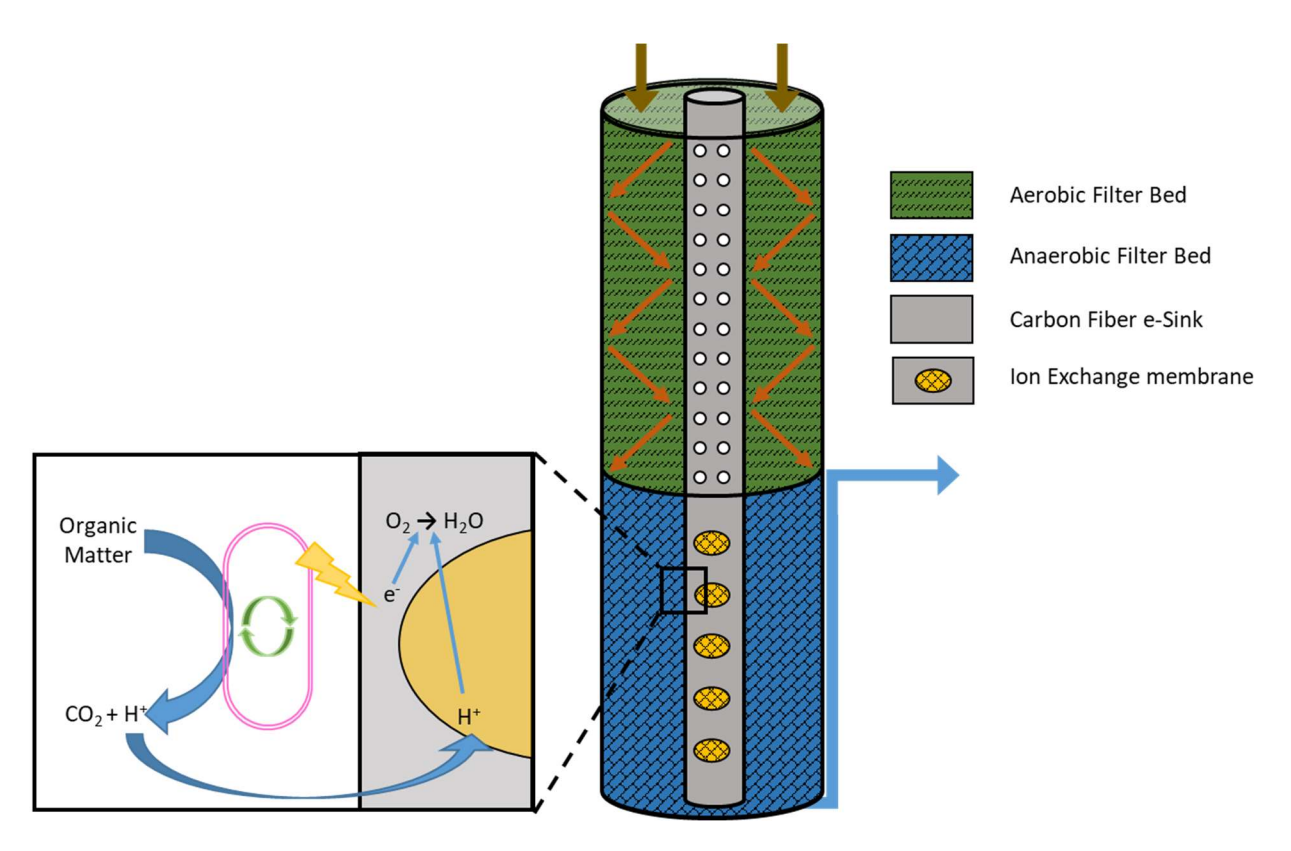


Figure 3: Schematic of the Chimney Hybrid Bed showing the differing aerobic and anaerobic areas and route of media flow. The model of the e-sink's function.

2.2 - Reactor Operation

2.2.1 - Synthetic Wastewater

All the reactors were fed with the same synthetic HC WW designed to mimic a waste stream from an oil refinery. The HC WW minimal media base contains 740 mg*L-1 NaCl and 350 mg*L-1 NaHCO₃. The contaminates of interest were nitrogen, emulsified oils, alkanes, and alkenes. Ammonia chloride was used to represent nitrogen, cutting oil (Multisol, Rocol) was used for emulsified oil, and automotive gasoline was used for alkanes and alkenes. Different combinations of the contaminants of interest were tested in the reactors. These combinations produced COD ranges from 130 to 500 g/m³*day and N-NH₄ from 7 to 30 g/m³*day. The ratio of cutting oil to gasoline was ca. 1:4.

2.2.2 - Operational Modes

All three reactors were inoculated with biological material from an aerobic hydrocarbon wastewater reactor and urban wastewater. The reactors were operated under different loading rates and operational modes to explore the limits of the reactor designs. Both flow rate and contaminant concentration were used to control the loading rate. The maximum new media introduced in one day was 1 L. The variable application of recirculation would

create flow rates of between 1 and 3 liters per day. Differing operational modes were tried. These include the application of pumped aeration (HEB & MPHB), recirculation (all reactors), and the bypass of fresh WW (HEB). When recirculation was used, the effluent was directly mixed with influent at the point of entry for the AAH and MPHB, whereas for the HEB, a mixing tank of 200 ml was used.

2.3 - Chemical Analysis

All the different operational modes were allowed to reach a steady state before any sampling regime was undertaken. Sampling regimes were at least two weeks to a maximum of 3 months. Depending on the system's flow rate, samples were taken 3-5 times weekly. All samples were analyzed for HC concentration (COD) and soluble nitrogen species (N-NH₄, N-NO₂, & N-NO₃). Samples were taken from the influent, effluent, and at any bed transition. COD was determined by photometric analysis (Hach LCI cuvette tests & Hach DR 3900 spectrophotometer). Ammonia (N-NH₄), nitrite (N-NO₂), and nitrate (N-NO₃) were analyzed by ionic chromatography (Metrohm 930 Compact Ion Chromatograph Flex). All samples not measured during sampling were frozen at -20C for short-term storage. Removal efficiencies were calculated as such (Eq.1)

$$E = \frac{c_{in} - c_{eff}}{c_{in}} \times 100$$
 Eq. 1

Where the efficiency of removal (E) is the quotient of the difference between the influent concentration (C_{in}) and effluent concertation (C_{eff}), and the influent concentration, multiplied by 100, Eq. 1 produces a unitless percentage. Removal (R) and loading (L) rates are represented by Eq. 2 and Eq. 3, respectively.

$$R = \frac{\frac{g_{COD}}{d}}{m^3_{bed}} \times E$$
 Eq.2

$$L = \frac{\frac{g_{COD}}{d}}{m^3_{had}}$$
 Eq. 3

Where g_{COD}/d is the grams of COD entering the reactor per day, and m_{bed}^3 is the volume of bed material in cubic meters. All error bars represent standard error.

2.4 - Microbial Community Analysis

Bed material (50ml) was harvested in triplicate from the center of each section in all three reactors. In brief, DNA was extracted, the V3-V4 region of the 16S genes was amplified via PCR, and all samples were Illumina sequenced (DNA Sequencing Unit from Autonomous University of Barcelona, Spain)

3 - Results & Discussion

Three different configurations of electroactive biofilters were operated to maximize COD and nitrogen removal rates from synthetic HC-based WW.

3.1 - COD and Nitrogen Removal

3.1.1 - Hybrid E-sink Biofilter

The HEB was run using a variety of operating schemas. At its simplest, it was run in a downflow configuration (Fig. 4A). The reactor in this configuration had a loading rate of 134 \pm 5 gCOD/m³*day and 8.7 \pm 0.3 gN-NH₄ /m³*day. The HEB eliminated COD at a rate of 91 \pm 3.5 gCOD/m³*day. It nitrified at a rate of 2.4 \pm 0.2 gN-NH₄ /m³*day. Of this ammonia, 53% remained in the effluent as N-NO₃, meaning that the HEB denitrified 47% of the nitrified ammonia at a rate of 1.1 \pm 0.3 gN-NO₃ /m³*day. Next, the aerobic section of the bed was supplemented with air via pumping to increase nitrogen removal (Fig. 4B). A similar loading rate was used, 129 \pm 9 gCOD/m³*day and 9.5 \pm 0.1 gN-NH₄ /m³*day. This pumped aeration had a negligible effect on the COD removal rate (93 \pm 7.1 gCOD/m³*day). The greater effect was upon the ammonia removal rate at 3.9 \pm 0.4 gN-NH₄ /m³*day. Nitrification converted 63% of the N-NH₄ as N-NO₃ in the effluent, meaning the removal rate was 1.5 \pm 0.2 gN-NO₃ /m³*day. There is a limit to the denitrification ability of the filter, which may be linked to the readily available organic matter. An ideal C:N ratio of 4:1 is required for proper denitrification, but it is unknown what carbon was bioavailable after the aerobic section.

In this case, the following operational mode to try was to recirculate the effluent (Fig. 4C). A 2:1 recirculation to influent ratio was tested to maximize the removal of nitrogen and COD. This recirculation resulted in a loading rate of 165 ± 7 gCOD/m3*day and 8.9 ± 0.1 gN-NH₄ /m³*day. The recirculation had a negligible effect on the COD removal rate of 97 ± 5 gCOD/m3*day and decreased the overall nitrification rate to 1.3 ± 0.1 gN-NH₄ /m³*day. A hybrid strategy was designed to try to increase the removal of nitrogen further. In this case, the recirculation was decreased to 0.5:1, and 1/3 of the influent was directly bypassed to the anaerobic section of the bed. This way, the anaerobic bed could have fresh organic matter to denitrify (Fig. 4D).

Chapter 4: Electrochemical Biofilters Treating Hydrocarbon Wastewater

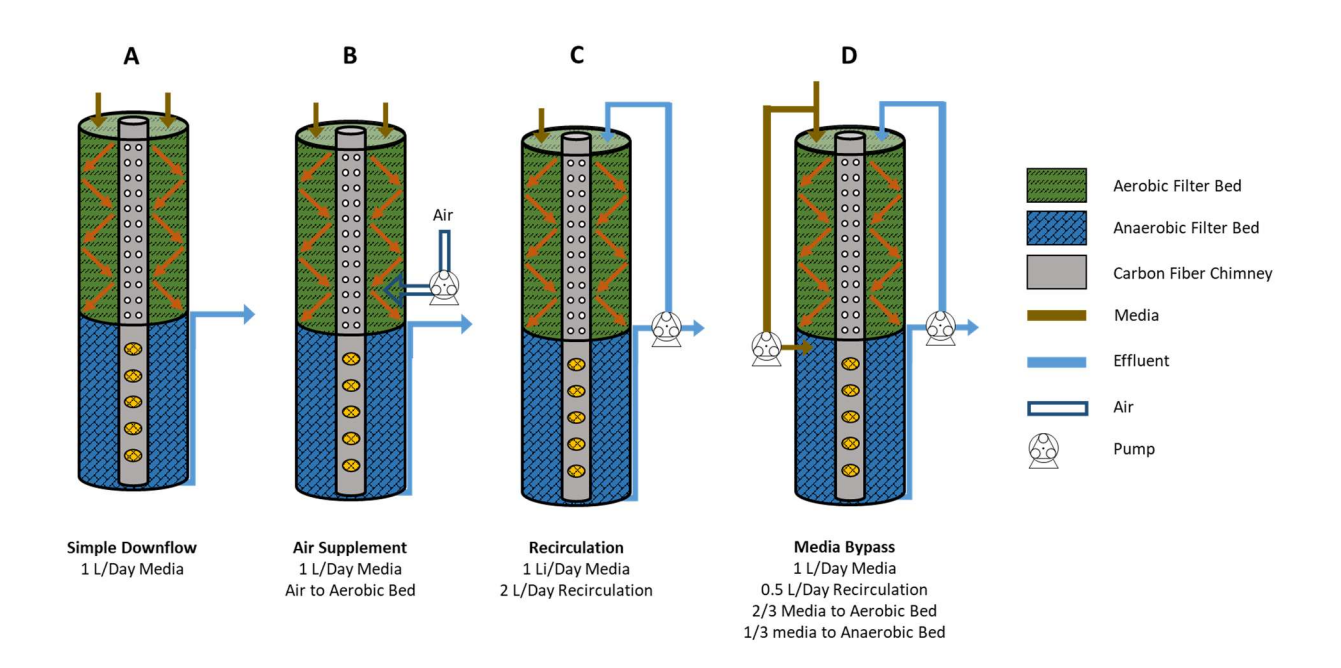


Figure 4: Operating conditions of the different tests run in HEB.

This operational scheme had a loading rate of 103 ± 5 gCOD/m³*day and 3.0 ± 0.3 gN-NH₄/m³*day. This scheme resulted in a COD removal rate of 74 ± 7 gCOD/m3*day rate. Furthermore, ammonia was nitrified at a rate of 2.9 ± 0.3 gNH₄-N/m³*day. The nitrification efficiency increased considerably, as did the denitrification, accounting for 28% of the initial nitrogen content, over a 2-fold increase. A novel design feature of the HEB is the esink device. This device produces a highly electronegative redox force in the system. The carbon fiber tube of the e-sink is conductive, allowing electrons to flow from the conductive filter bed to the interior of the e-sink. Inside the e-sink is oxygenated water, acting as an electron acceptor and pulling excess electrons out of the filter bed. Previous studies have shown that this process (Prado et al., 2020) increases the efficiency of urban wastewater treatment at a lab scale.

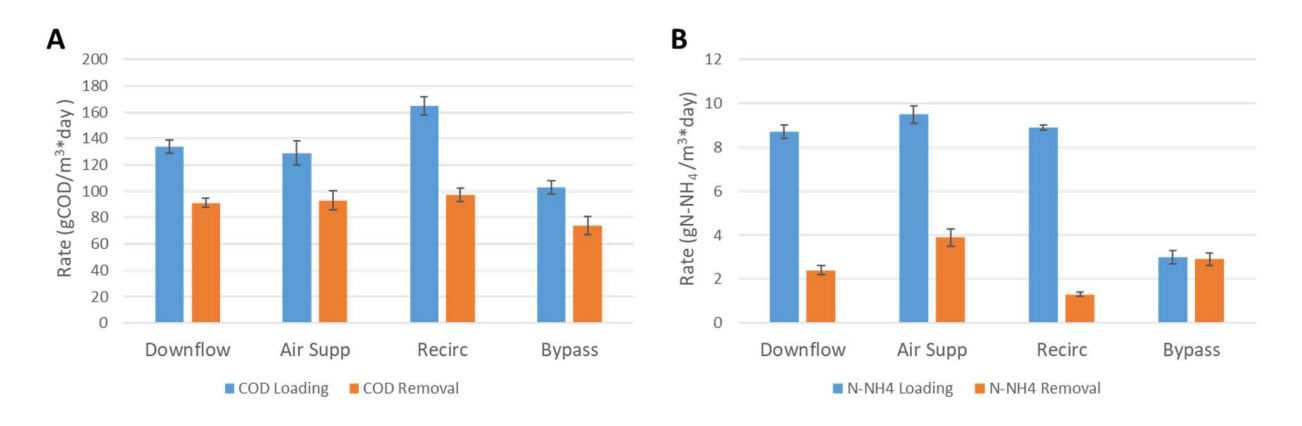


Figure 5: A) COD loading rates (Blue) vs. COD removal rates (Orange) for Downflow (Fig. 4A), Air Supp (Fig. 4B), Recirc (Fig. 4C), and Bypass in HEB. (Fig. 4D). B) N-NH₄ loading rates (Blue) vs N-NH₄ removal rates (Orange) for Downflow (Fig. 4A), Air Supp (Fig. 4B), Recirc (Fig. 4C), and Bypass in HEB. (Fig. 4D).

3.1.2 - Anaerobic-Aerobic Hybrid Biofilter

The AAH was run through experiments similar to the HEB. First, a simple upflow scheme (Fig. 6A) ran the system with a loading rate of $119 \pm 9 \, \text{gCOD/m}^3 \pm \text{day}$ and $7.4 \pm 0.1 \, \text{gN-NH}_4$ /m³*day. The AAH had a COD removal rate of $85 \pm 2.5 \, \text{gCOD/m}^3 \pm \text{day}$. This loading rate corresponded to a nitrification rate of $1.8 \pm 0.2 \, \text{gN-NH}_4$ /m³*day. There was no apparent denitrification present in the system. Unlike HEB, this lack of denitrification was expected because this system has the anaerobic section first proceeding to the aerobic. Nitrification requires the presence of oxygen to convert ammonia to nitrate. Ideally, this system would operate better with recirculation to have fresh organic matter with nitrate in an anaerobic stage. Thus, the system was tested with a 200% recirculation rate (Fig. 6B), resulting in a $198 \pm 7 \, \text{gCOD/m} 3^* \text{day}$ loading rate and $15.7 \pm 0.3 \, \text{gN-NH}_4$ /m³*day. With recirculation, the COD removal rate was $85 \pm 12 \, \text{gCOD/m} 3^* \text{day}$. This system seems to be limited in its COD removal abilities. This limitation can also be observed because the COD removal rate does not change with the flow and loading rate increase. This new mode of operation nearly doubled the nitrification rate to $3.7 \pm 0.4 \, \text{gN-NH}_4$ /m³*day but also doubled the gN-NH4 loading rate. The nitrogen removal by denitrification was still low, at only 5%.

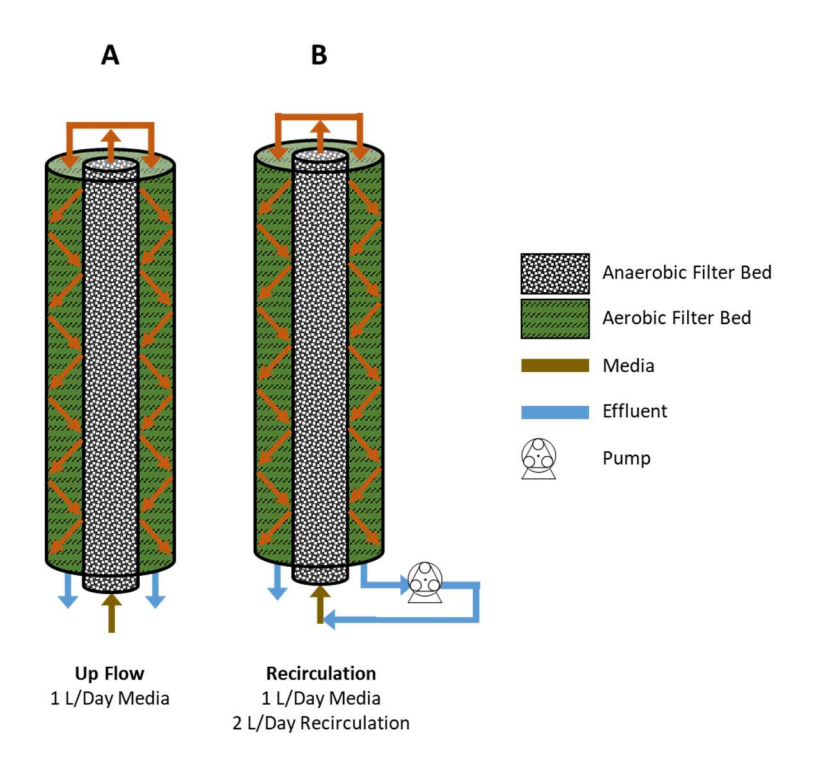


Figure 6: Operational schematic of the AAH for basic up flow (A) and 200% recirculation (B).

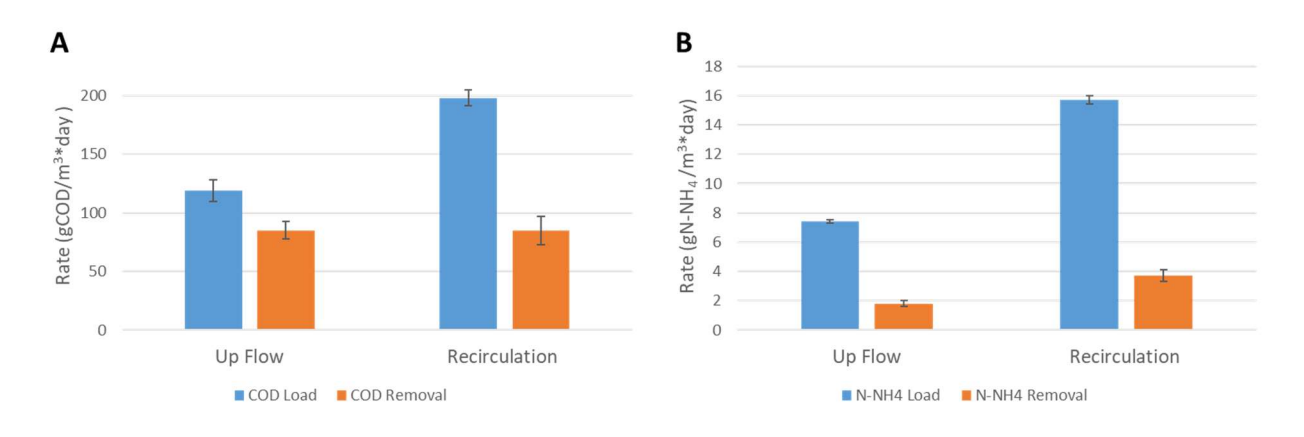


Figure 7: A) COD loading rates (Blue) vs. COD removal rates (Orange) for Up Flow (Fig. 6A) and Recirculation (Fig. 6B) in the AAH. B) N-NH₄ loading rates (Blue) vs N-NH₄ removal rates (Orange) Up Flow (Fig. 6A) and Recirculation (Fig. 6B) in the AAH.

3.1.3 - Multi-Phase Hybrid Bed Biofilter

The MPHB starts with an anaerobic section of the bed housed in a conductive carbon fiber tube. The WW exits the first anaerobic section and enters the surrounding bed between the central tube and the reactor housing. This bed's sections are divided into two sections in the same layout as the HEB, first with an aerobic section and a second anaerobic section. The idea is that the overall efficiency and removal rate can be increased by alternating between anaerobic and aerobic and then back to anaerobic.

The MPHB saw the highest average removal rates of the three reactor designs. The first experiment was run with a loading rate of $133 \pm 2 \, \text{gCOD/m}^3\text{*}$ day and $8.2 \pm 0.1 \, \text{gN-NH}_4$ /m³*day (Fig. 7A). The COD removal rate was $98 \pm 3 \, \text{gCOD/m}^3\text{*}$ day. As for nitrogen, the MHB could nitrify at $2.4 \pm 0.2 \, \text{gNH}_4\text{-N/m}^3\text{*}$ day. The MHB was able to denitrify 6% of the total influent N-NH₄. Following a strategy similar to HEB, excess atmospheric air was pumped into the aerobic bed to increase nitrification. This run had a loading rate of $115 \pm 6 \, \text{gCOD/m}^3\text{*}$ day and $8.5 \pm 0.5 \, \text{gN-NH}_4$ /m³*day (Fig. 8B). The added oxygen from the pumped aeration did increase the average COD removal rate to $104 \pm 6 \, \text{gCOD/m}^3\text{*}$ day. An increase in the nitrification with a removal rate of $3.4 \pm 0.3 \, \text{gN-NH}_4$ /m³*day. The total denitrification also doubled to 13%.

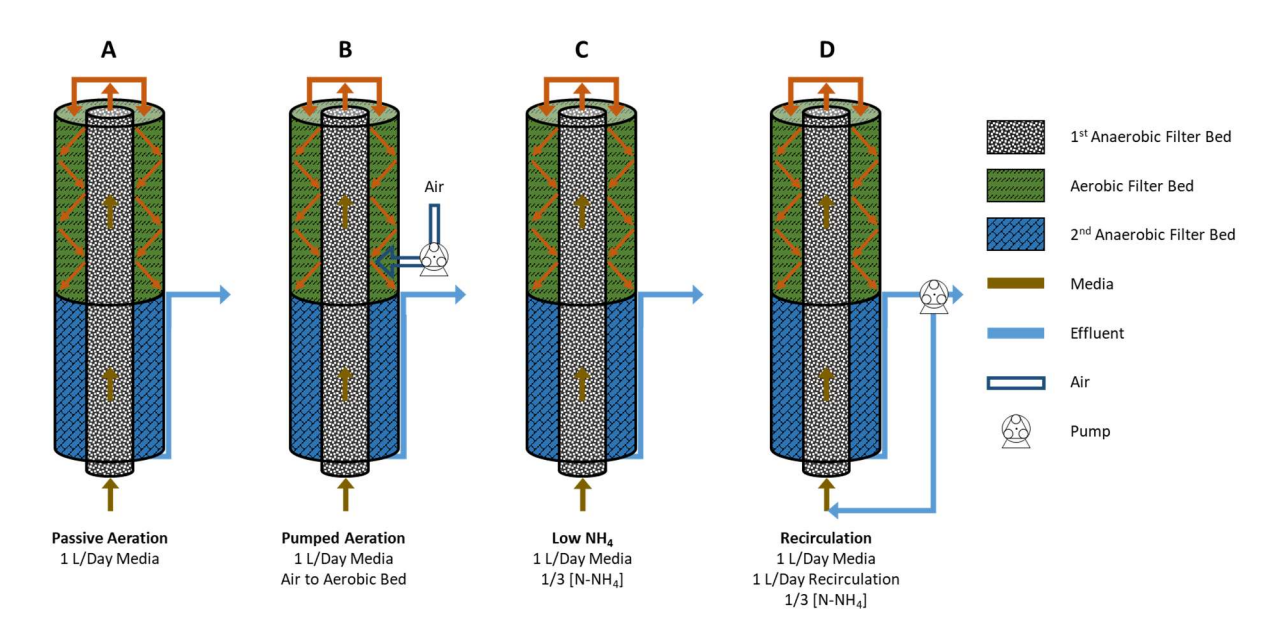


Figure 8: Operation schematics for MHB biofilter.

To increase the system's overall denitrification by altering the C:N, the nitrogen loading rate was decreased while maintaining the COD load (Fig. 8C). We ran the system under the same conditions but with a decreased concentration of nitrogen and a loading rate of $104 \pm 5 \text{ gCOD/m}^3$ *day and $3.1 \pm 0.1 \text{ gN-NH}_4$ /m³*day. The COD removal rate was slightly lower at $88 \pm 1 \text{ gCOD/m}^3$ *day. The biofilter could nitrify at a rate of $2.4 \pm 0.2 \text{ gNH}_4$ -N/m³*day. So, the nitrification efficiency increased by increasing the C:N ratio, but N-NH4 still remained. To try and increase nitrification further, the same higher C:N loading rate was used, but 100 percent recirculation was added. This recirculation effectively doubled residency time while maintaining the same flow of fresh media into the system. The loading rate was $57 \pm 5 \text{ gCOD/m}^3$ *day and $2.1 \pm 0.2 \text{ gN-NH}_4$ /m³*day. Again, it was about the same COD removal efficiency but about half the removal rate at $46 \pm 5 \text{ gCOD/m}^3$ *day. The nitrification rate decreased slightly to $2.1 \pm 0.3 \text{ gNH4-N/m}^3$ *day, but the biofilter removed all of the NH₄-N.

Chapter 4: Electrochemical Biofilters Treating Hydrocarbon Wastewater

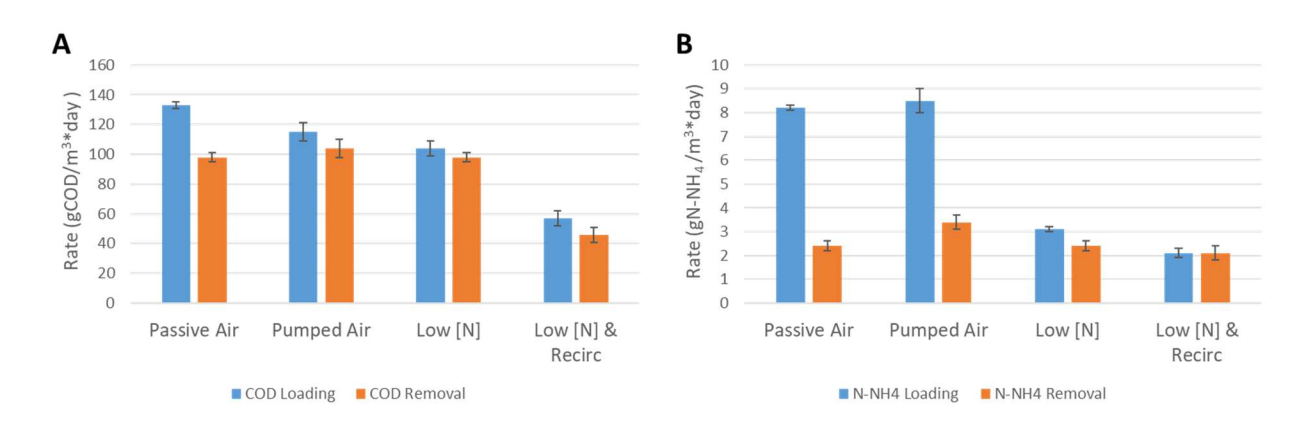


Figure 9: A) COD loading rates (Blue) vs. COD removal rates (Orange) for Passive Aeration (Fig. 8A), Pumped Aeration (Fig. 8B), Low [N] (Fig. 8C), and Low [N] & Recirc (Fig. 8D). B) N-NH4 loading rates (Blue) vs N-NH4 removal rates (Orange).

3.2 - Microbial Community Analysis

Given the austere nature of the media, low salinity, and hydrocarbons as the sole carbon source, the communities from the different biofilters able to degrade this media would be very specialized and similar. Of the genera that comprised more than 2.5% of the total abundance of the communities, 59 % of the genera for the anaerobic sections of all the bioreactors were the same, and 62% were the same in the aerobic sections. This similarity means that independent of the reactor but dependent on the presence of oxygen, these communities were very similar to one another.

Chapter 4: Electrochemical Biofilters Treating Hydrocarbon Wastewater

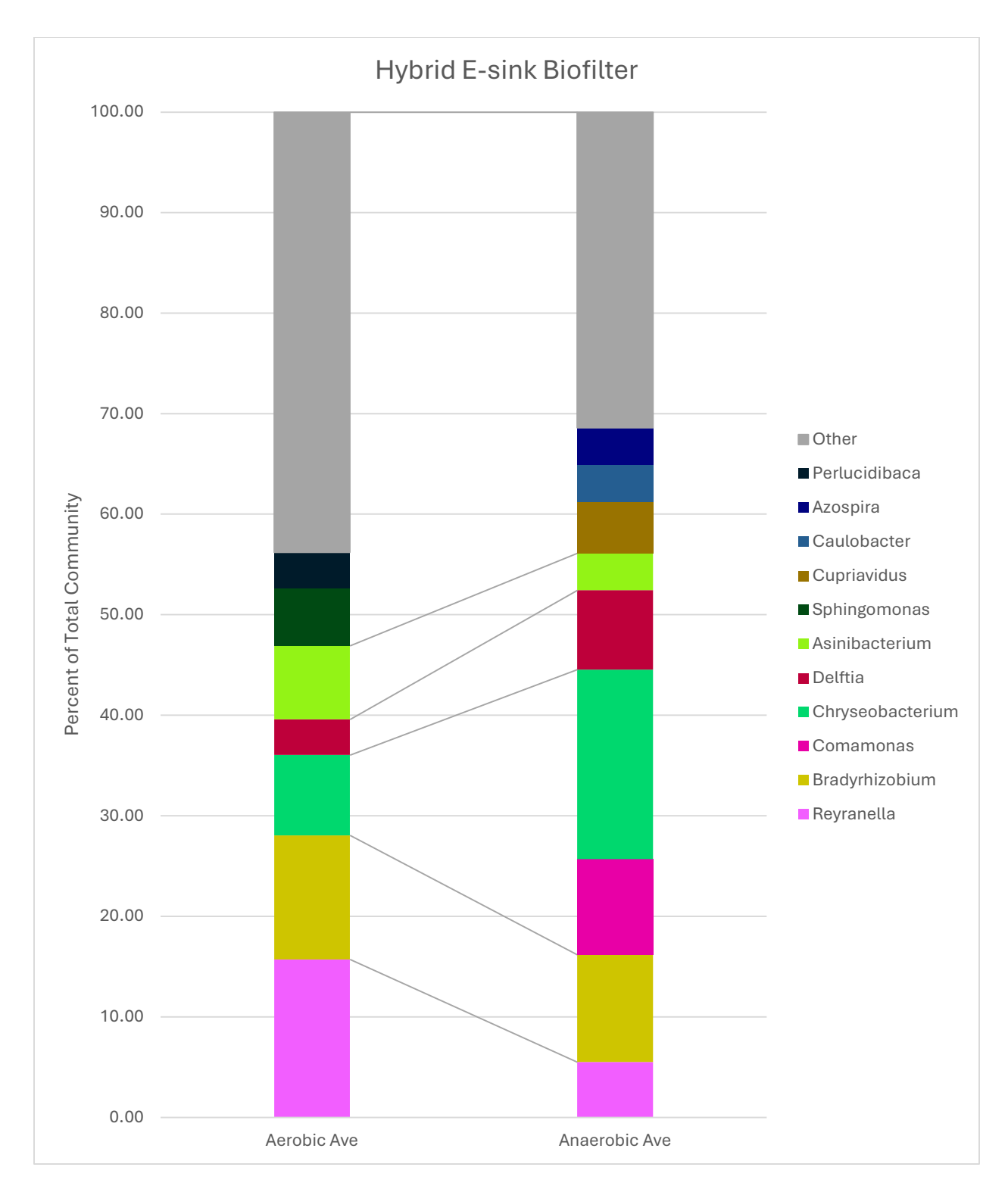


Figure 10: Average abundance of genera in the HEB. All genera shown have an abundance greater than 2.5%.

Chapter 4: Electrochemical Biofilters Treating Hydrocarbon Wastewater

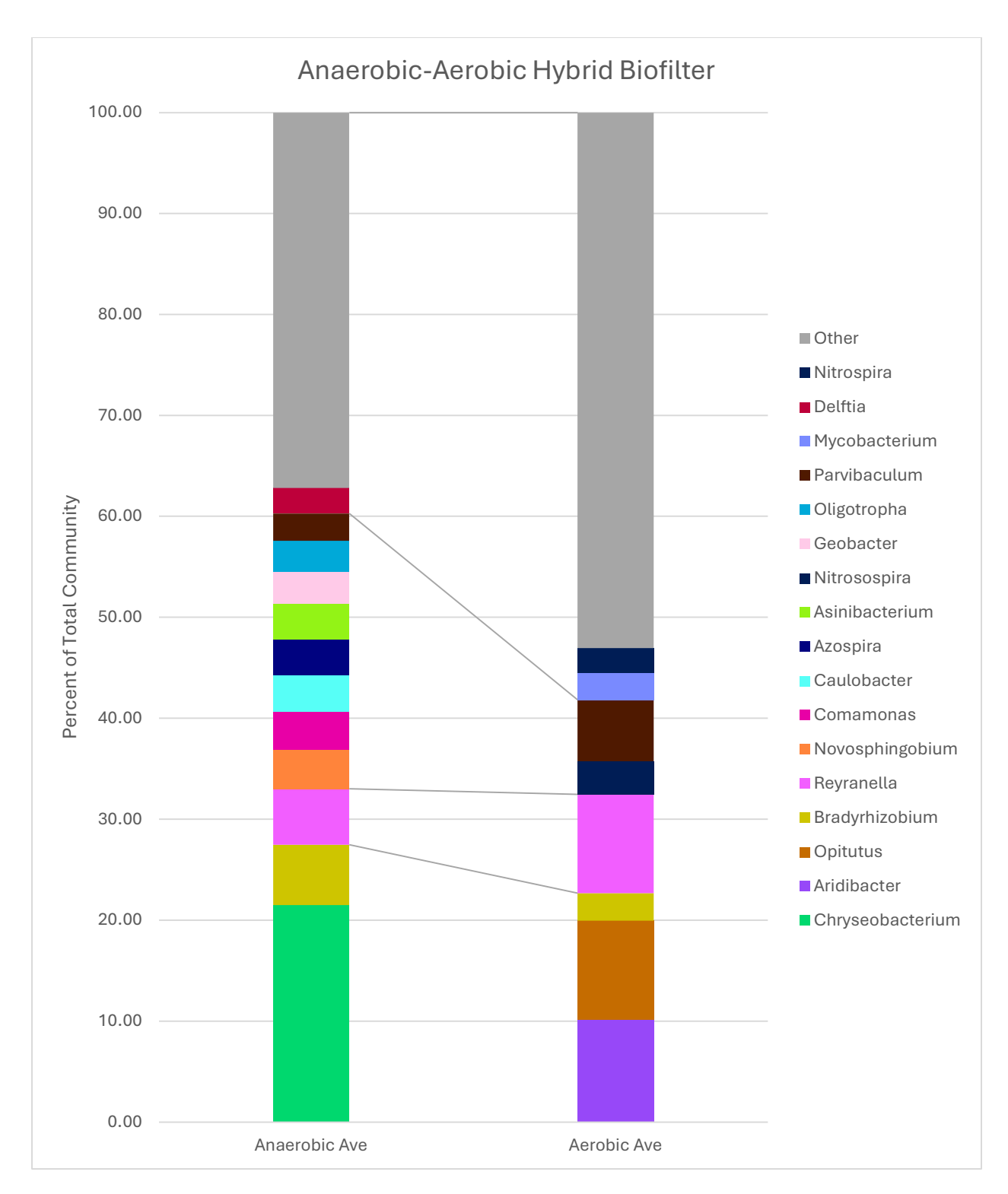


Figure 11: Average abundance of genera in the AAH biofilter. All genera shown have an abundance greater than 2.5%.

Chapter 4: Electrochemical Biofilters Treating Hydrocarbon Wastewater

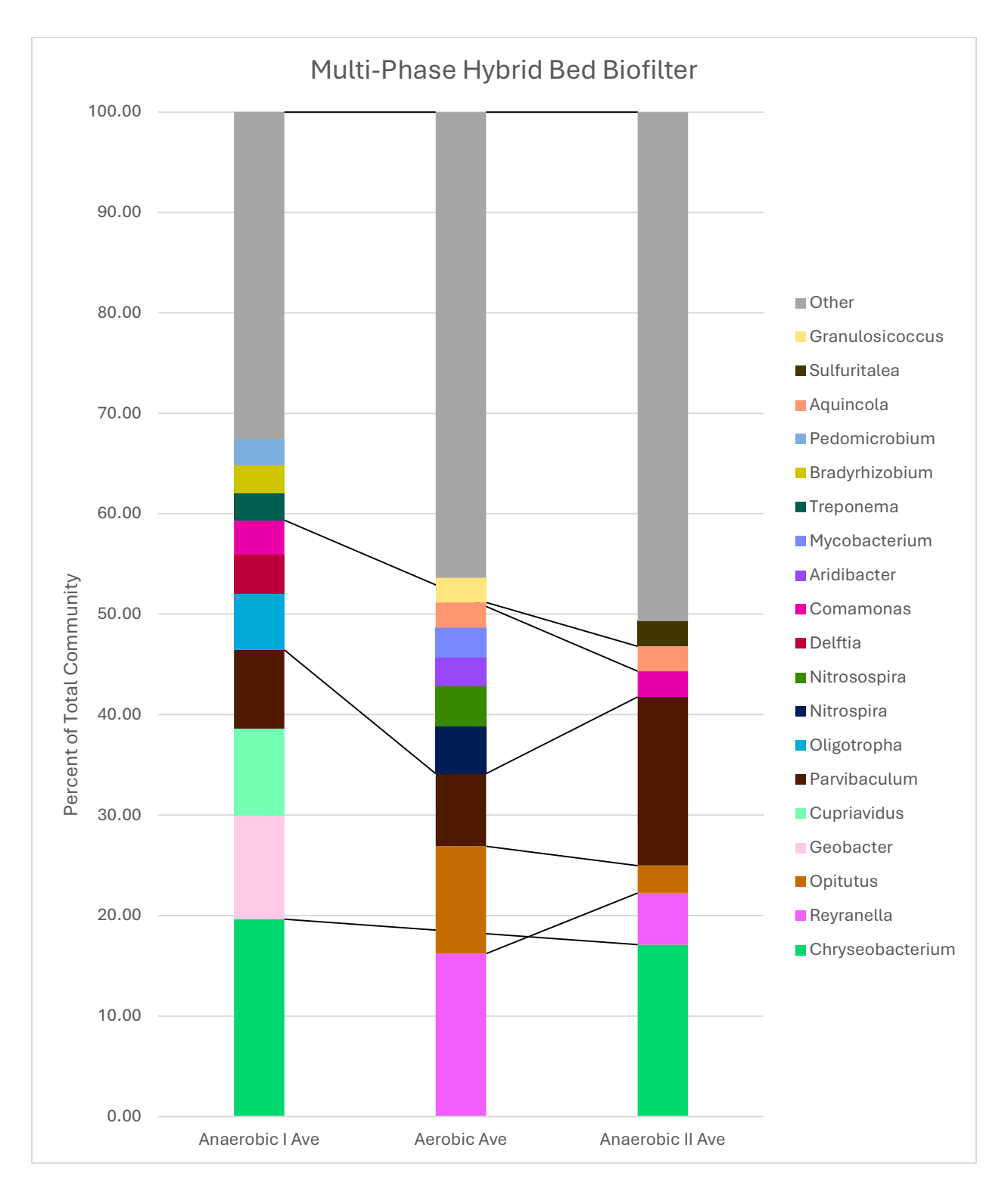


Figure 12: Average abundance of genera in the MPHB biofilter. All genera shown have an abundance greater than 2.5%.

3.2.1 - Aerobic Microbial Communities

The different aerobic sections of the HEB, AAH, and MPHB shared 8 genera: Reyranella, Bradyrhizobium, Parvibaculum, Nitrospira, Opitutus, Mycobacterium, Nitrosospira, and

Aridibacter. Most of these genera were previously reported as capable of polycyclic aromatic hydrocarbon (PAH) degradation or alkane degradation, or are found at HC-contaminated sites. Parvibaculum has been identified in high abundance at the Deepwater Horizon oil spill site as a genus associated with the ability to degrade HCs (Looper et al., 2013). Furthermore, members of the genus have shown the ability to degrade alkanes. One species, Parvibaculum hydrocarboniclasticum, can use n-alkanes as its sole carbon source (Rosario-Passapera et al., 2012). Others have been isolated from seawater greatly enriched with PAH (over 200 PPM) (Lai et al., 2011) or identified at contaminated sites that contain PAHs (Xia et al., 2018).

Parvibaculum is not the only community member ubiquitous to all the reactors that can degrade PAHs. At least 16 strains or species of *Mycobacterium* have been shown to have the function genes required to degrade pyrene and its metabolites (Qutob *et al.*, 2022). Furthermore, a degradation pathway has been proposed through transcriptional analysis (Yuan *et al.*, 2018). Another genus is *Bradyrhizobium*. *Bradyrhizobium* has been identified as a PAH degrader. Multiple genes involved in the breakdown of PAHs and their metabolites have been identified in the genus (Sandhu, Paul and Jha, 2022). Though not all genera have been identified as PAH degraders, one species of *Nitrospira* has been shown through a correlation-based network to be critical to communities involved in PAH degradation (Geng *et al.*, 2020). While not all common genera have been identified as HC degraders, many have been isolated or identified in high abundance in HC-contaminated sites.

Reyranella has been identified in petroleum-contaminated aquifers. There, it was one of the most abundant genera found. Furthermore, it is possible that Reyanella could be a facultative autotroph and is breaking HC down to inorganic carbon (Ning, Cai and Zhang, 2024). Opitutus is another genus that is very common in HC-contaminated soils. In a study of oilfields, Opitutus was found in high abundance and was a core genera in three separate oilfields (Sun et al., 2015). Aridibacter was also found in HC-contaminated soil at a shale gas well site (Ren et al., 2024). The final common genus is Nitrosospira. It was detected in the activated sludge plant treating PRW (Figuerola and Erijman, 2010). One unique standout genus was found in the aerobic section of the HEB. Asinibacterium is not identified from HC-comatmetied sites but has been identified in biofilms that form on metal (Akita, Shinto and Kimura, 2022). The presence of Asinibacterium makes sense since the conductive bed material has a high iron content.

3.2.1 - Anaerobic Microbial Communities

The anaerobic section of the different reactors also contained a group of genera that were present in all of them. The HEB, AAH, and MPHB shared 10 genera: *Chryseobacterium*, *Delftia*, *Comamonas*, *Bradyrhizobium*, *Parvibaculum*, *Geobacter*, *Cupriavidus*,

Caulobacter, Oligotropha, and Azospira. Almost all of these genera are either HC degraders or isolated from HC-contaminated sites. Multiple strains of Delftia have been isolated from HC-contaminated sites with the ability to degrade chlorobenzene (Ye et al., 2019), dimethylphenols (Vásquez-Piñeros et al., 2018), or diesel (Lenchi et al., 2020). Another strain can grow on hexane, crude oil, or various PAHs as its sole carbon source (Eren and Güven, 2022). Comamonas was supplemented in co-composting to eliminate PAHs. It was determined that C. testosterone could degrade PAHs (Jiang et al., 2023). Cupriavidus is another genus with strains isolated from oilfields that can oxidize PAHs and alkanes (Bacosa et al., 2021). Pyrene is a complex PAH degraded by Caulobacter (Al-Thukair and Malik, 2016). Finally, Chryseobacterium has been isolated from many HC-contaminated environments, though not confirmed to degrade HCs (Szoboszlay et al., 2008; Benmalek et al., 2010; Hugo et al., 2019).

Maybe the most critical genus seen in these electroactive biofilters is *Geobacter*. *Geobacter* is the model electroactive microorganism (Gralnick and Bond, 2023) due to its well-proven extracellular electron transfer capacity. *Geobacter* is also critical in transferring electrons from heterotrophs to the electroconductive bed of the biofilter. It has been shown that *Geobacter* acts as a keystone microbe in conductive biofilms that increase efficiency (Tejedor-Sanz *et al.*, 2018). These abilities allow for *Geobacter* to act as an intermediate and help perform conductive-particle-mediated interspecies electron transfer (Prado de Nicolás, Berenguer and Esteve-Núñez, 2022). Furthermore, during urban wastewater biodegradation, this electroactive genus was previously reported to colonize METland aerobic beds (Aguirre-Sierra et al., 2020). Members of the *Geobacter* genus were also reported as capable of biodegrading aromatic pollutants (Zhang *et al.*, 2012), so their presence could also directly contribute to the removal of HCs.

4 - Conclusions

Inspired by the METland concept, several hybrid configurations have been designed to combine oxidative and reductive reactions in the same device. HEB and MPHB had the highest COD removal rates, 97 ± 5 gCOD/m3*day and 104 ± 6 gCOD/m3*day, respectively. HEB and MPHB also had the highest rates for nitrification, 3.9 ± 0.4 gN-NH4 /m3*day and 3.1 ± 0.1 gN-NH4 /m3*day, respectively. While the two reactors had similar rates, the MPHB had better efficiency, removing a higher percentage of the initial loads. The microbial communities were highly conserved in the aerobic and anaerobic zones. Almost all the major genera present had shown previous activity in or isolation from HC-contaminated sites. *Geobacter* was present in all of the biofilters, as would be expected by their electroconductive nature.

Chapter 4: Electrochemical Biofilters Treating Hydrocarbon Wastewater

The next step is to build a pilot-scale biofilter to treat HC WW. The new generation of electroactive biofilters seems promising for removing HC-polluted WW, although significant modifications are required to enhance total nitrogen removal. The chemical nature of the recalcitrant pollutants after the treatment should be characterized to understand the technology's limits.

Chapter 5:

Novel Use of The Gradostat for the Adaptation of Microbes

Custom Workforce: Novel Use of The Gradostat for the Adaptation of Microbes for Microbial Electrochemical Devices

1 - Introduction

The study of microbial physiology has dramatically influenced our understanding of our environment, medicine, and microbiology's application to industrial and commercial processes. Knowing that certain bacteria can respire using an electrode as a terminal electron acceptor(Daniel R. Bond and Lovley, 2003), many novel microbial electrochemical technologies (METs) and applications have arisen to harvest energy (Potter, 1911; Liu and Logan, 2004), convert CO2 into organics (Nevin et al., 2010; Llorente et al., 2024), desalinate seawater (Cao et al., 2009; Ortiz et al., 2021; Ramírez-Moreno, Esteve-Núñez and Ortiz, 2021), and electrobioremediation (Wang et al., 2020; Tucci et al., 2021). These technologies apply considerably to water treatment (Ramírez-Vargas et al., 2018; Esteve-Núñez, 2025). All these technologies mentioned above rely on microbes to catalyze reactions or generate electrical potential. Much work has been done recently to increase the efficiency of microbial electrochemical systems, such as reactor design (Kadier et al., 2016), electrode design (Xie, Criddle and Cui, 2015), and electrolyte composition (Logan et al., 2015). Adapting and customizing microbes and microbial communities through selective pressure is vital in unlocking these devices' potential.

Geobacter sulfurreducens (Caccavo et al., 1994) is the model organism for Geobacter physiology(Lovley, 2003; Gralnick and Bond, 2023) performing extracellular electron transfer (Butler, Young and Lovley, 2010; Costa et al., 2018). The genome has been sequenced (Methé et al., 2003), and a genetic system (Coppi et al., 2001) is in place for modification. G. sulfurreducens can reduce iron through direct cell wall contact (Daniel R. Bond and Lovley, 2003) and using pilli, also known as nanowires (Reguera et al., 2005). G. sulfurreducens can reduce extracellular iron, technetium, uranium, vanadium, and cobalt (Lovley et al., 2011). The conductivity of pili structures called nanowires has been demonstrated in G. sulfurreducens by removing 5 aromatic amino acids from a PilA gene (Vargas, Nikhil S Malvankar, et al., 2013).

Furthermore, the current density on a graphite electrode has been well-studied (Daniel R. Bond and Lovley, 2003; Logan *et al.*, 2015). Long-term selection of varieties of *G. sulfurreducens* has shown increased efficiency in respiring an electrode (Yi *et al.*, 2009;

Malvankar, Tuominen and Lovley, 2012). If the speed of the selection process can be improved, the overall efficiencies can also be increased more quickly.

Researchers can force gain of function and loss of function mutations on specific organisms by applying specific selective pressure (Mills, Peterson and Spiegelman, 1967). This process can be very labor-intensive because a single round of mutation, gene expression, screening, and replication requires days or longer with frequent monitoring and interaction from researchers (Esvelt, Carlson and Liu, 2011). The mutation rate depends on the number of rounds of selection performed (Avoigt, Kauffman and Wang, 2001). Continuous culture can increase the mutation rate and decrease the amount of human intervention (Badran and Liu, 2015). The chemostat (Novick and Szilard, 1950) is a reactor that can maintain the exponential growth of a microorganism while maintaining a specific selective pressure. The chemostat has been modified to, for example, change selective pressure based on cell density(Lee *et al.*, 2010) or to select against biofilm formation (Marlière *et al.*, 2011).

Salinity constantly changes along an estuary from the freshwater river to the saltwater bay or ocean. There is a continually changing gradient of salinity as one moves from one to the other. To try and replicate this gradient in a laboratory, it is necessary to section off each specific salinity into a reactor that flows into another reactor (Cooper and Copeland, 1973). This segregation creates a group of interconnect reactors that produce a salinity gradient analogous to that estuary. This first system was passive, in which diffusion creates a gradient across a set of different vessels. This system was improved upon using bidirectional pumping between sealed chemostats. The gradostat was a system that could be used to study the individual steps along the analogous estuary. Beyond mimicking a natural system, the gradostat could be used to study opposing gradients of substrates (Lovitt and J. W. T. Wimpenny, 1981).

The gradostat can apply a gradient of selective pressures to a population of microorganisms (Lovitt and J. W. . Wimpenny, 1981). As a set of interconnected chemostats individually fed by two media types, the fresh media feeds into the first and final reactor, with one or both media containing a solute of interest (Fig. 1). The bidirectional communication between chemostats produces a gradient of the solute(s) of interest. Furthermore, this solute gradient combined with bidirectional communication provides for the continuous growth of microorganisms while constantly applying differential selective pressures (Wimpenny, 1982). This pressure allows the unique selection of minority members that have mutated or adapted to have greater efficiency under the selective pressure choice. The gradostat was modeled after the idea that many

environments are not static in nature, and the conditions microbes experience are not stable.

All bacteria are sensitive to osmotic stress in one way or another. Still, they can be used in the microbial desalination cell (MDC), a unique way to remove cations and anions from saltwater. The MDC uses METs to remove salt from water. To achieve this, the MDC uses three chambers: an anodic, a cathodic, and a saline chamber. In the anode's anodic chamber, a biofilm oxidizes organic matter, and electrons are donated to the anode. These electrons are passed through a resistor to a cathode, where a reductive process occurs. This process creates a positive-to-negative charge differential to form across the saline chamber in between. The anode and cathode chamber are separated by a saline chamber in which the salt water is to be desalinated. The saline chamber is separated from the anode chamber by an anion exchange member and the cathode chamber by a cation exchange membrane. This membrane separation allows cations like sodium to pass into the cathode chamber and anions like chlorine to pass into the anode chamber (Ramírez-Moreno, Esteve-Núñez and Ortiz, 2021, 2023). As the desalination process proceeds, the anodic chamber will increase in salinity, eventually affecting the anode biofilm. Osmotic stress may inhibit the biofilm's ability to respire the anode and, eventually, desalinate water. If microbes like G. sulfurreducens, which are fundamental for electron transfer to the anode (Borjas, Esteve-Núñez and Ortiz, 2017; Ramírez-Moreno et al., 2024), could be adapted to higher saline conditions and, therefore, osmotic stress, it could increase the efficiency of the MDC.

This study uses a gradostat combined with METs to study G. sulfurreducens' ability to adapt to a saline environment while studying its ability to respire an electrode by combining the gradostat concept with single-chamber microbial electrolysis cells (MECs). This study aims to show, for the first time, that the gradostat, combined with electromicrobiology concepts, is effective for understanding the G. sulfurreducens' ability to transfer electrons to electrodes in a biofilm and planktonically. The goal is first to show that G. sulfurreducens can grow under a diminishing electron acceptor gradient and to understand how salinity affects G. sulfurreducens' ability to transfer electrons to the anode.

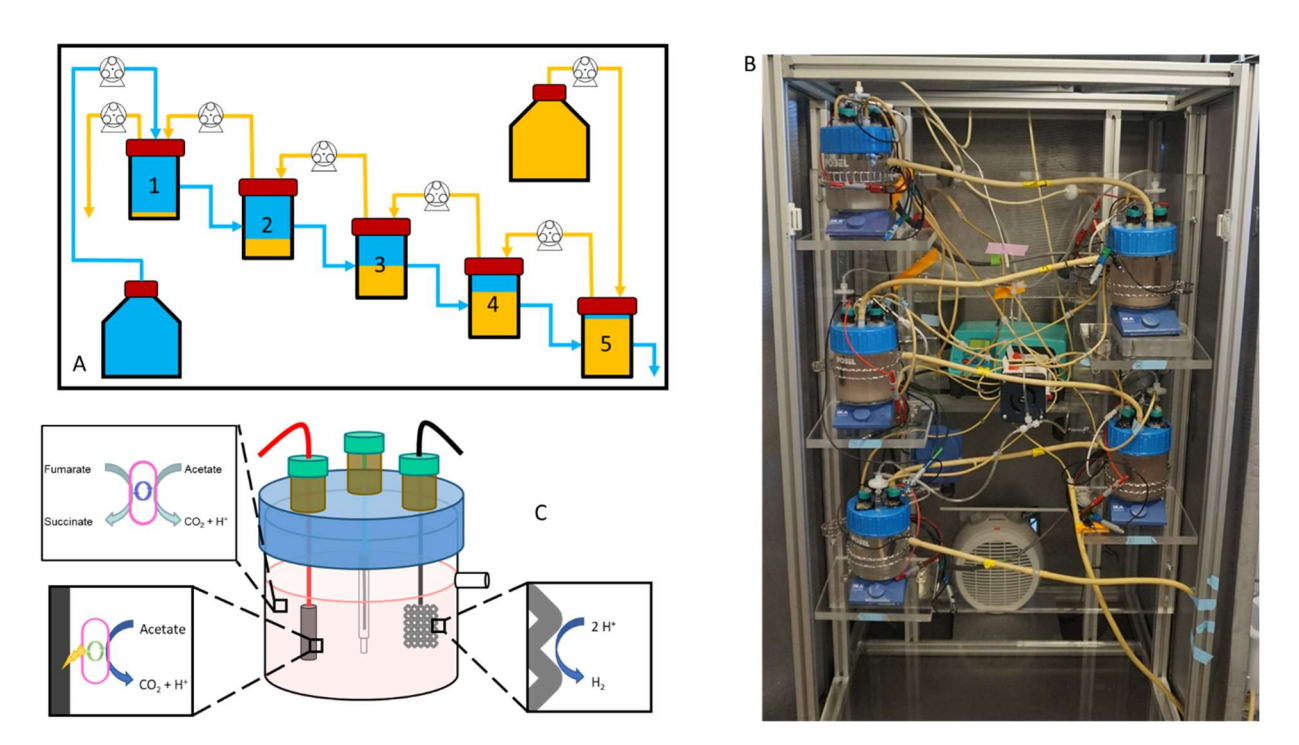


Figure 1: A) A conceptual diagram of the gradostat's operation. B) An inoculated gradostat in a temperature control cabinet. C) A diagram of the major metabolic and chemical reactions in the media on the working and counter electrodes.

2 - Materials and Methods

2.1 - Gradostat Design

The system comprised 5 glass bioreactors of ca.0.5 liters (Pobel, Madrid, Spain). The bioreactors were interconnecting with a bidirectional flow as described in Lovitt and Wimpenny 1981 (Fig. 1A). The significant difference in the design is using an alternating stacked configuration (Figure 1B) with a central Watson-Marlow pump (Falmouth, United Kingdom). All bioreactors were maintained in anaerobic conditions through the constant bubbling of N₂:CO₂ (80:20) (Airgas, Madrid, Spain). Sampling was done through stainless steel valves and cannulas through the bioreactor's enclosure caps. The basal media in the bioreactors was freshwater (2.5 g/L NaHCO₃, 0.36 g/L NaH₂PO₄, 0.25 g/L NH₄Cl, 0.10 g/L KCl supplemented with vitamins and minerals)(Kuzume *et al.*, 2014) for the cultivation of *G. sulfurreducens*. The electron donor and acceptor used were acetate and fumarate, respectively. The bioreactors were inoculated (1:10) with exponential phase *G. sulfurreducens* (ATCC 51573).

2.2 - Test Conditions

2.2.1 - Electron Acceptor Gradient

To validate *G. sulfurreducens* growth in a gradostat, a gradient of the electron acceptor was created by supplying bioreactor 1 with freshwater media containing 20 mM acetate as the electron donor and 40 mM fumarate as the electron acceptor. Bioreactor 5 was fed with the same media, excluding fumarate. This feeding scheme created a gradient where the highest fumarate concentration was in bioreactor 1 and the lowest was in bioreactor 5.

2.2.2 - Salt Gradient with Electrochemical Cells

The gradient was established using sodium chloride. Bioreactor 1 was supplied with freshwater media with 20 mM acetate and 40 mM fumarate to not limit the electron donor or acceptor. Bioreactor 5 had the same media as reactor 1 but with 10-30 g/L of NaCl. A graphite working electrode (~10 cm²) was added to each bioreactor. The counter electrode was a platinized titanium mesh (Inagasa, Spain) with excessive surface area to eliminate the possibility of cathode limitation. The working electrode was poised at 0.2 volts (vs. Ag/AgCl reference) (Solrayo, Madison, USA) versus an Ag/AgCl 3 M NaCl reference electrode (Basi, West Lafayette, USA).

2.2.3 - Planktonic Test Reactor

The planktonic test bioreactor was a 100 ml media Pyrex bottle (ThermoFisher, Waltham, USA). The planktonic bioreactor used the same three-electrode system as in each of gradostat's bioreactors. The working volume of the planktonic bioreactor was 50 mL and was operated in the same manner as each bioreactor in the gradostat. The salinity and OD were replicated and normalized to test the planktonic cells of the different bioreactors of the gradostat in the 100 ml vessel at the same conditions in the gradostat. All samples taken from the different bioreactors during a single run of the gradostat were normalized to the bioreactor with the lowest OD. OD was normalized with media without an electron donor (acetate) or electron acceptor (fumarate) but with the matching NaCl concentration of the gradostat bioreactor of origin. Once the planktonic bioreactor was inoculated, the working electrode was poised for 5 hours at 0.2 V (vs Ag/AgCl reference). After G. sulfurreducens was acclimatized to the planktonic bioreactor and a baseline current density was established, two cyclic voltammetries (CVs) were run at 1 mV/s and 5 mV/s between 0.6 V and -0.6 V (vs. Ag/AgCl reference). The working electrode was poised at 0.2 V (vs. Ag/AgCl reference) for 40 minutes between CVs to reestablish the baseline current density.

2.3 - Sample Analysis

Acetate concentration was determined through ionic chromatography, and fumarate concentration was performed using HPLC (Prado, Berenguer and Esteve-Núñez, 2019). Salinity was monitored through the ionic conductivity of the media (Borjas *et al.*, 2015). Growth was monitored through spectrophotometry (OD600) (Hach, Loveland, USA). Electrode potential was controlled via a multichannel potentiostat (Solrayo, Madison, Wisconsin). The current density was observed through the same system.

3 - Results & Discussion

The gradostat was first tested to validate its ability to grow *G. sulfurreducens* with an electron acceptor limiting gradient. Fumarate was used as a gradient to see how *G.* sulfurreducens would react and verify that the gradostat could maintain the conditions necessary for *G. sulfurreducens* growth. The second set of tests incorporated a three-electrode MEC into each of the bioreactors of the gradostat. Therein, *G. sulfurreducens* was adapted to growth in saline conditions. Furthermore, *G. sulfurreducens* was tested to understand how saline conditions would affect its ability to transfer electrons extracellularly in biofilm and planktonic form. The second set of tests aims to produce more resilient *G. sulfurreducens* for MDCs.

3.1 - Fumarate Limitation

The first test of the gradostat was to determine and verify its ability to grow organisms like *G. sulfurreducens* anaerobically as proof of concept. In this case, fumarate was selected as a solute to establish the gradient because it is a well-known electron acceptor for this microbial strain. Without electrodes, a fumarate gradient was formed along the five bioreactors. The gradient followed an exponential pattern (Fig. 2) from an initial concentration of 10.5 mM of fumarate in bioreactor R1 to fumarate-limiting conditions (0.02 mM) in bioreactor R5. The cell density followed a similar pattern to the fumarate except for R2 (Fig. 3), which showed the highest cell density. While it might seem surprising because bioreactor 1 had the highest available carbon source, this does not consider the dilutionary effect of the new media entering the first bioreactor. Furthermore, the cell density was not deleteriously affected until the fumarate concentration dropped below the one mM range. Cell density was not electron donor limited in any bioreactor (Fig. 4). acetate showed an inverse pattern to cell density in bioreactor 2, where cell density was highest.

Chapter 5: Novel Use of The Gradostat for the Adaptation of Microbes

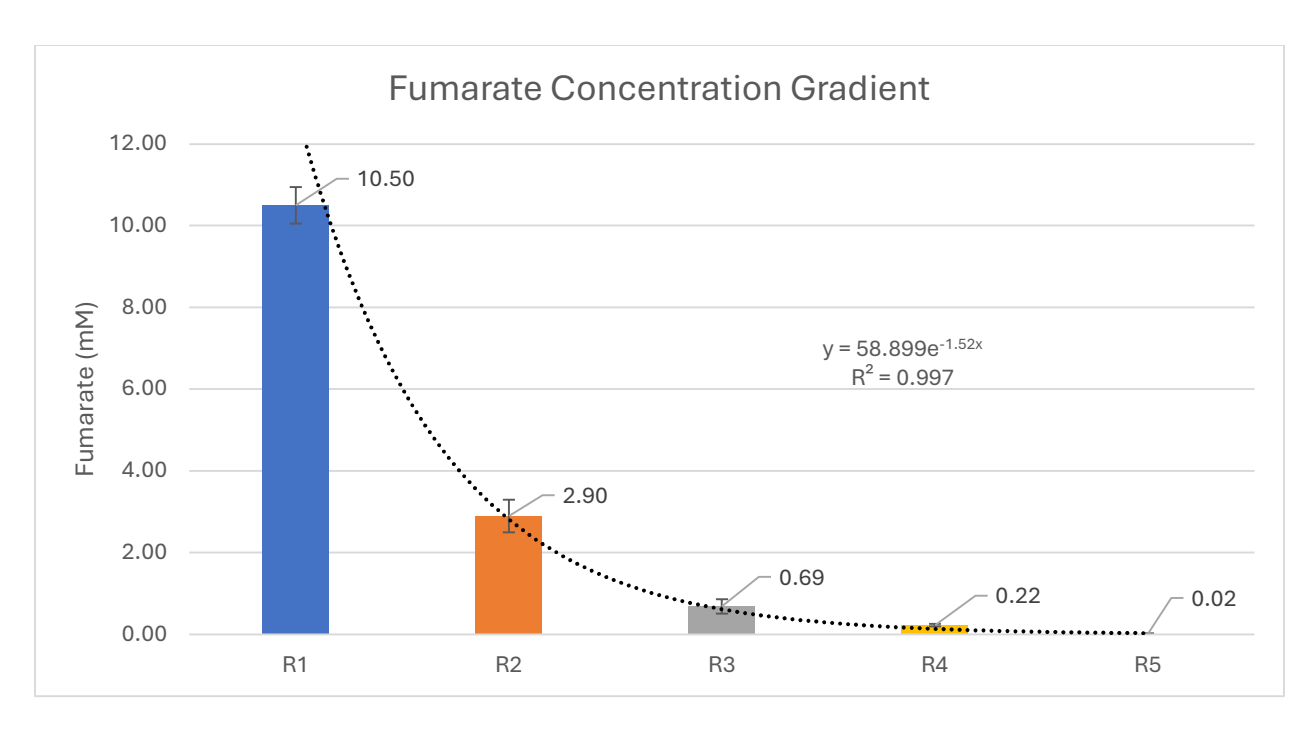


Figure 2: The fumarate concentration correlated to an exponential regression (R^2 =0.997).

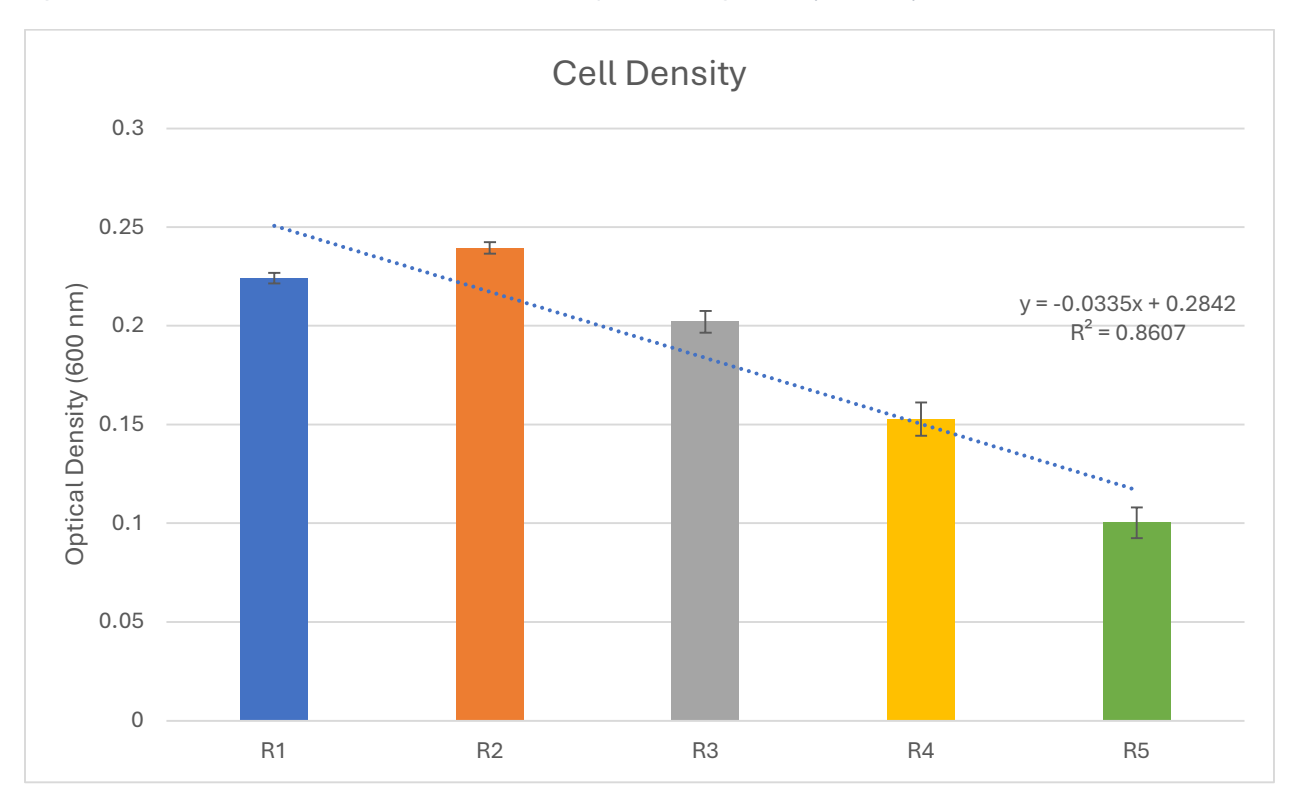


Figure 3: Cell density as observed through optical density.

Chapter 5: Novel Use of The Gradostat for the Adaptation of Microbes

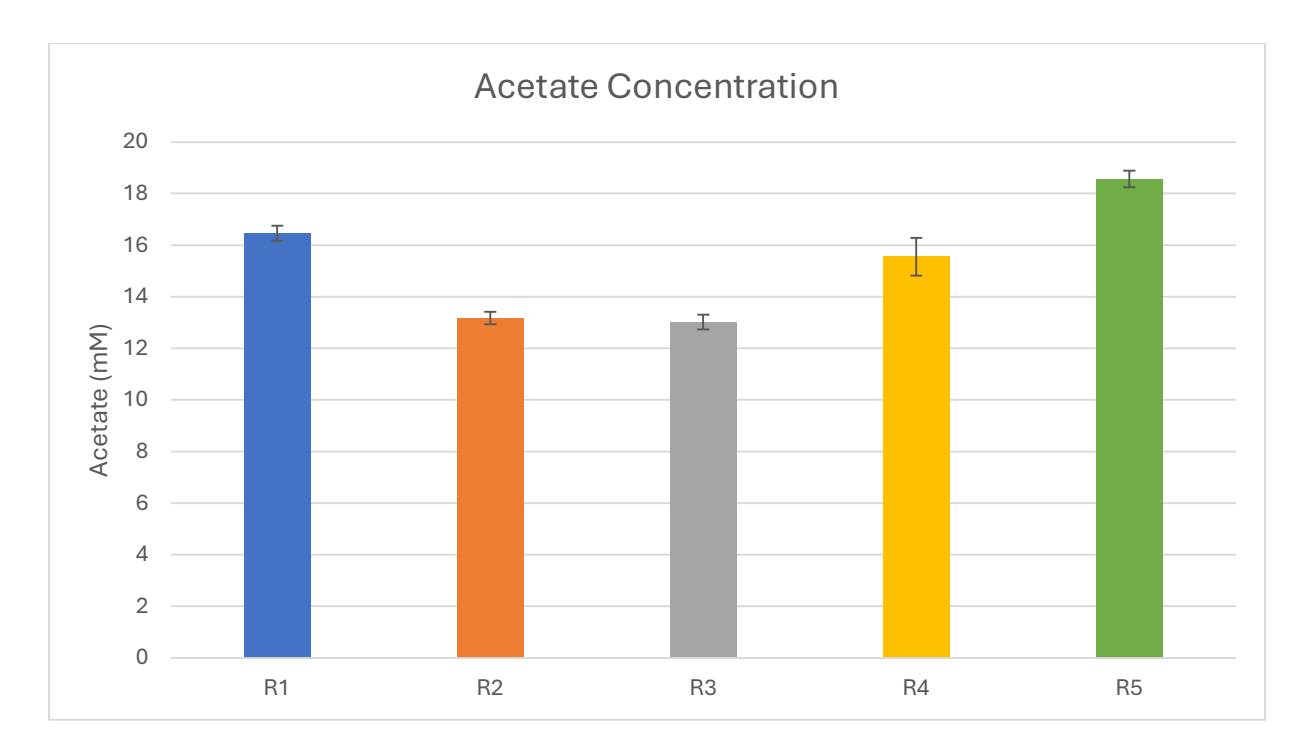


Figure 4: Electron donor limitation was never observed in the reactors.

3.2 - In situ Biofilm Growth under a Saline Gradient

The following experiments were to understand how *G. sulfurreducens* would react electrochemically to increasing concentrations of sodium chloride (NaCl). Initially, bioreactor 1 of the gradostat was fed with freshwater media and into bioreactor 5 with NaCl at 20 g/L. Throughout these experiments, the concentration of NaCl in the feed solutions varied in the range of 10-30 g/L. The initial set of experiments focused on 20 g/L NaCl vs. freshwater media. *G. sulfurreducens* was supplied with 20 mM acetate and 40 mM fumarate in both media feeds. It was shown that the concentration of NaCl across the reactors had a strong linear relationship with an R² value of 0.99 (Fig. 5), with the lowest salinity in reactor 1 and the highest in reactor 5. Furthermore, the concentration of NaCl remained steady over time, with less than 1 g/L fluctuation over a week (Fig. 6). These

bioreactors of the gradostat differed from the fumarate experiment because they included *in situ* three-electrode electrochemical systems.

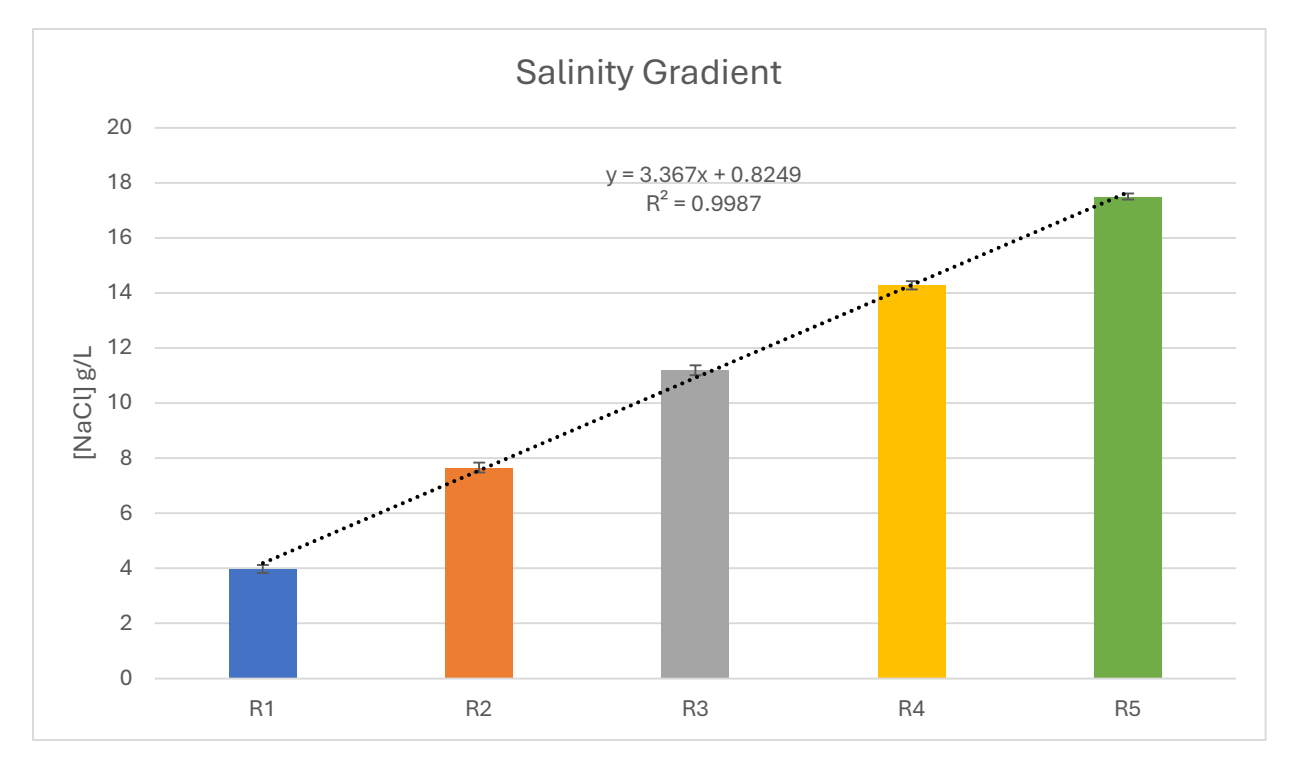


Figure 5: The salt concentration across the reactors showed a strong linear relationship (R^2 =0.99)

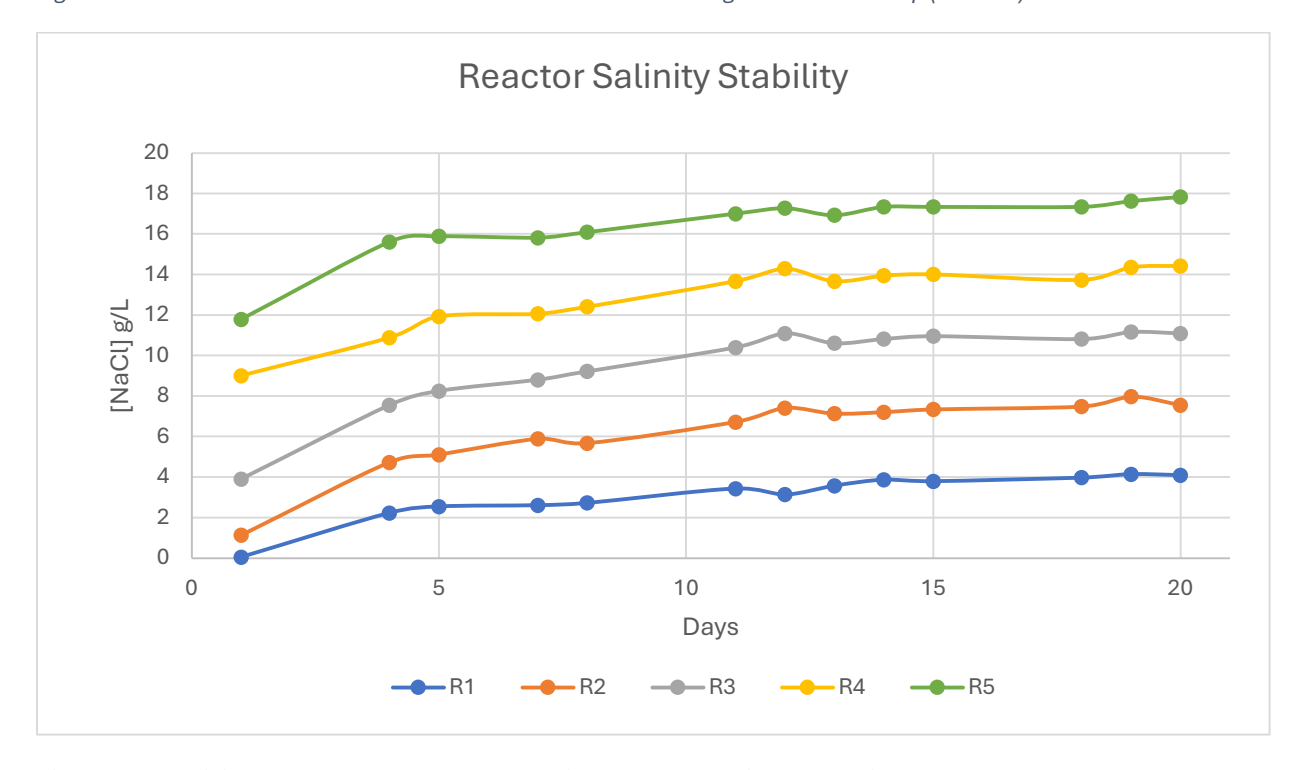


Figure 6: The salinity of the system was stable over time and showed little fluctuation.

Each bioreactor of the gradostat had a working electrode made of a graphite rod, a platinized titanium counter electrode, and an Ag/AgCl reference electrode. The biofilms generally formed and reached a steady-state current density over 3-5 days (Fig. 7).

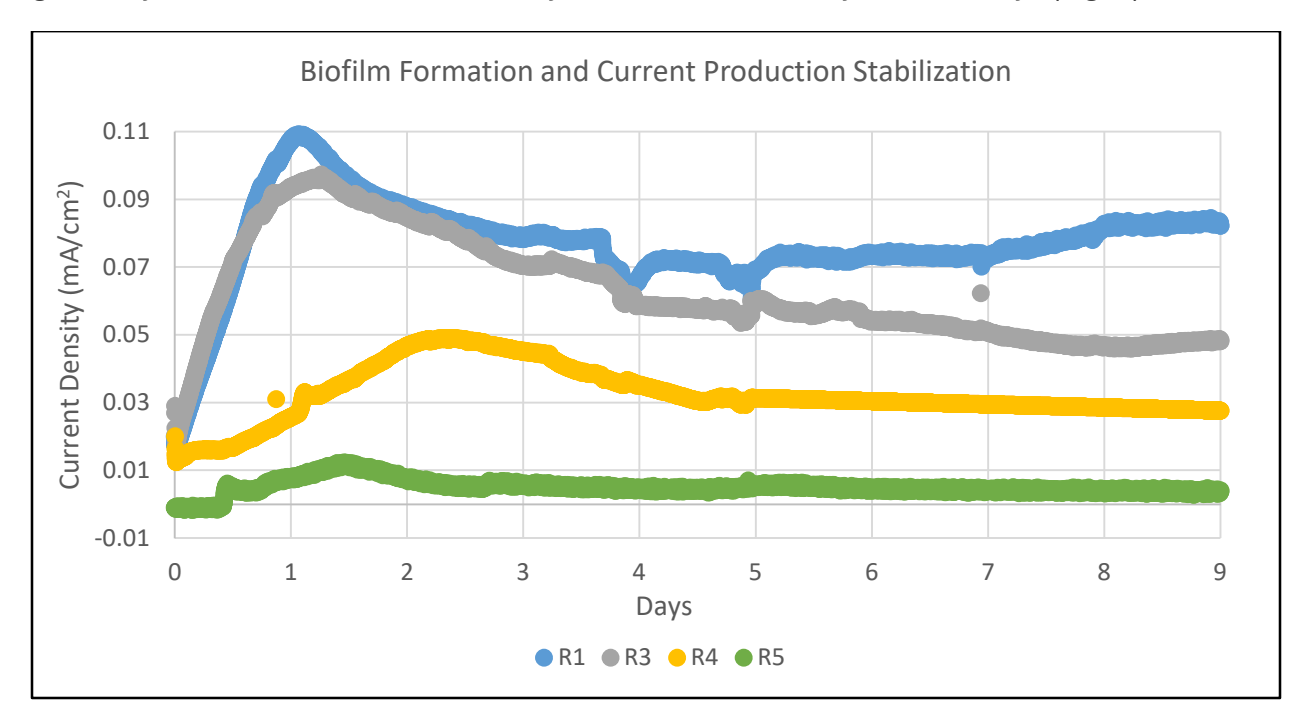


Figure 7: Current density showing biofilm formation and steady-state current productions after 3 days. Reactor 2 (R2) was not included due to a defective reference electrode.

The working electrode was poised at 0.2 A (vs. Ag/AgCl reference). The *in situ* biofilms have a marked negative correlation (R²=0.94) between current density and NaCl concentration (Fig. 8). As the salinity increases, the resistance in the electrochemical cell will decrease, which should cause an increase in efficacy, but that was not observed. Therefore, this decrease in current density must be related to microbial physiology, not the electrochemical cell's physical properties. Cell density could have been negatively affected by salinity. While biofilms were present at all salinities, the number of cells in those biofilms could be lower at higher salinity. Furthermore, as previously reported, *G. sulfurreducens* produces excess exopolysaccharide (EPS)(Borjas, 2016) under salinity osmotic stress. This EPS could lead to decreased mass transfer rates when growing as a biofilm, limiting the availability of acetate for producing electrical current (Sun *et al.*, 2016).

Additionally, a decrease in mass transfer rates could lead to acidification of the biofilm. With a lower mass transfer, it is easier for the proton formation associated with acetate oxidation and the respiration of the electrode to outpace the neutralizing effect of the bicarbonate in the media(Torres, Marcus and Rittmann, 2008). As previously shown, acetate was not limited in the reactors (Fig. 4) cyclic voltammetry (CV) analysis demonstrated that the effect on current density was related to microbial physiology.

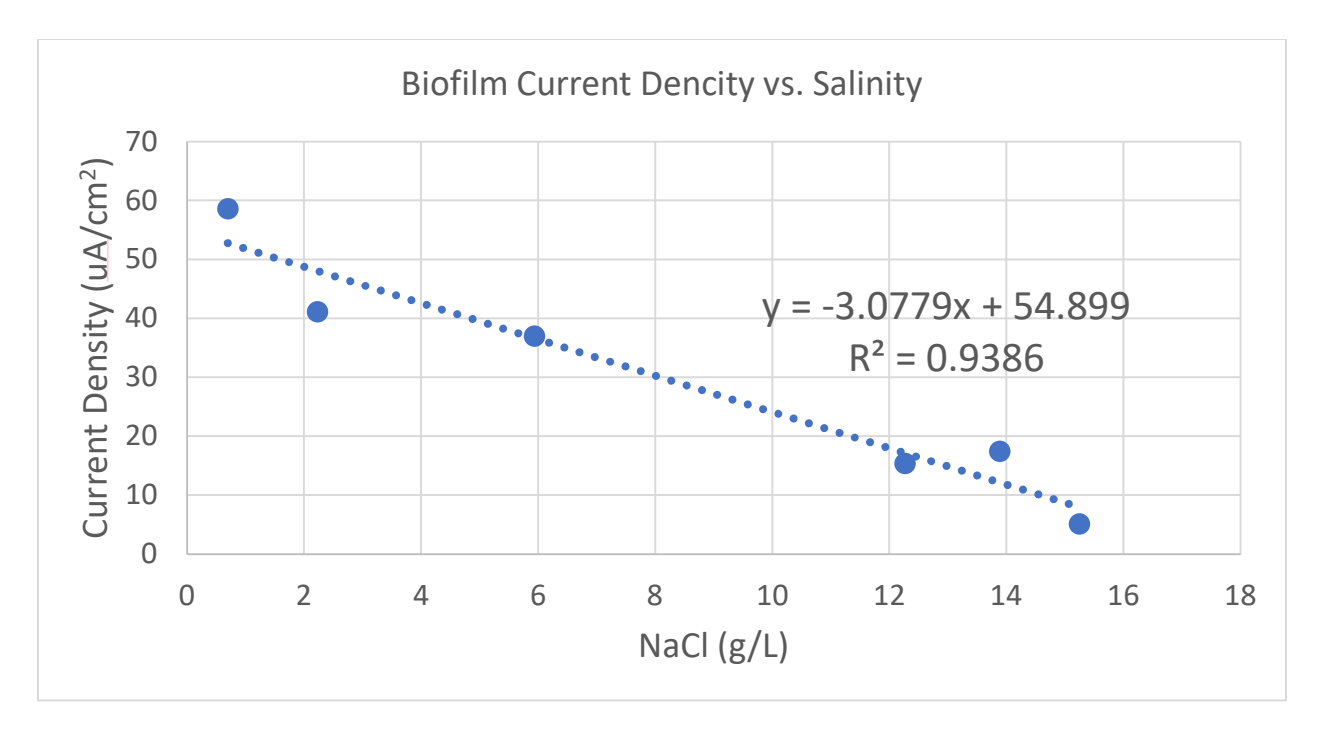


Figure 8: The linear correlation between current density and NaCl concentration for G. sulfurreducens grown on the anode under non-limiting availability for acetate and fumarate.

According to results from CVs analysis, ranging from 3.9 - 20.1 g/L NaCl, there was a marked decrease in the sigmoidal shape associated with a turnover CV (Fig. 9). Typically, a turnover CV is performed in the presence of an electron donor. The presence of the donor allows for the electrochemical study of, in this case, respiration using the anode as the terminal electron acceptor. In *G. sulfurreducens*, the inflection point between the reduction and oxidative reaction with acetate occurs at about -0.34 V (Fricke, Harnisch and Schröder, 2008). As salinity increases, there is a decrease in the difference between the oxidated and reduced states of the cells on the anode. As the salinity increased above 9.7 g/L, the CV was flattened, thus becoming more similar to a typical abiotic CV. This shift occurs such that at 20.1 g/L NaCl, the sigmoidal shape was almost wholly lost. This loss of detectable oxidation and reduction states was consistent with the diminished current density revealed by chronoamperometry (CA) when salinity was increased (Fig. 8). Thus, respiration was decreased due to saline stress. It would negatively affect the current density, and consequently, the CV would stop showing active respiration.

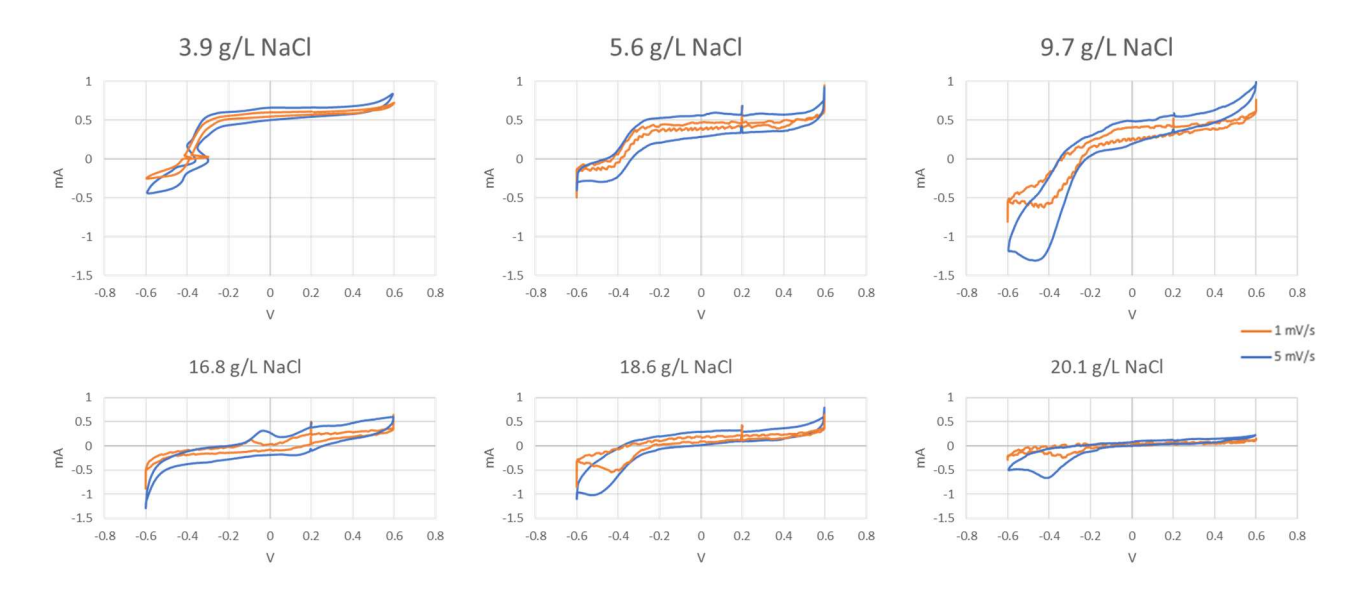


Figure 9: CV run at 1 mV/s (orange line) and 5 mV/s (blue line) between 0.6 V and -0.6 V.

3.3 - Electrochemical Analysis of Cells in the Planktonic Phase

To understand the effect of salinity on the planktonic cells, *G. sulfurreducens* adapted to different salinities were tested electrochemically without forming a biofilm. Biofilm formation follows a typical pattern revealed by CA. First, there was an initial increase and peak of current density followed by a decrease and stabilization (Yi *et al.*, 2009) in a process that typically takes ca. 4 days (Fig.7). Thus, for testing the planktonic cells from the gradostat, *G. sulfurreducens* cells were in contact with the poised electrode just for 5 hours before cyclic voltammetry was performed.

Furthermore, when looking at the CA, none of the typical features of biofilm formation (Fig. 10) were observed. A comparison between current density and salinity revealed a clear positive linear correlation (R2=0.88) (Fig. 11), which is the opposite of the response of biofilm cells. Moreover, the highest current density for planktonic (105 uA) nearly doubles the density of the biofilm's highest density. The extracellular electron transfer exhibited by planktonic cells of electroactive bacteria is not a new phenomenon, and it was previously reported after growing this strain in the presence of an electroconductive fluidized bed (Manchon, Asensio, et al., 2023; Manchon, Muniesa-Merino, Llorente, et al., 2023; Manchon, Muniesa-Merino, Serna, et al., 2023; Llorente et al., 2024). Furthermore, G. sulfurreducens grown exponentially in the presence of salt showed an increased ability to interchange electrons with an electrode (Borjas, 2016) without an acclimation period to the electrode. Indeed, microbial growing conditions seem to be vital for performing EET. It has been previously shown that G. sulfurreducens grown in a chemostat can reduce the start-

up time of microbial electrochemical systems and produce higher current densities than batch-grown cells (Borjas *et al.*, 2015).

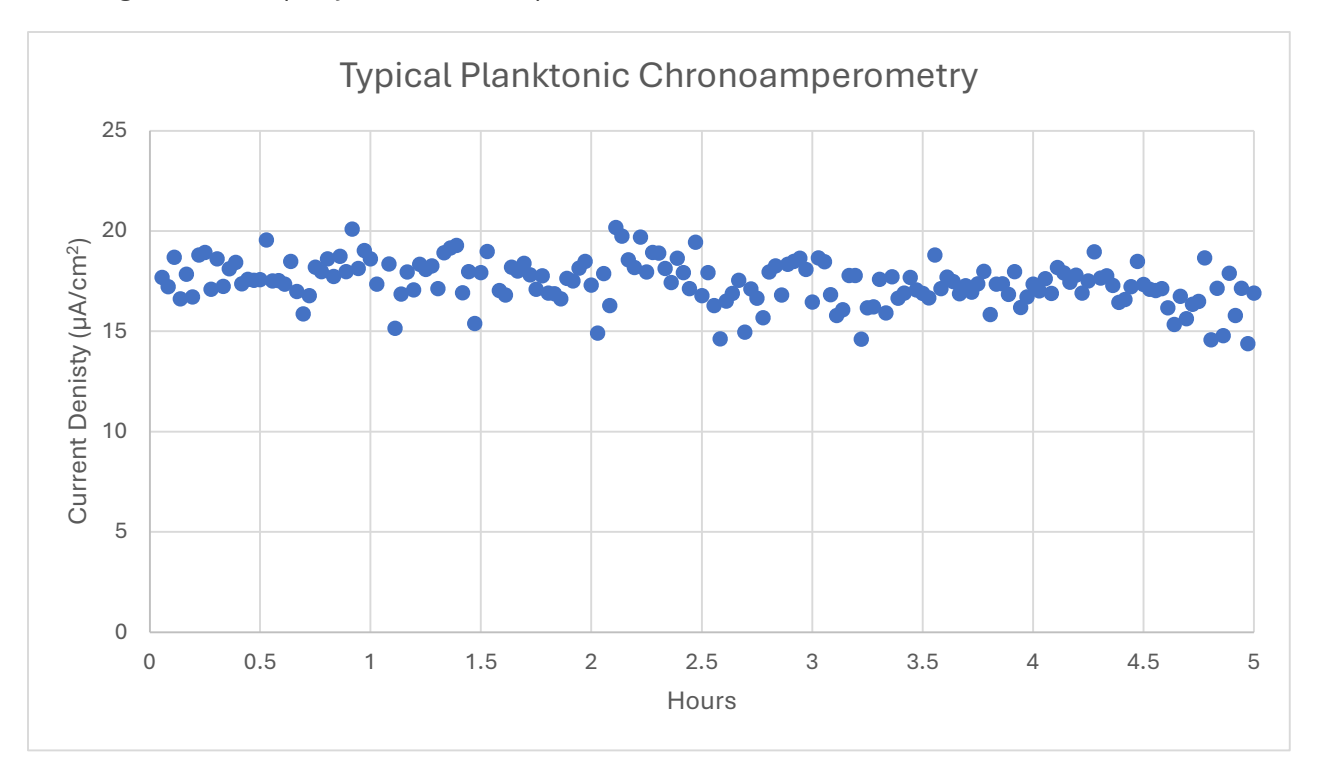


Figure 10: An example of the planktonic CA poised at 0.2 V for 5 hours at 2 g/L NaCl.

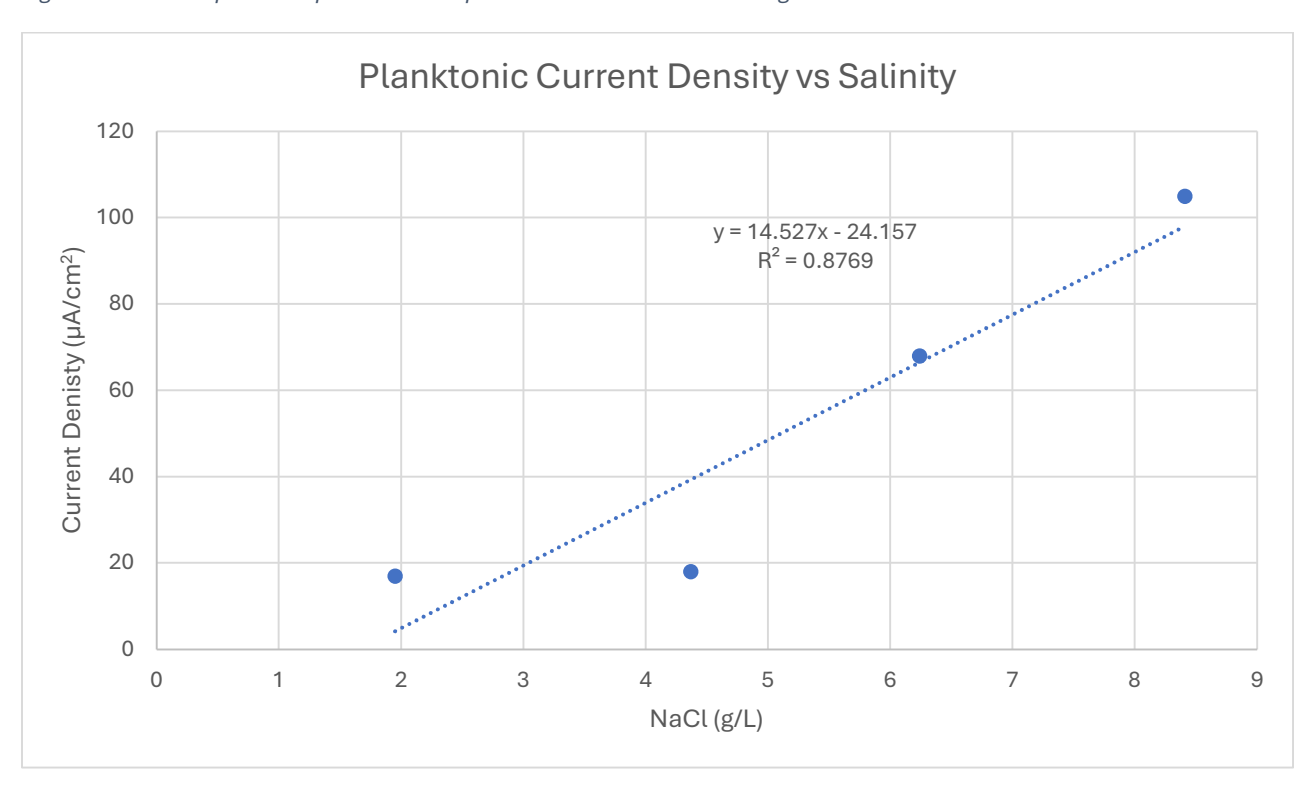


Figure 11: Planktonic G. sulfurreducens shows a positive correlation between current density and salinity.

Furthermore, cells grown exponentially in chemostats are known to overexpress cytochrome C (Esteve-Núñez et al., 2011), which could further explain the greater ability of the planktonic cells to respire the electrode. It appears that that is the situation here. When looking at the CV for the planktonic *G. sulfurreducens* at different salinity levels, there was a clear interaction with the electrode between 0.3 - 0.5 V when the voltammogram read returned to 0 V (Fig. 12). This oxidative/reductive peak was a clear sign of planktonic interaction due to its absence from an abiotic CV. Unlike the biofilm, the typical sigmoidal shape observed in a turnover CV was absent in the planktonic CV. No inflection point at -0.34 V in the planktonic CVs corresponded to the reduction and oxidative reactions with acetate. This lack of sigmoidal shape and inflection point and the presence of an oxidative/reductive peak show clear evidence that the planktonic cells interact with the electrode but do not form a biofilm during the 5 hours of the assay.

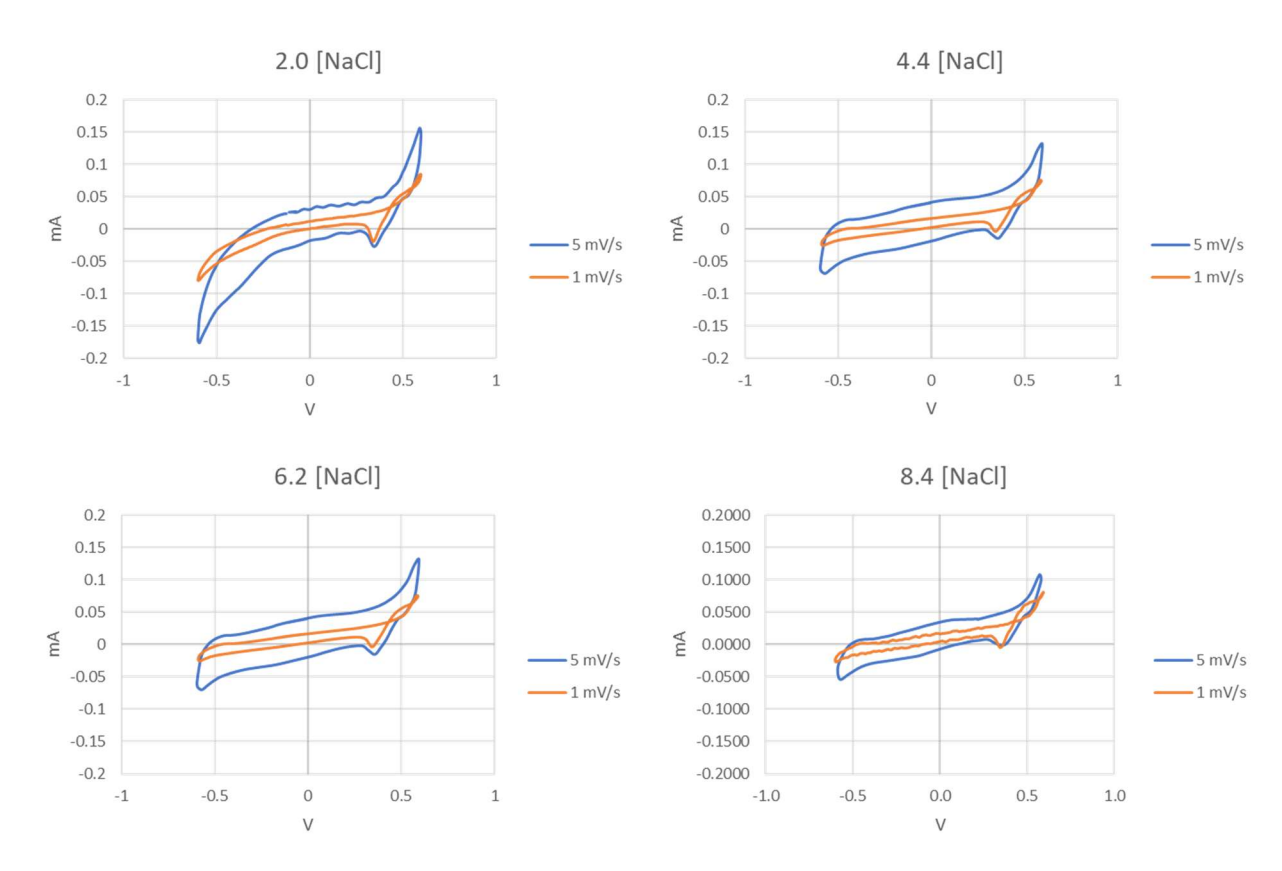


Figure 12: CVs from planktonic cells exposed to different salinities.

4 - Conclusions

Overall, salinity has very different effects on the respiration of a working electrode by *G. sulfurreducens*, depending on its growth-associated physiology. As a biofilm, *G. sulfurreducens*' defense against osmotic stress, such as the production of EPS, while protecting the cell from harm, decreases its ability to respire the electrode, most likely due to reduced availability of an electron donor. Furthermore, salinity may decrease the cell density of the biofilm. This fundamental suppression of the metabolism leads to a reduction in the current density. By contrast, the planktonic *G. sulfurreducens* increases its ability to respire the working electrode as salinity increases. This ability is likely due to the increased presence of EPS but the lack of mass transfer limitation caused by biofilm formation. The gradostat has shown that it can maintain a stable gradient of a solute of interest, that it can grow *G. sulfurreducens*, that it is capable of adapting to *G. sulfurreducens* high saline environments in a short amount of time, and allow for the study of the effects of salinity on *G. sulfurreducens* ability to respire an electrode.

Chapter 6:

General Discussion, Conclusions, and Future Work

General Discussion

The main objective of this thesis is to demonstrate the potential of microbial electrochemical technologies (METs) in addressing environmental and industrial challenges such as wastewater management, wastewater (WW) treatment, and water scarcity. The research presented here strongly supports the idea that METs can effectively monitor water quality, treat WW, and direct the evolution of microbes and microbial communities for processes like bioelectrochemical water desalination and WW treatment. This discussion, structured in a question-and-answer format, will show the practical benefits of METs.

How can METs significantly enhance the monitoring of contaminated sites in real time?

In Chapter 2, this thesis focuses on the abilities of METs to determine the *in situ* biological activity of sediments in real time. To accomplish this goal, an anode-resistor-cathode or microbial fuel cell (MFC)-based biosensor was used to examine the biological activity of three sediment types.

The goal of the MFC biosensor was to show that metabolic rates, or, in this case, acetate turnover rates, could be directly correlated to the electrical current produced by the MFC. Conventional methods of determining the metabolic rates in anaerobic subsurface environments are time consuming. They require detailed analysis of molecules and metabolites, which need complex procedures and highly technical apparatuses. Furthermore, different methods and equipment can affect the observed metabolic rates (Chapelle and Lovley, 1990; Phelps et al., 1994). The metabolic processes of subsurface microbes are critical to understanding the movement of contamination plumes by monitoring for increases in organic matter that increase microbial metabolism or a toxin that may slow microbial metabolism. The MFC allows metabolism to be turned into a signal that can be monitored, even remotely, in real time.

It is demonstrated that independent of the terminal electron-accepting process in the surrounding sediment, the MFC can determine the turnover rate of acetate. Acetate is the most common and vital intermediate in anaerobic sediments for microbial metabolism (Lovley and Chapelle, 1995). The MFC showed a strong linear correlation between the current generated and acetate turnover rates in sediments where the following reduction processes were predominant: methanogenic ($R^2 = 0.86$), Fe-reducing ($R^2 = 0.74$), and sulfate-reducing ($R^2 = 0.77$).

These results align with MFC biosensors' ability to respond to changes in BOD. MFC biosensors have been calibrated to be used across a variety of feedstock. Like changing terminal electron-accepting processes, the MFC can be used in various urban and commercial WWs. Furthermore, this biosensor can measure BOD concentration within the error limit of conventional tests (Salvian *et al.*, 2024). MFC biosensors can detect changes in organic matter reliably over long timelines in raw WW (Spurr *et al.*, 2021), as in this study with sediments.

This application of METs allows *in-situ* monitoring of subsurface sediments, aquifers, and marine environments. This monitoring can be done without needing more complex equipment than a data logger. Furthermore, it allows long-term monitoring of contamination plumes, chemical or oil pipelines, and storage tanks. This monitoring can all be achieved with sustainable materials and at a minimal cost. The MET-based biosensors are capable of protecting not only the environment but also the equipment that treats water entering our environment.

Can a poised-electrode biosensor determine the health of fast-changing treatment systems like anaerobic digestors?

Chapter 3 shows that the MEC-based biosensor can provide essential data to understand the health of a prevalent wastewater treatment method. The up-flow anaerobic sludge blanket (UASB) anaerobic digester is a stalwart for treating many types of WW. USAB can handle heavy but can be very sensitive to variations in organic loading rate (OLR) and pH (Tomei and Garrido, 2024). The conventional indicators monitored for stability are biogas production, pH, volatile fatty acids (VFAs), and chemical oxygen demands (COD) removal rates (Wu *et al.*, 2019). Most of these indicators, apart from pH, are slow to measure. The COD removal rate is a good indicator of USAB health (Li *et al.*, 2018). Therefore, the ability to monitor COD directly would help assess the health of the reactors.

As shown in Chapter 2, MFC-based biosensors can be used to monitor the biological activity of sediments; another type of biosensor can be used for more dynamic and changeable environments. The three-electrode microbial electrolysis cell or MEC-based biosensor has been shown to detect organic compounds like VFAs (Li *et al.*, 2018). Furthermore, this biosensor type can reliably detect COD (Estevez-Canales *et al.*, 2015). MEC biosensors have been shown to monitor the turnover rate of terminal electron donors (Estevez-Canales *et al.*, 2018). These abilities for sensitivity to VFA, COD, and terminal electron donors make the MEC ideal for monitoring the health of the USAB. The biosensor used in Chapter 3 detected COD concentration with a correlation coefficient of 0.85 and an R² of 0.72. This correlation shows that the current produced in the MEC biosensor increased or decreased to match COD concentrations. While other studies showed higher

levels of calculated correlation (Di Lorenzo *et al.*, 2009)(Salvian *et al.*, 2024), the above figures are similar to more real-world or pilot scale studies (Corbella *et al.*, 2019b). Monitoring the effluent with its low concentration of COD (Gao *et al.*, 2021) and the possibility of COD being less bioavailable (You *et al.*, 2015) these factors could increase the noise in the signal and decrease the observed correlation.

While COD is a good indicator of health for a USAB, the reaction of the sludge and the microbes therein to toxicity can take time to manifest as a change in COD concentration. It may take days from introducing a toxic biocide before the COD removal rate shows that the USAB was having a problem. It could take anywhere from 5 to 8 days before the problem could be identified. This lack of fidelity can cause severe damage to the system's granular sludge before mitigation can be applied. When an MEC biosensor was used to detect the presence of a biocide, it only took 6 hours to start showing effects on the signal produced by the biosensor. This level of response is close to real-time when compared to testing COD removal. These experiments were only a proof of concept, and further work needs to be done to validate this biosensor. Even at this stage in development, the MEC biosensor has excellent potential to increase detection speed by a degree of magnitude.

Can METs create the correct selective pressures to enable microorganisms to perform a specific task, such as treating austere and recalcitrant industrial waste like cutting oil and gasoline?

One of the challenges of METs is to have the right microbe or microbial community to complete the desired task. By creating the proper environment to select for the desired community, one can make a MET biofilter that can treat almost any contaminant. The METland concept has previously had great success with this. The METland concept combines the unique abilities of electroactive bacteria (EAB) with a well-known WW treatment technology, the treatment wetland. Using an electroconductive bed and a WW of interest, the METland has been able to treat a variety of WWs. First shown to treat urban WW (Aguirre-Sierra, Bacchetti-De Gregoris, Antonio Berná, et al., 2016), the METland could remove organic matter and nitrogen more efficiently than conventional treatment wetlands. Large-scale METlands have been shown to work in both northern and southern latitudes, including wastewater from urban and industrial sectors (Mosquera-Romero et al., 2023; Esteve-Núñez, 2025).

Furthermore, the METland concept has been applied to more resilient substances and has been able to treat them by selecting the correct microbial community (Noriega Primo, López-Heras and Esteve-Núñez, 2024). A horizontal flow METland-like biofilter could efficiently treat complex pharmaceutical and pesticide mixtures (Pun, Boltes, Letón and

Esteve-Nuñez, 2019; Pun et al., 2025). In Chapter 4, this same feat was accomplished with hydrocarbons (HCs).

Three electroactive biofilters were designed to create alternating aerobic and anaerobic electroconductive filter beds. The concept was to create conditions for different microbial communities to form and treat an austere and recalcitrant HC WW media. The reactors were iterative, building one concept off of the other. The first had an aerobic bed followed by an anaerobic bed, while the second reversed that with an anaerobic bed followed by an aerobic bed. All the beds were connected by electroconductive material to allow electrons from the treatment process to naturally form redox potentials between anodic and cathodic zones, depending on the processes involved. This segregation of bed types further allowed for the selection of more specialized communities. The third and final reactor was a combination of the previous two. It started with an anaerobic bed, an aerobic bed, and a second anaerobic bed. Ultimately, this configuration allowed for efficient treatment of emulsified oils, alkanes, and alkenes. COD removal efficiency of 86 ± 1 % and a rate of 88 ± 1 gCOD/m³*day were observed. The biofilter also could achieve 100% nitrification at a rate of 3.1 ± 0.1 gNH₄-N/m³*day. Furthermore, different but well-conserved microbial communities could develop by alternating the oxic state of the beds.

Almost all of the main genera of microbes, greater than 2.5% of total abundance, in the different biofilters were microbes that were either abundant in or isolated from HC-contaminated environments or could degrade HCs. This conservation causes a similar pattern in the aerobic and anaerobic sections of the biofilter.

A combination of the 8 genera were present in all the aerobic sections of the 3 biofilters: Reyranella, Bradyrhizobium, Parvibaculum, Nitrospira, Opitutus, Mycobacterium, Nitrosospira, and Aridibacter. Of these, Parvibaculum(Looper et al., 2013), Mycobacterium (Yuan et al., 2018), and Bradyrhizobium (Sandhu, Paul and Jha, 2022) are genera known to have alkane or polycyclic aromatic hydrocarbon (PAH) degraders. Nitrospira has been shown to be critical to communities involved in PAH degradation (Geng et al., 2020). Reyranella(Ning, Cai and Zhang, 2024), Opitutus (Sun et al., 2015), Aridibacter (Ren et al., 2024), and Nitrosospira (Figuerola and Erijman, 2010) have been isolated from or found in high abundance at HC-contaminated sites or aquifers.

A similar pattern was seen in the anaerobic sections of the three biofilter with 10 genera: Chryseobacterium, Delftia, Comamonas, Bradyrhizobium, Parvibaculum, Geobacter, Cupriavidus, Caulobacter, Oligotropha, and Azospira. Of these genera, Delftia, Comamonas, Cupriavidus, Caulobacter, Chryseobacterium, Oligotropha, Azospira, and Geobacter are not seen in the aerobic sections. Delftia (Vásquez-Piñeros et al., 2018; Ye et al., 2019; Lenchi et al., 2020; Eren and Güven, 2022), Comamonas (Jiang et al., 2023),

Cupriavidus (Bacosa et al., 2021), and Caulobacter (Al-Thukair and Malik, 2016) have been shown to degrade PAHs, alkanes, and transportations fuels like diesel. While Chryseobacterium had been isolated from many HC-contaminated environments (Szoboszlay et al., 2008; Benmalek et al., 2010; Hugo et al., 2019). The most important for an electroconductive biofilter is Geobacter. Geobacter is more than a model organism for extracellular electron transfer (Gralnick and Bond, 2023) but acts as a keystone microbe for the transfer of electrons from heterotrophs of a biofilm to the conductive material to which it is attached (Tejedor-Sanz et al., 2018). Without Geobacter, the movement of electrons through the conductive bed to form redox gradients (Ramírez-Vargas et al., 2018; Peñacoba-Antona et al., 2022a) through the process of conductive-particle-mediated interspecies electron transfer (Prado de Nicolás, Berenguer and Esteve-Núñez, 2022) could be greatly reduced or impossible.

Electroactive biofilters have shown great success in terms of scalability. The METland was able to transition from a laboratory-scale electroconductive biofilter (Prado de Nicolás, Berenguer and Esteve-Núñez, 2022) to a full-scale treatment option (Peñacoba-Antona et al., 2022b; Esteve-Núñez, 2025) for residential WW treatment. Beyond scalability, METlands and electroconductive biofilters can be placed geographically to optimize their efficiency and minimize their environmental impact (Peñacoba-Antona, Gómez-Delgado and Esteve-Núñez, 2021). Furthermore, this technology has been shown to have similar environmental impacts as other nature-based treatment options, which are ideal for where lower energy expenditure and high efficiency are required. The electroconductive biofilter has a significantly lower environmental impact than conventional treatment methods like activated sludge. The environmental impact of the METland has been confirmed using Life Cycle Assessment and Net Eutrophication Balance (Peñacoba-Antona et al., 2021). These factors, along with the electroconductive biofilter's ability to use already existing infrastructure, such as old constructed wetlands and conventional biofilters, give this technology many advantages over other conventional treatment methods.

In the end, the electroconductive material, design of the reactors, and manipulation of access to oxygen selected a specialized microbial community for the efficient treatment of HC WW.

If METs can select entire microbial communities for a task, can they adapt or evolve a single microbe to a selective pressure of choice?

Adapting or selecting microbial phenotypes for a specific purpose is lengthy and costly. The process requires large amounts of work. First, a single round of mutation or selective pressure is applied, followed by gene expression, screening, and replication. One round of this process can take days or longer and requires constant monitoring and interaction from

the researcher (Esvelt, Carlson and Liu, 2011). Continuous culture can improve this by increasing the mutation rate, but it can only supply a single condition and will select for the majority phenotype. This method does not allow the isolation of the minority phenotype that may be better adapted to the selective pressure of interest. The gradostat can solve this issue.

In brief, the gradostat uses an interconnected set of chemostats to create a gradient of selective pressure (Lovitt and Wimpenny, 1981). In Chapter 5, merging the single-chamber 3-electrode MEC concept with the gradostat allows it to apply a gradient of selective pressures while simultaneously selecting for electroactive bacteria. This system has applications like selecting for saline tolerance in microbes used for microbial desalination cells (MDC) (Ramírez-Moreno, Esteve-Núñez and Ortiz, 2021). Chapter 5 focuses on the effects of salinity on *Geobacter sulfurreducens* and its ability for extracellular electron transfer. It shows that salinity's impact can be elucidated for biofilms growing on the electrode and for planktonic cells.

Chapter 5 shows that the gradostat can maintain a stable salinity gradient and grow G. sulfurreducens in saline conditions. Furthermore, salinity has a marked effect on G. sulfurreducens ability to transfer electrons extracellular, and the effect depends on whether the cells were grown in a biofilm or planktonically. The current density of the biofilm at low salinity (0.7 g/L NaCl) is $58.6~\mu\text{A/cm}^2$, but when exposed to high salinity (15.2 g/L NaCl), the biofilms only generate $5.1~\mu\text{A/cm}^2$. That is a tenfold decrease in current density, and over that range of salinity, there is a robust negative linear correlation (R²=0.94) for the intermediate salinities tested. For the planktonic cells, there is a much different effect.

Planktonic cells at low salinity (2.0 g/L NaCl) had a very low current density of 17.0 μ A/cm². While the highest salinity (8.4 g/L NaCl) had the highest current density of 105 μ A/cm². The salinity and current density relationship had a strong positive linear correlation (R²=0.88). These two opposite responses show that osmotic stress affects *G. sulfurreducens* differently based on the growth mode. As a biofilm, *G. sulfurreducens*' defense against osmotic stress, such as the production of EPS, while protecting the cells from harm, decreases its ability to respire the electrode, most likely due to reduced availability of an electron donor. This fundamental suppression of the metabolism leads to a reduction in the current density. By contrast, the planktonic *G. sulfurreducens* increases its ability to respire the working electrode as salinity increases. This ability is likely due to the increased presence of EPS but the lack of mass transfer limitation caused by biofilm formation (Borjas, 2016).

Overall, Chapter 5 shows that this novel combination of the MEC and gradostat has excellent potential for the directed adaptation or evolution of microbes and microbial communities. It could adapt *G. sulfurreducens* to different saline conditions in as little as 5 days and to higher salinity than ever reported. This ability could increase the efficiency of many different METs by producing adapted microbes or microbial communities for specific applications.

Final Conclusions

The main conclusions presented in this thesis are as follows:

- An MFC-based biosensor can monitor the metabolic rates of microbes in sediments independent of the terminal electron-accepting process. This system can be used *in situ* and give data in real time.
- A MEC-based biosensor can monitor USAB's health by measuring the effluent's COD, giving real-time information on the system's microbial activity and health.
- MEC-based biosensors can react to toxins present in a USAB faster than granulated sludge and predict problems faster than other indicators like VFA and COD.
- Electroconductive biofilters can create an environment for treating austere and recalcitrant WWs by selecting for a community of microbes specially tailored to the task created by the biofilter's environment.
- HC-contaminated WW can be efficiently treated by alternating aerobic and anaerobic conditions in a single electroactive biofilter.
- Combining an MEC and a gradostat makes it possible to select minority community members and quickly adapt microbes to a chosen selective pressure.
- *G. sulfurreducens* ability to transfer electrons extracellularly responds differently to salinity depending on its growth form. Growing as a biofilm decreases *G.* sulfurreducens' ability to respire an electrode as salinity increases. When *G. sulfurreducens* is grown planktonically, salinity has the opposite effect; as salinity increases, so does its ability to respire an electrode.

Future Work

The main objective of this thesis was to show that by applying METs to various problems using various devices, one could protect the environment, improve treatment management, and increase treatment efficiency. These goals were achieved while also understanding how environments select for different microbial communities and how

microbes can be adapted to desired environments. Future research can be expanded upon the studies presented here in the following ways:

- The *in-situ* real-time subsurface biosensor can be a quantitative instrument with further research. The biosensor worked independently of the terminal electron-accepting process for the sediments in which it was used, but each of the signals produced was of a very different magnitude. Understanding further the effect of the terminal electron accepting on the signal and being able to calibrate the system to its environment could lead to a device that would not only give a qualitative understanding of the subsurface environment but also a quantitative one. Through collaboration with designers and engineers, the biosensor above could be refined into a viable product for research in remote locations and as an early warning system for oil pipelines.
- The MEC-based biosensor needs more research as it is a proof-of-concept. The first task would be to decrease the system's response time. Placing another biosensor in the influent line may increase the signal strength and reduce the USAB's exposure time to the toxic effects of a biocide. This placement would also allow for monitoring the influent COD and loading rates, which can affect the USAB's health. Furthermore, different potentials of the working electrode should be tested to see if sensitivity to biocides can be increased. Testing different stress conditions of the USAB outside of biocides and determining if the biosensor can detect conditions like overloading, starvation, and low temperature (Asensio, Llorente, Fernández, et al., 2021). Much can be tested, but the overall concept should work with the USAB and other anaerobic digester designs. Ideally, this system should be tested in a full-size anaerobic digestor to determine the viability of it as a warning system.
- The biofilters successfully used alternating aerobic and anaerobic conditions to treat HC WW. These systems allowed electrons to flow freely in different areas to increase removal efficiency. Understanding how this is happening would help improve the design and efficiency of these biofilters. Testing the redox potential of the flooded sections could shed light on how electrons flow in the system (Ramírez-Vargas et al., 2019). Further testing of different electroconductive bed materials like conductive biochar (Prado, Berenguer and Esteve-Núñez, 2019; Jiménez-Conde, 2024) could improve the microbial community and treatment efficiency. These biofilters should scale up well as has been seen with METLands from laboratory scale to full scale.
- The gradostat integrated with an MEC could adapt *G. sulfurreducens* to saline conditions and elucidate trends in extracellular electron transfer. Next, understanding the metabolic effects of the salinity on *G. sulfurreducens* would be of

Chapter 6: General Discussion, Conclusions, and Future Work

great importance. For example, understanding how the metabolomics of *G. sulfurreducens* change at different salinity would give an insight into how the tricarboxylic acid cycle is affected and if that is part of the reason for the differing current density at various salinities (Song *et al.*, 2016). Furthermore, different selective pressures on microbial communities, such as if the microbial communities of Chapter 4, could be replicated using an HC WW media. Ther gradostat has the potential to create custom communities for many applications in METs.

References

Abbasi, T. and Abbasi, S.A. (2012) 'Formation and impact of granules in fostering clean energy production and wastewater treatment in upflow anaerobic sludge blanket (UASB) reactors', *Renewable and Sustainable Energy Reviews*, 16(3), pp. 1696–1708. Available at: https://doi.org/10.1016/j.rser.2011.11.017.

Aguirre-Sierra, A., Bacchetti-De Gregoris, T., Berná, A., et al. (2016) 'Microbial electrochemical systems outperform fixed-bed biofilters in cleaning up urban wastewater', *Environmental Science: Water Research and Technology*, 2(6), pp. 984–993. Available at: https://doi.org/10.1039/c6ew00172f.

Aguirre-Sierra, A., Bacchetti-De Gregoris, T., Berná, Antonio, *et al.* (2016) 'Microbial electrochemical systems outperform fixed-bed biofilters in cleaning up urban wastewater', *Environmental Science: Water Research & Technology*, 2(6), pp. 984–993. Available at: https://doi.org/10.1039/C6EW00172F.

Aguirre-Sierra, A. et al. (2020) 'A new concept in constructed wetlands: Assessment of aerobic electroconductive biofilters', *Environmental Science: Water Research and Technology*, 6(5), pp. 1312–1323. Available at: https://doi.org/10.1039/c9ew00696f.

Akita, H., Shinto, Y. and Kimura, Z. (2022) 'Bacterial Community Analysis of Biofilm Formed on Metal Joint', *Applied Biosciences 2022, Vol. 1, Pages 221-228*, 1(2), pp. 221–228. Available at: https://doi.org/10.3390/APPLBIOSCI1020014.

Al-Thukair, A.A. and Malik, K. (2016) 'Pyrene metabolism by the novel bacterial strains Burkholderia fungorum (T3A13001) and Caulobacter sp (T2A12002) isolated from an oil-polluted site in the Arabian Gulf', *International Biodeterioration and Biodegradation*, 110, pp. 32–37. Available at: https://doi.org/10.1016/j.ibiod.2016.02.005.

Alva-Argáez, A., Kokossis, A.C. and Smith, R. (2007) 'The design of water-using systems in petroleum refining using a water-pinch decomposition', *Chemical Engineering Journal*, 128(1), pp. 33–46. Available at: https://doi.org/10.1016/j.cej.2006.10.001.

Alwared, A.I. and Jaber, W.S. (2020) 'Spiral path three phase fluidized bed reactor for treating wastewater contaminated with engine oil', *Applied Water Science*, 10(9), pp. 1–11. Available at: https://doi.org/10.1007/s13201-020-01290-4.

An, C. et al. (2017) 'Emerging usage of electrocoagulation technology for oil removal from wastewater: A review', *Science of The Total Environment*, 579, pp. 537–556. Available at: https://doi.org/10.1016/j.scitotenv.2016.11.062.

Anderson, R.T. *et al.* (2003) 'Stimulating the In Situ Activity of Geobacter Species to Remove Uranium from the Groundwater of a Uranium-Contaminated Aquifer', *Applied and Environmental Microbiology*, 69(10), pp. 5884–5891. Available at: https://doi.org/10.1128/AEM.69.10.5884-5891.2003.

Arantes, M.K. et al. (2017) 'Treatment of brewery wastewater and its use for biological

References

production of methane and hydrogen', *International Journal of Hydrogen Energy*, 42(42), pp. 26243–26256. Available at: https://doi.org/10.1016/j.ijhydene.2017.08.206.

Asensio, Y., Llorente, M., Sánchez-Gómez, A., *et al.* (2021) 'Microbial Electrochemical Fluidized Bed Reactor: A Promising Solution for Removing Pollutants From Pharmaceutical Industrial Wastewater', *Frontiers in Microbiology*, 12(November), pp. 1–10. Available at: https://doi.org/10.3389/fmicb.2021.737112.

Asensio, Y., Llorente, M., Fernández, P., et al. (2021) 'Upgrading fluidized bed bioelectrochemical reactors for treating brewery wastewater by using a fluid-like electrode', *Chemical Engineering Journal*, 406(July 2020). Available at: https://doi.org/10.1016/j.cej.2020.127103.

Avoigt, C., Kauffman, S. and Wang, Z.-G. (2001) 'Rational evolutionary design: The theory of in vitro protein evolution', in *Advances in Protein Chemistry*, pp. 79–160. Available at: https://doi.org/10.1016/S0065-3233(01)55003-2.

Bacosa, H.P. *et al.* (2021) 'Biodegradation of binary mixtures of octane with benzene, toluene, ethylbenzene or xylene (BTEX): insights on the potential of Burkholderia, Pseudomonas and Cupriavidus isolates', *World Journal of Microbiology and Biotechnology*, 37(7), pp. 1–8. Available at: https://doi.org/10.1007/S11274-021-03093-4/TABLES/2.

Badran, A.H. and Liu, D.R. (2015) 'In vivo continuous directed evolution', *Current Opinion in Chemical Biology*, 24, pp. 1–10. Available at: https://doi.org/10.1016/j.cbpa.2014.09.040.

Baldoni-Andrey, P. et al. (2006) 'Impact of high salinity of produced water on the technical feasibility of biotreatment for E&P onshore applications', 8th SPE International Conference on Health, Safety and Environment in Oil and Gas Exploration and Production 2006, 2, pp. 889–893.

Barlett, M. *et al.* (2012) 'Uranium reduction and microbial community development in response to stimulation with different electron donors', *Biodegradation*, 23(4), pp. 535–546. Available at: https://doi.org/10.1007/s10532-011-9531-8.

Benmalek, Y. *et al.* (2010) 'Chryseobacterium solincola sp. nov., isolated from soil', *International Journal of Systematic and Evolutionary Microbiology*, 60(8), pp. 1876–1880. Available at: https://doi.org/10.1099/ijs.0.008631-0.

Bond, Daniel R. and Lovley, D.R. (2003) 'Electricity Production by Geobacter sulfurreducens Attached to Electrodes', *Applied and Environmental Microbiology*, 69(3), pp. 1548–1555. Available at: https://doi.org/10.1128/AEM.69.3.1548-1555.2003.

Bond, Daniel R and Lovley, D.R. (2003) 'Electricity Production by Geobacter sulfurreducens Attached to Electrodes Electricity Production by Geobacter sulfurreducens Attached to Electrodes', *Applied and Environmental Microbiology*, 69(3), pp. 1548–1555. Available at: https://doi.org/10.1128/AEM.69.3.1548.

References

Borjas, Z. *et al.* (2015) 'Strategies for reducing the start-up operation of microbial electrochemical treatments of urban wastewater', *Energies*, 8(12), pp. 14064–14077. Available at: https://doi.org/10.3390/en81212416.

Borjas, Z. (2016) *Physiological and Operation Strategies for Optimizing Geobacter-based Electrochemical Systems*. University of Alcalá.

Borjas, Z., Esteve-Núñez, A. and Ortiz, J.M. (2017) 'Strategies for merging microbial fuel cell technologies in water desalination processes: Start-up protocol and desalination efficiency assessment', *Journal of Power Sources*, 356, pp. 519–528. Available at: https://doi.org/10.1016/j.jpowsour.2017.02.052.

Bose, D. et al. (2018) 'Analysis of sediment-microbial fuel cell power production in series and parallel configurations', *Nature Environment and Pollution Technology*, 17(1), pp. 311–314.

BP (2019) BP Statistical Review of World Energy Statistical Review of World.

Broadaway, B.J. and Hannigan, R.E. (2012) 'Elemental fingerprints used to identify essential habitats: Nantucket bay scallop', *Journal of Shellfish Research*, 31(3), pp. 671–676. Available at: https://doi.org/10.2983/035.031.0310.

Butler, J.E., Young, N.D. and Lovley, D.R. (2010) *Evolution of electron transfer out of the cell: comparative genomics of six Geobacter genomes*. Available at: http://www.biomedcentral.com/1471-2164/11/40 (Accessed: 23 April 2020).

Caccavo, F. et al. (1994) 'Geobacter sulfurreducens sp. nov., a hydrogen- and acetate-oxidizing dissimilatory metal-reducing microorganism.', *Applied and environmental microbiology*, 60(10), pp. 3752–9. Available at: https://doi.org/10.1128/aem.60.10.3752-3759.1994.

Call, D. and Logan, B.E. (2008) 'Hydrogen production in a single chamber microbial electrolysis cell lacking a membrane', *Environmental Science and Technology*, 42(9), pp. 3401–3406. Available at: https://doi.org/10.1021/es8001822.

Canfield, D.E. *et al.* (1993) 'Pathways of organic carbon oxidation in three continental margin sediments.', *Marine geology*, 113, pp. 27–40. Available at: http://www.ncbi.nlm.nih.gov/pubmed/11539842.

Cao, X. et al. (2009) 'A new method for water desalination using microbial desalination cells', *Environmental Science and Technology*, 43(18), pp. 7148–7152. Available at: https://doi.org/10.1021/es901950j.

Chapelle, F.H. *et al.* (1997) 'Practical considerations for measuring hydrogen concentrations in groundwater', *Environmental Science and Technology*, 31(10), pp. 2873–2877. Available at: https://doi.org/10.1021/es970085c.

Chapelle, F.H. and Lovley, D.R. (1990) 'Rates of microbial metabolism in deep coastal plain aquifers', *Applied and Environmental Microbiology*, 56(6), pp. 1865–1874. Available

at: https://doi.org/10.1128/aem.56.6.1865-1874.1990.

Chen, C. et al. (2019) 'Characterization of aerobic granular sludge used for the treatment of petroleum wastewater', *Bioresource Technology*, 271, pp. 353–359. Available at: https://doi.org/10.1016/J.BIORTECH.2018.09.132.

Chen, L. et al. (2021) 'Uncover the secret of granule calcification and deactivation in upflow anaerobic sludge bed (UASB) reactor with long-term exposure to high calcium', *Water Research*, 189, p. 116586. Available at: https://doi.org/10.1016/j.watres.2020.116586.

Coelho, A. *et al.* (2006) 'Treatment of petroleum refinery sourwater by advanced oxidation processes', *Journal of Hazardous Materials*, 137(1), pp. 178–184. Available at: https://doi.org/10.1016/j.jhazmat.2006.01.051.

Cooper, D.C. and Copeland, B.J. (1973) 'Responses of Continuous-Series Estuarine Microecosystems to Point-Source Input Variations', *Ecological Monographs*, 43(2), pp. 213–236. Available at: https://doi.org/10.2307/1942195.

Coppi, M. V. *et al.* (2001) 'Development of a Genetic System for Geobacter sulfurreducens', *Applied and Environmental Microbiology*, 67(7), pp. 3180–3187. Available at: https://doi.org/10.1128/AEM.67.7.3180-3187.2001.

Corbella, C. et al. (2019a) 'MFC-based biosensor for domestic wastewater COD assessment in constructed wetlands', *Science of the Total Environment*, 660, pp. 218–226. Available at: https://doi.org/10.1016/j.scitotenv.2018.12.347.

Corbella, C. et al. (2019b) 'MFC-based biosensor for domestic wastewater COD assessment in constructed wetlands', *Science of The Total Environment*, 660, pp. 218–226. Available at: https://doi.org/10.1016/J.SCITOTENV.2018.12.347.

Costa, N.L. *et al.* (2018) 'Electron transfer process in microbial electrochemical technologies: The role of cell-surface exposed conductive proteins', *Bioresource Technology*, 255, pp. 308–317. Available at: https://doi.org/10.1016/j.biortech.2018.01.133.

Crini, G. and Lichtfouse, E. (2019) 'Advantages and disadvantages of techniques used for wastewater treatment', *Environmental Chemistry Letters*, 17(1), pp. 145–155. Available at: https://doi.org/10.1007/s10311-018-0785-9.

Czudar, A. *et al.* (2011) 'Removal of Organic Materials and Plant Nutrients in a Constructed Wetland for Petrochemical Wastewater Treatment', 21(1), pp. 109–114.

Deatherage, D.E. et al. (2017) 'Specificity of genome evolution in experimental populations of Escherichia coli evolved at different temperatures', (4). Available at: https://doi.org/10.1073/pnas.1616132114.

Diya'uddeen, B.H. *et al.* (2011) 'Treatment technologies for petroleum refinery effluents: A review', *Process Safety and Environmental Protection*, 89(2), pp. 95–105. Available at: https://doi.org/10.1016/j.psep.2010.11.003.

Do, M.H. et al. (2020) 'Performance of mediator-less double chamber microbial fuel cell-based biosensor for measuring biological chemical oxygen', *Journal of Environmental Management*, 276(August), p. 111279. Available at: https://doi.org/10.1016/j.jenvman.2020.111279.

El-Naas, M.H. *et al.* (2009) 'Assessment of electrocoagulation for the treatment of petroleum refinery wastewater', *Journal of Environmental Management*, 91(1), pp. 180–185. Available at: https://doi.org/10.1016/j.jenvman.2009.08.003.

Erable, B., Etcheverry, L. and Bergel, A. (2011) 'From microbial fuel cell (MFC) to microbial electrochemical snorkel (MES): maximizing chemical oxygen demand (COD) removal from wastewater.', *Biofouling*, 27(3), pp. 319–326. Available at: https://doi.org/10.1080/08927014.2011.564615.

Eren, A. and Güven, K. (2022) 'Isolation and characterization of alkane hydrocarbons-degrading Delftia tsuruhatensis strain D9 from petroleum-contaminated soils', *Biotech Studies*, 31(1), pp. 36–44. Available at: https://doi.org/10.38042/biotechstudies.1103695.

Espinosa, M.I. *et al.* (2020) 'Adaptive laboratory evolution of native methanol assimilation in Saccharomyces cerevisiae', *Nature Communications*, 11(1). Available at: https://doi.org/10.1038/s41467-020-19390-9.

Esteve-Núñez, A. et al. (2011) 'Opportunities behind the unusual ability of geobacter sulfurreducens for exocellular respiration and electricity production', *Energy and Environmental Science*, 4(6), pp. 2066–2069. Available at: https://doi.org/10.1039/c1ee01067k.

Esteve-Núñez, A. (2025) 'Bioelectrochemically assisted constructed wetlands: the METland concept', *Emerging Developments in Constructed Wetlands*, pp. 293–310. Available at: https://doi.org/10.1016/B978-0-443-14078-5.00011-8.

Estevez-Canales, M. *et al.* (2015) 'Screen-printed electrodes: New tools for developing microbial electrochemistry at microscale level', *Energies*, 8(11), pp. 13211–13221. Available at: https://doi.org/10.3390/en81112367.

Estevez-Canales, M. *et al.* (2018) 'Silica immobilization of Geobacter sulfurreducens for constructing ready-to-use artificial bioelectrodes', *Microbial Biotechnology*, 11(1), pp. 39–49. Available at: https://doi.org/10.1111/1751-7915.12561.

Esvelt, K.M., Carlson, J.C. and Liu, D.R. (2011) 'A system for the continuous directed evolution of biomolecules', *Nature*, 472(7344), pp. 499–503. Available at: https://doi.org/10.1038/nature09929.

Fakhru'l-Razi, A. *et al.* (2009) 'Review of technologies for oil and gas produced water treatment', *Journal of Hazardous Materials*, 170(2–3), pp. 530–551. Available at: https://doi.org/10.1016/j.jhazmat.2009.05.044.

Figuerola, E.L.M. and Erijman, L. (2010) 'Diversity of nitrifying bacteria in a full-scale petroleum refinery wastewater treatment plant experiencing unstable nitrification', *Journal*

of Hazardous Materials, 181(1–3), pp. 281–288. Available at: https://doi.org/10.1016/j.jhazmat.2010.05.009.

Freire, D.D.C., Cammarota, M.C. and Sant'Anna, G.L. (2001) 'Biological treatment of oil field wastewater in a sequencing batch reactor', *Environmental Technology*, 22(10), pp. 1125–1135. Available at: https://doi.org/10.1080/09593332208618203.

Fricke, K., Harnisch, F. and Schröder, U. (2008) 'On the use of cyclic voltammetry for the study of anodic electron transfer in microbial fuel cells', *Energy and Environmental Science*, 1(1), pp. 144–147. Available at: https://doi.org/10.1039/b802363h.

Gaki, A. et al. (2009) 'Complex dynamics of microbial competition in the gradostat', *Journal of Biotechnology*, 139(1), pp. 38–46. Available at: https://doi.org/10.1016/j.jbiotec.2008.08.006.

Gao, Y. et al. (2021) 'Enhancing sensitivity of microbial fuel cell sensors for low concentration biodegradable organic matter detection: Regulation of substrate concentration, anode area and external resistance', *Journal of Environmental Sciences (China)*, 101, pp. 227–235. Available at: https://doi.org/10.1016/j.jes.2020.08.020.

Garbini, G.L., Barra Caracciolo, A. and Grenni, P. (2023) 'Electroactive Bacteria in Natural Ecosystems and Their Applications in Microbial Fuel Cells for Bioremediation: A Review', *Microorganisms*, 11(5). Available at: https://doi.org/10.3390/microorganisms11051255.

Geng, S. et al. (2020) 'Microbial diversity and co-occurrence patterns in deep soils contaminated by polycyclic aromatic hydrocarbons (PAHs)', *Ecotoxicology and Environmental Safety*, 203(July), p. 110931. Available at: https://doi.org/10.1016/j.ecoenv.2020.110931.

Gong, Y. et al. (2013) 'Sul fi de-Driven Microbial Electrosynthesis'.

Gralnick, J.A. and Bond, D.R. (2023) 'Electron Transfer beyond the Outer Membrane: Putting Electrons to Rest', *Annual Review of Microbiology*, 77, pp. 517–539. Available at: https://doi.org/10.1146/annurev-micro-032221-023725.

Haandel, A.C. van and Lubbe, J.G.. van der (2012) *Handbook of Biological Wastewater Treatment: Design and Optimisation of Activated Sludge Systems*. 2nd edn. London: IWA Publishing.

Hayes, L.A., Nevin, K.P. and Lovley, D.R. (1999) 'Role of prior exposure on anaerobic degradation of naphthalene and phenanthrene in marine harbor sediments', *Organic Geochemistry*, 30(8 B), pp. 937–945. Available at: https://doi.org/10.1016/S0146-6380(99)00077-7.

van Hees, W. (1965) 'A Bacterial Methane Fuel Cell', *Journal of The Electrochemical Society*, 112(3), p. 258. Available at: https://doi.org/10.1149/1.2423519.

Hoareau, M., Erable, B. and Bergel, A. (2019) 'Microbial electrochemical snorkels (MESs): A budding technology for multiple applications. A mini review', *Electrochemistry*

Communications, 104(May), p. 106473. Available at: https://doi.org/10.1016/j.elecom.2019.05.022.

Holmes, D.E., Bond, D.R. and Lovley, D.R. (2004) 'Electron Transfer by Desulfobulbus propionicus to Fe(III) and Graphite Electrodes', *Applied and Environmental Microbiology*, 70(2), pp. 1234–1237. Available at: https://doi.org/10.1128/AEM.70.2.1234-1237.2004.

Hugo, C. et al. (2019) Chryseobacterium, Bergey's Manual of Systematics of Archaea and Bacteria. Available at: https://doi.org/10.1002/9781118960608.gbm00301.pub2.

Ingelman, H. et al. (2024) 'Autotrophic adaptive laboratory evolution of the acetogen Clostridium autoethanogenum delivers the gas-fermenting strain LAbrini with superior growth, products, and robustness', *New Biotechnology*, 83(April), pp. 1–15. Available at: https://doi.org/10.1016/j.nbt.2024.06.002.

Jafarinejad, S. (2017) 'Recent developments in the application of sequencing batch reactor (SBR) technology for the petroleum industry wastewater treatment', *Chem. Int.*, 3(3), pp. 342–350.

Jager, W. et al. (1987) 'Competition in the gradostat', *Journal of Mathematical Biology*, 25(1), pp. 23–42. Available at: https://doi.org/10.1007/BF00275886.

Jiang, F. *et al.* (2023) 'Exploration of potential driving mechanisms of Comamonas testosteroni in polycyclic aromatic hydrocarbons degradation and remodelled bacterial community during co-composting', *Journal of Hazardous Materials*, 458(May), p. 132032. Available at: https://doi.org/10.1016/j.jhazmat.2023.132032.

Jiménez-Conde, M. (2024) Electrobioremediation Strategies for Removing Nitrogen and Emerging Pollutants in Urban Wastewater: The METland Solution as Tertiary & Quaternary Treatment. University of Alcalá.

Kadier, A. *et al.* (2016) 'A comprehensive review of microbial electrolysis cells (MEC) reactor designs and configurations for sustainable hydrogen gas production', *Alexandria Engineering Journal*, 55(1), pp. 427–443. Available at: https://doi.org/10.1016/j.aej.2015.10.008.

Kadlec, R. and Wallace, S. (2001) 'Treatment Wetlands', *Angewandte Chemie International Edition*, 40(6), p. 9823. Available at: https://doi.org/10.1002/1521-3773(20010316)40:6<9823::AID-ANIE9823>3.3.CO;2-C.

Kuyukina, M.S., Krivoruchko, A. V. and Ivshina, I.B. (2020) 'Advanced bioreactor treatments of hydrocarbon-containing wastewater', *Applied Sciences (Switzerland)*, 10(3). Available at: https://doi.org/10.3390/app10030831.

Kuzume, A. et al. (2014) 'An in situ surface electrochemistry approach towards whole-cell studies: The structure and reactivity of a Geobacter sulfurreducens submonolayer on electrified metal/electrolyte interfaces', *Physical Chemistry Chemical Physics*, 16(40). Available at: https://doi.org/10.1039/c4cp03357d.

Lai, Q. et al. (2011) 'Parvibaculum indicum sp. nov., isolated from deep-sea water', International Journal of Systematic and Evolutionary Microbiology, 61(2), pp. 271–274. Available at: https://doi.org/10.1099/IJS.0.021899-0/CITE/REFWORKS.

LaPanse, A.J., Krishnan, A. and Posewitz, M.C. (2021) 'Adaptive Laboratory Evolution for algal strain improvement: methodologies and applications', *Algal Research*, 53(November 2020), p. 102122. Available at: https://doi.org/10.1016/j.algal.2020.102122.

Lee, H.H. *et al.* (2010) 'Bacterial charity work leads to population-wide resistance', *Nature*, 467(7311), pp. 82–85. Available at: https://doi.org/10.1038/nature09354.

Lenchi, N. *et al.* (2020) 'Diesel Biodegradation Capacities and Biosurfactant Production in Saline-Alkaline Conditions by Delftia sp NL1, Isolated from an Algerian Oilfield', *Geomicrobiology Journal*, 37(5), pp. 454–466. Available at: https://doi.org/10.1080/01490451.2020.1722769.

Leong, M.L. *et al.* (2011) 'Sludge characteristics and performances of the sequencing batch reactor at different influent phenol concentrations', *Desalination*, 270(1–3), pp. 181–187. Available at: https://doi.org/10.1016/j.desal.2010.11.043.

Li, L. *et al.* (2018) 'Anaerobic digestion of food waste: A review focusing on process stability', *Bioresource Technology*, 248(174), pp. 20–28. Available at: https://doi.org/10.1016/j.biortech.2017.07.012.

Li, T. et al. (2016) 'Bioelectrochemical Sensor Using Living Biofilm to in Situ Evaluate Flocculant Toxicity', *ACS Sensors*, 1(11), pp. 1374–1379. Available at: https://doi.org/10.1021/acssensors.6b00571.

Liesack, W., Schnell, S. and Revsbech, N.P. (2000) 'Microbiology of flooded rice paddies', *FEMS Microbiology Reviews*, 24(5), pp. 625–645. Available at: https://doi.org/10.1016/S0168-6445(00)00050-4.

Lin, W.C., Coppi, M. V. and Lovley, D.R. (2004) 'Geobacter sulfurreducens Can Grow with Oxygen as a Terminal Electron Acceptor', *Applied and Environmental Microbiology*, 70(4), pp. 2525–2528. Available at: https://doi.org/10.1128/AEM.70.4.2525-2528.2004.

Liu, H. and Logan, B.E. (2004) 'Electricity generation using an air-cathode single chamber microbial fuel cell (MFC) in the absence of a proton exchange membrane', *ACS National Meeting Book of Abstracts*, 228(1), pp. 4040–4046. Available at: https://doi.org/10.1021/es0499344.

Llorente, M. et al. (2024) 'Novel electrochemical strategies for the microbial conversion of CO2 into biomass and volatile fatty acids using a fluid-like bed electrode in a three-phase reactor', *Microbial Biotechnology*, 17(1), pp. 1–13. Available at: https://doi.org/10.1111/1751-7915.14383.

Logan, B.E. *et al.* (2006) 'Microbial fuel cells: Methodology and technology', *Environmental Science and Technology*, 40(17), pp. 5181–5192. Available at: https://doi.org/10.1021/es0605016.

Logan, B.E. *et al.* (2015) 'Assessment of Microbial Fuel Cell Configurations and Power Densities', *Environmental Science & Technology Letters*, 2(8), pp. 206–214. Available at: https://doi.org/10.1021/acs.estlett.5b00180.

Looper, J.K. *et al.* (2013) 'Microbial community analysis of Deepwater Horizon oil-spill impacted sites along the Gulf coast using functional and phylogenetic markers', *Environmental Sciences: Processes and Impacts*, 15(11), pp. 2068–2079. Available at: https://doi.org/10.1039/c3em00200d.

Di Lorenzo, M. *et al.* (2009) 'A single-chamber microbial fuel cell as a biosensor for wastewaters', *Water Research*, 43(13), pp. 3145–3154. Available at: https://doi.org/10.1016/j.watres.2009.01.005.

Lovitt, R.W. and Wimpenny, J.W.. (1981) The Gradostat: a Bidirectional Compound Chemostat and its Application in Microbiological Research, Journal of General Microbiology.

Lovitt, R.W. and Wimpenny, J.W.T. (1981) *Physiological Behaviour of Escherichia coli Grown in Opposing Gradients of Oxidant and Reductant in the Gradostat, Journal of General Microbiology*.

LOVITT, R.W. and WIMPENNY, J.W.T. (1981) 'The Gradostat: a Bidirectional Compound Chemostat and its Application in Microbiological Research', *Microbiology*, 127(2), pp. 261–268. Available at: https://doi.org/10.1099/00221287-127-2-261.

Lovley, D.D.R. and Goodwin, S. (1988) 'Hydrogen concentrations as an indicator of the predominant terminal electron-accepting reactions in aquatic sediments', *Geochimica et Cosmochimica Acta*, 52(Iv), pp. 2993–3003. Available at: https://doi.org/10.1016/0016-7037(88)90163-9.

Lovley, D.R. (2003) 'Cleaning up with genomics: Applying molecular biology to bioremediation', *Nature Reviews Microbiology*, 1(1), pp. 35–44. Available at: https://doi.org/10.1038/nrmicro731.

Lovley, D.R. et al. (2011) Geobacter: the microbe electric's physiology, ecology, and practical applications., Advances in microbial physiology. Available at: https://doi.org/10.1016/B978-0-12-387661-4.00004-5.

Lovley, D.R. and Chapelle, F.H. (1995) 'Deep subsurface microbial processes', *Reviews of Geophysics*, 33(3), p. 365. Available at: https://doi.org/10.1029/95RG01305.

Lovley, D.R., Chapelle, F.H. and Woodward, J.C. (1994) 'Use of Dissolved H2 Concentrations To Determine Distribution of Microbially Catalyzed Redox Reactions in Anoxic Groundwater', *Environmental Science and Technology*, 28(7), pp. 1205–1210. Available at: https://doi.org/10.1021/es00056a005.

Lovley, D.R. and Klug, M.J. (1983) 'Sulfate reducers can outcompete methanogens at freshwater sulfate concentrations', *Applied and Environmental Microbiology*, 45(1), pp. 187–192. Available at: https://doi.org/10.1128/aem.45.1.187-192.1983.

Lovley, D.R. and Klug, M.J. (1986) 'Model for the distribution of sulfate reduction and methanogenesis in freshwater sediments', *Geochimica et Cosmochimica Acta*, 50(1), pp. 11–18. Available at: https://doi.org/10.1016/0016-7037(86)90043-8.

Lovley, D.R. and Phillips, E.J.P. (1987) 'Competitive Mechanisms for Inhibition of Sulfate Reduction and Methane Production in the Zone of Ferric Iron Reduction in Sediments', *Applied and Environmental Microbiology*, 53(11), pp. 2636–2641. Available at: https://doi.org/10.1128/aem.53.11.2636-2641.1987.

Lovley, D.R. and Phillips, E.J.P. (1988) 'Novel Mode of Microbial Energy Metabolism: Organic Carbon Oxidation Coupled to Dissimilatory Reduction of Iron or Manganese', *Applied and Environmental Microbiology*, 54(6), pp. 1472–1480. Available at: https://doi.org/10.1128/aem.54.6.1472-1480.1988.

Lu, J. et al. (2022) 'Transformation and toxicity dynamics of polycyclic aromatic hydrocarbons in a novel biological-constructed wetland-microalgal wastewater treatment process', *Water Research*, 223(June), p. 119023. Available at: https://doi.org/10.1016/j.watres.2022.119023.

Mainardis, M., Buttazzoni, M. and Goi, D. (2020) 'Up-flow anaerobic sludge blanket (Uasb) technology for energy recovery: A review on state-of-the-art and recent technological advances', *Bioengineering*, 7(2). Available at: https://doi.org/10.3390/bioengineering7020043.

Malvankar, N.S. *et al.* (2011) 'Tunable metallic-like conductivity in microbial nanowire networks', *Nature Nanotechnology*, 6(9), pp. 573–579. Available at: https://doi.org/10.1038/nnano.2011.119.

Malvankar, N.S., Tuominen, M.T. and Lovley, D.R. (2012) 'Biofilm conductivity is a decisive variable for high-current-density Geobacter sulfurreducens microbial fuel cells', *Energy and Environmental Science*, 5(2), pp. 5790–5797. Available at: https://doi.org/10.1039/c2ee03388g.

Manchon, C., Asensio, Y., et al. (2023) 'Fluid-like cathode enhances valuable biomass production from brewery wastewater in purple phototrophic bacteria', *Frontiers in Microbiology*, 14(March), pp. 1–9. Available at: https://doi.org/10.3389/fmicb.2023.1115956.

Manchon, C., Muniesa-Merino, F., Serna, D., et al. (2023) 'Fluid-like electrodes and Purple Phototrophic Bacteria: bridging the gap in wastewater biorefineries', *Chemical Engineering Journal*, 453, p. 139828. Available at: https://doi.org/10.1016/J.CEJ.2022.139828.

Manchon, C., Muniesa-Merino, F., Llorente, M., *et al.* (2023) 'Microbial photoelectrosynthesis: Feeding purple phototrophic bacteria electricity to produce bacterial biomass', *Microbial Biotechnology*, 16(3), pp. 569–578. Available at: https://doi.org/10.1111/1751-7915.14190.

Marlière, P. et al. (2011) 'Chemical evolution of a bacterium's genome', Angewandte

Chemie - International Edition, 50(31), pp. 7109–7114. Available at: https://doi.org/10.1002/anie.201100535.

McCloskey, D. *et al.* (2018) 'Evolution of gene knockout strains of E. coli reveal regulatory architectures governed by metabolism', *Nature Communications*, 9(1). Available at: https://doi.org/10.1038/s41467-018-06219-9.

Methé, B.A. *et al.* (2003) 'Genome of Geobacter sulfurreducens: Metal Reduction in Subsurface Environments', *Science*, 302(5652), pp. 1967–1969. Available at: https://doi.org/10.1126/science.1088727.

Mills, D.R., Peterson, R.L. and Spiegelman, S. (1967) 'An extracellular Darwinian experiment with a self-duplicating nucleic acid molecule.', *Proceedings of the National Academy of Sciences*, 58(1), pp. 217–224. Available at: https://doi.org/10.1073/pnas.58.1.217.

Molaei, S. et al. (2022) 'Biodegradation of the petroleum hydrocarbons using an anoxic packed-bed biofilm reactor with in-situ biosurfactant-producing bacteria', *Journal of Hazardous Materials*, 421(July 2021), p. 126699. Available at: https://doi.org/10.1016/j.jhazmat.2021.126699.

Mosquera-Romero, S. et al. (2023) 'Water treatment and reclamation by implementing electrochemical systems with constructed wetlands', *Environmental Science and Ecotechnology*, 16. Available at: https://doi.org/10.1016/j.ese.2023.100265.

Muñoz Sierra, J.D. *et al.* (2019) 'Comparative performance of upflow anaerobic sludge blanket reactor and anaerobic membrane bioreactor treating phenolic wastewater: Overcoming high salinity', *Chemical Engineering Journal*, 366(December 2018), pp. 480–490. Available at: https://doi.org/10.1016/j.cej.2019.02.097.

Mustapha, H.I., van Bruggen, J.J.A. and Lens, P.N.L. (2015) 'Vertical subsurface flow constructed wetlands for polishing secondary Kaduna refinery wastewater in Nigeria', *Ecological Engineering*, 84, pp. 588–595. Available at: https://doi.org/10.1016/j.ecoleng.2015.09.060.

Nevin, K.P. et al. (2010) 'Microbial electrosynthesis: feeding microbes electricity to convert carbon dioxide and water to multicarbon extracellular organic compounds.', mBio, 1(2). Available at: https://doi.org/10.1128/mBio.00103-10.

Ning, Z., Cai, P. and Zhang, M. (2024) 'Metagenomic analysis revealed highly diverse carbon fixation microorganisms in a petroleum-hydrocarbon-contaminated aquifer', *Environmental Research*, 247(July 2023), p. 118289. Available at: https://doi.org/10.1016/j.envres.2024.118289.

Noriega Primo, E., López-Heras, I. and Esteve-Núñez, A. (2024) 'Electroactive biofilters outperform inert biofilters for treating surfactant-polluted wastewater by means of selecting a low-growth yield microbial community', *Journal of Hazardous Materials*, 477(August). Available at: https://doi.org/10.1016/j.jhazmat.2024.135415.

Novick, A. and Szilard, L. (1950) 'Experiments with the Chemostat on Spontaneous Mutations of Bacteria', *Proceedings of the National Academy of Sciences*, 36(12), pp. 708–719. Available at: https://doi.org/10.1073/pnas.36.12.708.

Ortiz, J.M. et al. (2021) Microbial Desalination Cells for Low Energy Drinking Water, Microbial Desalination Cells for Low Energy Drinking Water. Available at: https://doi.org/10.2166/9781789062120.

Panizza, M. and Cerisola, G. (2009) 'Direct and mediated anodic oxidation of organic pollutants', *Chemical Reviews*, 109(12), pp. 6541–6569. Available at: https://doi.org/10.1021/cr9001319.

Passos, F. *et al.* (2020) 'Potential applications of biogas produced in small-scale UASB-based sewage treatment plants in Brazil', *Energies*, 13(13). Available at: https://doi.org/10.3390/en13133356.

Patel, H. and Madamwar, D. (2002) 'Effects of temperatures and organic loading rates on biomethanation of acidic petrochemical wastewater using an anaerobic upflow fixed-film reactor', *Bioresource Technology*, 82(1), pp. 65–71. Available at: https://doi.org/10.1016/S0960-8524(01)00142-0.

Peñacoba-Antona, L. et al. (2021) 'Assessing METland® Design and Performance Through LCA: Techno-Environmental Study With Multifunctional Unit Perspective', *Frontiers in Microbiology*, 12(June), pp. 1–14. Available at: https://doi.org/10.3389/fmicb.2021.652173.

Peñacoba-Antona, L. *et al.* (2022a) 'Microbial Electrochemically Assisted Treatment Wetlands: Current Flow Density as a Performance Indicator in Real-Scale Systems in Mediterranean and Northern European Locations.', *Frontiers in Microbiology*, 13, pp. 843135–843135. Available at: https://doi.org/10.3389/FMICB.2022.843135.

Peñacoba-Antona, L. *et al.* (2022b) 'Microbial Electrochemically Assisted Treatment Wetlands: Current Flow Density as a Performance Indicator in Real-Scale Systems in Mediterranean and Northern European Locations', *Frontiers in Microbiology*, 13. Available at: https://doi.org/10.3389/fmicb.2022.843135.

Peñacoba-Antona, L., Gómez-Delgado, M. and Esteve-Núñez, A. (2021) 'Multi-Criteria Evaluation and Sensitivity Analysis for the Optimal Location of Constructed Wetlands (METland) at Oceanic and Mediterranean Areas', *International Journal of Environmental Research and Public Health 2021, Vol. 18, Page 5415*, 18(10), p. 5415. Available at: https://doi.org/10.3390/IJERPH18105415.

Pérez-Armendáriz, B. et al. (2010) 'Anaerobic biodegradability and inhibitory effects of some anionic and cationic surfactants', *Bulletin of Environmental Contamination and Toxicology*, 85(3), pp. 269–273. Available at: https://doi.org/10.1007/s00128-010-0096-8.

Pfeifer, E. et al. (2017) 'Adaptive laboratory evolution of Corynebacterium glutamicum towards higher growth rates on glucose minimal medium', *Scientific Reports*, 7(1), pp. 1–14. Available at: https://doi.org/10.1038/s41598-017-17014-9.

Phelps, T.J. *et al.* (1994) 'Comparison between geochemical and biological estimates of subsurface microbial activities', *Microbial Ecology*, 28(3), pp. 335–349. Available at: https://doi.org/10.1007/BF00662027.

Potter, M. (1911) 'Electrical effects accompanying the decomposition of organic compounds', *Proceedings of the Royal Society of London. Series B, ...*, 84(571), pp. 260–276. Available at: http://www.jstor.org/stable/10.2307/80609 (Accessed: 20 June 2013).

Prado, A. et al. (2020) 'Novel bioelectrochemical strategies for domesticating the electron flow in constructed wetlands', *Science of the Total Environment*, 735, p. 139522. Available at: https://doi.org/10.1016/j.scitotenv.2020.139522.

Prado, A., Berenguer, R. and Esteve-Núñez, A. (2019) 'Electroactive biochar outperforms highly conductive carbon materials for biodegrading pollutants by enhancing microbial extracellular electron transfer', *Carbon*, 146(January 2021), pp. 597–609. Available at: https://doi.org/10.1016/j.carbon.2019.02.038.

Prado de Nicolás, A., Berenguer, R. and Esteve-Núñez, A. (2022) 'Evaluating bioelectrochemically-assisted constructed wetland (METland®) for treating wastewater: Analysis of materials, performance and electroactive communities', *Chemical Engineering Journal*, 440(February). Available at: https://doi.org/10.1016/j.cej.2022.135748.

Pun, Á., Boltes, K., Letón, P., Esteve-Nuñez, A., *et al.* (2019) 'Detoxification of wastewater containing pharmaceuticals using horizontal flow bioelectrochemical filter', *Bioresource Technology Reports*, 7(July), p. 100296. Available at: https://doi.org/10.1016/j.biteb.2019.100296.

Pun, A., Boltes, K., Letón, P. and Esteve-Nuñez, A. (2019) 'Detoxification of wastewater containing pharmaceuticals using horizontal flow bioelectrochemical filter', *Bioresource Technology Reports*, 7, p. 100296. Available at: https://doi.org/10.1016/J.BITEB.2019.100296.

Pun, Á. et al. (2025) 'Enhanced removal of chiral emerging contaminants by an electroactive biofilter', *Environmental Science and Ecotechnology*, 23. Available at: https://doi.org/10.1016/j.ese.2024.100500.

Qutob, M. et al. (2022) 'A Review of Pyrene Bioremediation Using Mycobacterium Strains in a Different Matrix', *Fermentation 2022, Vol. 8, Page 260*, 8(6), p. 260. Available at: https://doi.org/10.3390/FERMENTATION8060260.

Rajagopal, R. et al. (2019) 'Influence of pre-hydrolysis on sewage treatment in an Up-Flow Anaerobic Sludge BLANKET (UASB) reactor: A review', *Water (Switzerland)*, 11(2), pp. 3–7. Available at: https://doi.org/10.3390/w11020372.

Ramírez-Moreno, M. *et al.* (2024) 'Study of the influence of nanoscale porosity on the microbial electroactivity between expanded graphite electrodes and Geobacter sulfurreducens biofilms', *Microbial Biotechnology*, 17(1), pp. 1–16. Available at: https://doi.org/10.1111/1751-7915.14357.

Ramírez-Moreno, M., Esteve-Núñez, A. and Ortiz, J.M. (2021) 'Desalination of brackish water using a microbial desalination cell: Analysis of the electrochemical behaviour', *Electrochimica Acta*, 388. Available at: https://doi.org/10.1016/j.electacta.2021.138570.

Ramírez-Moreno, M., Esteve-Núñez, A. and Ortiz, J.M. (2023) 'Study of microbial desalination cell performance with different saline streams: Analysis of current efficiency and freshwater production', *Journal of Environmental Chemical Engineering*, 11(1). Available at: https://doi.org/10.1016/j.jece.2022.109240.

Ramírez-Vargas, C.A. *et al.* (2018) 'Microbial Electrochemical Technologies for Wastewater Treatment: Principles and Evolution from Microbial Fuel Cells to Bioelectrochemical-Based Constructed Wetlands', *Water 2018, Vol. 10, Page 1128*, 10(9), p. 1128. Available at: https://doi.org/10.3390/W10091128.

Ramírez-Vargas, C.A. *et al.* (2019) 'Electroactive biofilm-based constructed wetland (EABB-CW): A mesocosm-scale test of an innovative setup for wastewater treatment', *Science of the Total Environment*, 659, pp. 796–806. Available at: https://doi.org/10.1016/j.scitotenv.2018.12.432.

Ramos, D.G. *et al.* (2016) 'Biotechnology for Biofuels A new laboratory evolution approach to select for constitutive acetic acid tolerance in Saccharomyces cerevisiae and identification of causal mutations', *Biotechnology for Biofuels*, pp. 1–18. Available at: https://doi.org/10.1186/s13068-016-0583-1.

Reguera, G. et al. (2005) 'Extracellular electron transfer via microbial nanowires.', *Nature*, 435(7045), pp. 1098–101. Available at: https://doi.org/10.1038/nature03661.

Ren, H. *et al.* (2024) 'Structures and diversities of bacterial communities in oil-contaminated soil at shale gas well site assessed by high-throughput sequencing', *Environmental Science and Pollution Research*, 31(7), pp. 10766–10784. Available at: https://doi.org/10.1007/s11356-023-31344-4.

Renault, F. et al. (2009) 'Chitosan for coagulation/flocculation processes - An eco-friendly approach', *European Polymer Journal*, 45(5), pp. 1337–1348. Available at: https://doi.org/10.1016/j.eurpolymj.2008.12.027.

Rosario-Passapera, R. *et al.* (2012) 'Parvibaculum hydrocarboniclasticum sp. nov., a mesophilic, alkane-oxidizing alphaproteobacterium isolated from a deep-sea hydrothermal vent on the East Pacific Rise', *International Journal of Systematic and Evolutionary Microbiology*, 62(12), pp. 2921–2926. Available at: https://doi.org/10.1099/ijs.0.039594-0.

Rotaru, A.E., Yee, M.O. and Musat, F. (2021) 'Microbes trading electricity in consortia of environmental and biotechnological significance', *Current Opinion in Biotechnology*, 67, pp. 119–129. Available at: https://doi.org/10.1016/j.copbio.2021.01.014.

Salas-Navarrete, P.C. *et al.* (2022) 'Evolutionary and reverse engineering to increase Saccharomyces cerevisiae tolerance to acetic acid, acidic pH, and high temperature',

Applied Microbiology and Biotechnology, 106(1), pp. 383–399. Available at: https://doi.org/10.1007/s00253-021-11730-z.

Salvian, A. *et al.* (2024) 'Resilience of anodic bio fi lm in microbial fuel cell biosensor for BOD monitoring of urban wastewater', *npj Clean Water*, pp. 1–12. Available at: https://doi.org/10.1038/s41545-024-00350-5.

Sandberg, T.E. *et al.* (2019) 'The emergence of adaptive laboratory evolution as an efficient tool for biological discovery and industrial biotechnology', *Metabolic Engineering*, 56(April), pp. 1–16. Available at: https://doi.org/10.1016/j.ymben.2019.08.004.

Sandhu, M., Paul, A.T. and Jha, P.N. (2022) 'Metagenomic analysis for taxonomic and functional potential of Polyaromatic hydrocarbons (PAHs) and Polychlorinated biphenyl (PCB) degrading bacterial communities in steel industrial soil', *PLoS ONE*, 17(4 April), pp. 1–22. Available at: https://doi.org/10.1371/journal.pone.0266808.

Santo, C.E. *et al.* (2013) 'Biological treatment by activated sludge of petroleum refinery wastewaters', *Desalination and Water Treatment*, 51(34–36), pp. 6641–6654. Available at: https://doi.org/10.1080/19443994.2013.792141.

Santos, M.R.G. *et al.* (2006) 'The application of electrochemical technology to the remediation of oily wastewater', *Chemosphere*, 64(3), pp. 393–399. Available at: https://doi.org/10.1016/j.chemosphere.2005.12.036.

Schneider, E.E., Cerqueira, A.C.F.P.F.P. and Dezotti, M. (2011) 'MBBR evaluation for oil refinery wastewater treatment, with post-ozonation and BAC, for wastewater reuse', *Water Science and Technology*, 63(1), pp. 143–148. Available at: https://doi.org/10.2166/wst.2011.024.

Sekman, E. et al. (2011) 'Treatment of oily wastewater from port waste reception facilities by electrocoagulation', *International Journal of Environmental Research*, 5(4), pp. 1079–1086.

Seok, W.H. *et al.* (2008) 'Field experiments on bioelectricity production from lake sediment using microbial fuel cell technology', *Bulletin of the Korean Chemical Society*, 29(11), pp. 2189–2194. Available at: https://doi.org/10.5012/bkcs.2008.29.11.2189.

Shepelin, D. *et al.* (2018) 'Selecting the best: Evolutionary engineering of chemical production in microbes', *Genes*, 9(5). Available at: https://doi.org/10.3390/genes9050249.

Shokri, A. and Sanavi Fard, M. (2022) 'A critical review in electrocoagulation technology applied for oil removal in industrial wastewater', *Chemosphere*, 288(P2), p. 132355. Available at: https://doi.org/10.1016/j.chemosphere.2021.132355.

Simate, G.S. *et al.* (2011) 'The treatment of brewery wastewater for reuse: State of the art', *Desalination*, 273(2–3), pp. 235–247. Available at: https://doi.org/10.1016/j.desal.2011.02.035.

Song, J. et al. (2016) 'Comprehensive metabolomic analyses of anode-respiring Geobacter

sulfurreducens cells: The impact of anode-respiration activity on intracellular metabolite levels', *Process Biochemistry*, 51(1), pp. 34–38. Available at: https://doi.org/10.1016/j.procbio.2015.11.012.

Spurr, M.W. et al. (2021) 'No re-calibration required? Stability of a bioelectrochemical sensor for biodegradable organic matter over 800 days', *Biosensors and Bioelectronics*, 190(March), p. 113392. Available at: https://doi.org/10.1016/j.bios.2021.113392.

Sun, D. *et al.* (2016) 'The effect of biofilm thickness on electrochemical activity of Geobacter sulfurreducens', *International Journal of Hydrogen Energy*, 41(37), pp. 16523–16528. Available at: https://doi.org/10.1016/j.ijhydene.2016.04.163.

Sun, W. et al. (2015) 'Profiling microbial community structures across six large oilfields in China and the potential role of dominant microorganisms in bioremediation', *Applied Microbiology and Biotechnology*, 99(20), pp. 8751–8764. Available at: https://doi.org/10.1007/s00253-015-6748-1.

Szoboszlay, S. *et al.* (2008) 'Chryseobacterium hungaricum sp. nov., isolated from hydrocarbon-contaminated soil', *International Journal of Systematic and Evolutionary Microbiology*, 58(12), pp. 2748–2754. Available at: https://doi.org/10.1099/ijs.0.65847-0.

Tejedor-Sanz, S. *et al.* (2018) 'Geobacter dominates the inner layers of a stratified biofilm on a fluidized anode during brewery wastewater treatment', *Frontiers in Microbiology*, 9(MAR). Available at: https://doi.org/10.3389/fmicb.2018.00378.

Tejedor-Sanz, S., Ortiz, J.M. and Esteve-Núñez, A. (2017) 'Merging microbial electrochemical systems with electrocoagulation pretreatment for achieving a complete treatment of brewery wastewater', *Chemical Engineering Journal*, 330, pp. 1068–1074. Available at: https://doi.org/10.1016/j.cej.2017.08.049.

Tellez, G.T., Nirmalakhandan, N. and Gardea-Torresdey, J.L. (2002) 'Performance evaluation of an activated sludge system for removing petroleum hydrocarbons from oilfield produced water', *Advances in Environmental Research*, 6(4), pp. 455–470. Available at: https://doi.org/10.1016/S1093-0191(01)00073-9.

Tender, L.M. *et al.* (2002) 'Harnessing microbially generated power on the seafloor.', *Nature biotechnology*, 20(8), pp. 821–5. Available at: https://doi.org/10.1038/nbt716.

Thakur, C., Srivastava, V.C. and Mall, I.D. (2014) 'Aerobic degradation of petroleum refinery wastewater in sequential batch reactor', *Journal of Environmental Science and Health - Part A Toxic/Hazardous Substances and Environmental Engineering*, 49(12), pp. 1436–1444. Available at: https://doi.org/10.1080/10934529.2014.928557.

Tilloy, V. and Ortiz-julien, A. (2014) 'Reduction of Ethanol Yield and Improvement of Glycerol Formation by Adaptive Evolution of the Wine Yeast Saccharomyces cerevisiae under Hyperosmotic Conditions'. Available at: https://doi.org/10.1128/AEM.03710-13.

Tomei, M.C. and Garrido, J.M. (eds) (2024) *Anaerobic Treatment of Domestic Wastewater*. London, UK: IWA Publishing. Available at: https://doi.org/10.2166/9781789063479.

Torres, C.I., Marcus, A.K. and Rittmann, B.E. (2008) 'Proton transport inside the biofilm limits electrical current generation by anode-respiring bacteria', *Biotechnology and Bioengineering*, 100(5), pp. 872–881. Available at: https://doi.org/10.1002/BIT.21821.

Tront, J.M. *et al.* (2008) 'Microbial fuel cell biosensor for in situ assessment of microbial activity.', *Biosensors & bioelectronics*, 24(4), pp. 586–90. Available at: https://doi.org/10.1016/j.bios.2008.06.006.

Tucci, M. et al. (2021) 'Empowering electroactive microorganisms for soil remediation: Challenges in the bioelectrochemical removal of petroleum hydrocarbons', *Chemical Engineering Journal*, 419(February). Available at: https://doi.org/10.1016/j.cej.2021.130008.

U.S. Energy Information Administration (2023) *International Energy Statistics*, *United States Department of Energy*. Available at: https://www.eia.gov/international/data/world.

United Nations (2024) Food and Agriculture Organization: Databases & Publications, Food and Agriculture Organization of the United Nations. Available at: https://www.fao.org/faostat/en/#data/QCL.

Uria, N. et al. (2020) 'Immobilisation of electrochemically active bacteria on screen-printed electrodes for rapid in situ toxicity biosensing', *Environmental Science and Ecotechnology*, 3. Available at: https://doi.org/10.1016/j.ese.2020.100053.

Vargas, M., Malvankar, Nikhil S, et al. (2013) 'Aromatic Amino Acids Required for Pili Conductivity and Long-', *Proceedings of the National Academy of Sciences*, 4(2), pp. 1–6. Available at: https://doi.org/10.1128/mBio.00105-13.Editor.

Vargas, M., Malvankar, Nikhil S., et al. (2013) 'Aromatic amino acids required for pili conductivity and long-range extracellular electron transport in Geobacter sulfurreducens', mBio, 4(2), pp. e00105-13. Available at: https://doi.org/10.1128/mBio.00105-13.

Vásquez-Piñeros, M.A. *et al.* (2018) 'Delftia sp. LCW, a strain isolated from a constructed wetland shows novel properties for dimethylphenol isomers degradation', *BMC Microbiology*, 18(1), pp. 1–12. Available at: https://doi.org/10.1186/s12866-018-1255-z.

Wang, X. *et al.* (2018) 'Tolerance improvement of Corynebacterium glutamicum on lignocellulose derived inhibitors by adaptive evolution', pp. 377–388.

Wang, X. et al. (2020) 'Microbial electrochemistry for bioremediation', *Environmental Science and Ecotechnology*, 1(January), p. 100013. Available at: https://doi.org/10.1016/J.ESE.2020.100013.

Wang, Y. et al. (2016) 'Electrocoagulation mechanism of perfluorooctanoate (PFOA) on a zinc anode: Influence of cathodes and anions', *Science of the Total Environment*, 557–558, pp. 542–550. Available at: https://doi.org/10.1016/j.scitotenv.2016.03.114.

Wei, S. et al. (2024) 'Application of adaptive laboratory evolution to improve the tolerance of Rhodotorula strain to methanol in crude glycerol and development of an effective

method for cell lysis', *Biotechnology Journal*, 19(1). Available at: https://doi.org/10.1002/biot.202300483.

Wei, T. (2024) Developing modular constructed treatment wetland: the idea, the strategy and the reality. Universidad de Alcalá.

Williams, K.H. *et al.* (2010) 'Electrode-based approach for monitoring in situ microbial activity during subsurface bioremediation.', *Environmental science & technology*, 44(1), pp. 47–54. Available at: https://doi.org/10.1021/es9017464.

Wimpenny, J.W. (1982) 'Responses of microorganisms to physical and chemical gradients', *Philosophical Transactions of the Royal Society of London. B, Biological Sciences*, 297(1088), pp. 497–515. Available at: https://doi.org/10.1098/rstb.1982.0057.

Wu, D. et al. (2019) 'Anaerobic digestion: A review on process monitoring', Renewable and Sustainable Energy Reviews, 103(July 2018), pp. 1–12. Available at: https://doi.org/10.1016/j.rser.2018.12.039.

Wu, J. et al. (2023) 'Device integration of electrochemical biosensors', *Nature Reviews Bioengineering*, 1(5), pp. 346–360. Available at: https://doi.org/10.1038/s44222-023-00032-w.

Xia, W. et al. (2018) 'Influence of Dispersant/Oil Ratio on the Bacterial Community Structure and Petroleum Hydrocarbon Biodegradation in Seawater', *Journal of Coastal Research*, 84(84 (10084)), pp. 77–81. Available at: https://doi.org/10.2112/SI84-011.1.

Xie, X., Criddle, C. and Cui, Y. (2015) 'Design and fabrication of bioelectrodes for microbial bioelectrochemical systems', *Energy and Environmental Science*, 8(12), pp. 3418–3441. Available at: https://doi.org/10.1039/c5ee01862e.

Yan, P., Feng, D. and Liu, S. (2024) 'Experimental study on the biodegradability of petroleum wastewater and improving the performance of a moving-bed biofilm reactor', *International Journal of Environmental Science and Technology* [Preprint]. Available at: https://doi.org/10.1007/s13762-024-06149-8.

Yavitt, J.B., Lang, G.E. and Wieder, R.K. (1987) 'Control of carbon mineralization to CH4 and CO2 in anaerobic, Sphagnum-derived peat from Big Run Bog, West Virginia', *Biogeochemistry*, 4(2), pp. 141–157. Available at: https://doi.org/10.1007/BF02180152/METRICS.

Yavuz, Y., Koparal, A.S. and Öğütveren, Ü.B. (2010) 'Treatment of petroleum refinery wastewater by electrochemical methods', *Desalination*, 258(1–3), pp. 201–205. Available at: https://doi.org/10.1016/j.desal.2010.03.013.

Ye, J.X. et al. (2019) 'Enhancing chlorobenzene biodegradation by delftia tsuruhatensis using awater-silicone oil biphasic system', *International Journal of Environmental Research and Public Health*, 16(9). Available at: https://doi.org/10.3390/ijerph16091629.

Yi, H. et al. (2009) 'Selection of a variant of Geobacter sulfurreducens with enhanced

capacity for current production in microbial fuel cells', *Biosensors and Bioelectronics*, 24(12), pp. 3498–3503. Available at: https://doi.org/10.1016/j.bios.2009.05.004.

You, J. et al. (2015) 'Stability and reliability of anodic biofilms under different feedstock conditions: Towards microbial fuel cell sensors', *Sensing and Bio-Sensing Research*, 6, pp. 43–50. Available at: https://doi.org/10.1016/j.sbsr.2015.11.007.

Yuan, K. *et al.* (2018) 'Transcriptional response of Mycobacterium sp. strain A1-PYR to multiple polycyclic aromatic hydrocarbon contaminations', *Environmental Pollution*, 243, pp. 824–832. Available at: https://doi.org/10.1016/J.ENVPOL.2018.09.001.

Zhang, T. et al. (2012) 'Anaerobic benzene oxidation by Geobacter species', *Applied and Environmental Microbiology*, 78(23), pp. 8304–8310. Available at: https://doi.org/10.1128/AEM.02469-12.

Zhang, T. et al. (2014) 'Sulfur oxidation to sulfate coupled with electron transfer to electrodes by Desulfuromonas strain TZ1', *Microbiology (United Kingdom)*, 160(PART 1), pp. 123–129. Available at: https://doi.org/10.1099/mic.0.069930-0.

Zhang, W. et al. (2018) 'Adaptive Evolution Relieves Nitrogen Catabolite Repression and Decreases Urea Accumulation in Cultures of the Chinese Rice Wine Yeast Strain Saccharomyces cerevisiae XZ-11', *Journal of Agricultural and Food Chemistry*, 66(34), pp. 9061–9069. Available at: https://doi.org/10.1021/acs.jafc.8b01313.

Zhang, Y. and Angelidaki, I. (2011) 'Submersible microbial fuel cell sensor for monitoring microbial activity and BOD in groundwater: Focusing on impact of anodic biofilm on sensor applicability', *Biotechnology and Bioengineering*, 108(10), pp. 2339–2347. Available at: https://doi.org/10.1002/bit.23204.

Chapter 1

Figure 1: Diagram showing iron reduction, direct reduction of the electrode, and	
planktonic reduction of the electrode.	3
Figure 2: Microbial interactions with the anode of an MFC biosensor.	4
Figure 3: Diagram of the mechanisms and function of a sediment microbial fuel	
cell.	6
Figure 4: Diagram of the three electrode biosensors with the working electrode	
(Red), counter electrode (Black), and reference electrode (Blue). Highlighted are	
interactions that are possible at the WE and CE surfaces.	7
Figure 5: Diagram of reactor used by Chen et al. 2019	10
Figure 6: Diagram of an electrooxidation cell.	12
Figure 7: Diagram of the mechanism for electrocoagulation.	13
Figure 8: Diagram of a fluidized bed reactor.	14
Figure 9: Diagram of proposed mechanisms for aerobic and anaerobic METfilers.	17
Figure 10: Diagram of the workflow for adaptive laboratory evolution.	18
Chapter 2	
Figure 1: Hypothetical model and mechanism of the current generation	
by microbial metabolism. Fermentation products and acetate will produce	
the majority of the current. Reactions distal to the electrode may also	
contribute to the current by producing Fe(II), sulfide, and subsequent abiotic	
oxidation at the anode.	24
Figure 2: A) Diagram of the sediment cylinder. B) Sediment cylinders in aquaria	
with current monitoring equipment.	26
Figure 3: Confocal laser scanning micrographs of a methanogenic sediment	
anode. Live cells are in green, and dead/compromised cells are in red. A) Total	
magnification is 100X. B) Total magnification is 1000X.	29
Figure 4: Direct correlation between current production and acetate	
mineralization in methanogenic sediments incubated at different temperatures	
(4° C, 25° C, 37° C) (R2=0.8565). Error bars are the standard deviation of the	
triplicate cores tested for acetate turnover rate.	29

Figure 5: Direct correlation between current production and acetate	
mineralization in sulfate-reducing sediments incubated at different	
temperatures (4° C, 15° C, 25° C) (R2=0.7409). Error bars are the standard	
deviation of the triplicate cores tested for acetate turnover rate.	30
Figure 6: Direct correlation between current production and acetate	
mineralization in iron-reducing sediments incubated at different temperatures	
(15°C, 25°C, 37°C) (R2=0.7409). Error bars are the standard deviation of the	
triplicate cores tested for acetate turnover rate.	31
Chapter 3	
Figure 1: A) The three-electrode biosensor used in the study. B) Biosensor	
diagram, poised at 0.2 V versus Ag/AgCl	36
Figure 2: A) photo of the lab scale UASB in the temperature control cabinet.	
B) Diagrams of the UASB and biosensor with the conditions and operating	
parameters of the UASB.	37
Figure 3: The removal rate of COD of anaerobic digestors over time	
after exposure to biocides. The red arrow denotes when the reactor	
started to have complications from the biocide. The green arrow denotes	
the cessation of biocides on day 12. Control represents an average of the	
multiple control UASBs during the biocides' initial round of testing, which did	
not operate for longer than ten days.	39
Figure 4: Average current produced (10 seconds) by the biosensor on the left	
axis (blue line). COD concentration on the right axis (orange line).	40
Figure 5: Shows the change in COD removal rate after being exposed to Biocide 3	
at day zero. The red arrow denotes where the biocide started negatively	
affecting the reactor's COD removal rate.	41
Figure 6: Exposure to the biocide started at day 0 (Red Arrow). Shortly after,	
the current dropped precipitously	41
Chapter 4	
Figure 1: Schematic of the Anaerobic-Aerobic Hybrid Reactor showing	
the differing anaerobic and aerobic areas and route of media flow.	48
Figure 2: Schematic of the Multi-Hybrid Bed biofilter showing the alternating	
anaerobic, aerobic, and anaerobic areas and route of media flow.	49

Figure 3: Schematic of the Chimney Hybrid Bed showing the differing aerobic	
and anaerobic areas and route of media flow. The model of the e-sink's function.	50
Figure 4: Operating conditions of the different tests run in HEB.	53
Figure 5: A) COD loading rates (Blue) vs. COD removal rates (Orange) for	
Downflow (Fig. 4A), Air Supp (Fig. 4B), Recirc (Fig. 4C), and Bypass in HEB.	
(Fig. 4D). B) N-NH4 loading rates (Blue) vs N-NH4 removal rates (Orange) for	
Downflow (Fig. 4A), Air Supp (Fig. 4B), Recirc (Fig. 4C), and Bypass in HEB.	
(Fig. 4D).	54
Figure 6: Operational schematic of the AAH for basic up flow (A) and 200%	
recirculation (B).	55
Figure 7: A) COD loading rates (Blue) vs. COD removal rates (Orange) for Up	
Flow (Fig. 6A) and Recirculation (Fig. 6B) in the AAH. B) N-NH4 loading rates	
(Blue) vs N-NH4 removal rates (Orange) Up Flow (Fig. 6A) and Recirculation	
(Fig. 6B) in the AAH.	55
Figure 8: Operation schematics for MHB biofilter.	56
Figure 9: A) COD loading rates (Blue) vs. COD removal rates (Orange) for	
Passive Aeration (Fig. 8A), Pumped Aeration (Fig. 8B), Low [N] (Fig. 8C), and	
Low [N] & Recirc (Fig. 8D). B) N-NH4 loading rates (Blue) vs N-NH4 removal	
rates (Orange).	57
Figure 10: Average abundance of genera in the HEB. All genera shown have	
an abundance greater than 2.5%.	58
Figure 11: Average abundance of genera in the AAH biofilter. All genera	
shown have an abundance greater than 2.5%.	59
Figure 12: Average abundance of genera in the MPHB biofilter. All genera	
shown have an abundance greater than 2.5%.	60
Chapter 5	
Figure 1: A) A conceptual diagram of the gradostat's operation. B) An	
inoculated gradostat in a temperature control cabinet. C) A diagram of the	
major metabolic and chemical reactions in the media on the working	
and counter electrodes.	68
Figure 2: The fumarate concentration correlated to an exponential egression	
(R2=0.997).	71
Figure 3: Cell density as observed through optical density.	71

Figure 4: Electron donor limitation was never observed in the reactors.	72
Figure 5: The salt concentration across the reactors showed a strong linear	
relationship (R2=0.99).	73
Figure 7: Current density showing biofilm formation and steady-state current	
productions after 3 days. Reactor 2 (R2) was not included due to a defective	
reference electrode.	74
Figure 8: The linear correlation between current density and NaCl concentration	
for G. sulfurreducens grown on the anode under non-limiting availability for	
acetate and fumarate.	75
Figure 9: CV run at 1 mV/s (orange line) and 5 mV/s (blue line) between	
0.6 V and -0.6 V.	76
Figure 10: An example of the planktonic CA poised at 0.2 V for 5 hours at	
2 g/L NaCl.	77
Figure 11: Planktonic G. sulfurreducens shows a positive correlation	
between current density and salinity.	77
Figure 12: CVs from planktonic cells exposed to different salinities.	78

Abbreviations

ALE Adaptive Laboratory Evolution

AAS Aerobic Activated Sludge systems

AAH Anaerobic-Aerobic Hybrid biofilter

AFBR Anaerobic Fluidized Bed Reactor

BBR Biofilm-Based Reactors

BOD Biological Oxygen Demand

CA Chrono**A**mperometry

COD Chemical Oxygen Demand

CW Constructed Wetland

CV Cyclic Voltammetry

EAB ElectroActive Bacteria

EPS ExoPolySaccharide

EET Extracellular Electron Transfer

FBR Fluidized Bed Reactors

HEB Hybrid E-sink Biofilter

HC HydroCarbon

MDC Microbial Desalination Cell

ME-FBR Microbial Electrochemical Fluidized Bed Reactor

MES Microbial Electrochemical Snorkel

MET Microbial Electrochemical Technology

MEC Microbial Electrolysis Cell

MFC Microbial Fuel Cell

MPHB Multi-Phase Hybrid Bed biofilter

OLR Organic Loading Rates

PRW Petroleum Refinery Wastewater

PAH Polycyclic Aromatic Hydrocarbon

PW Produce Water

S-MFC Sediment Microbial Fuel Cell

SBR Sequencing Batch Reactors

UASB Up-flow **A**naerobic **S**ludge **B**lanket anaerobic digesters

VFA Volatile Fatty Acid

WW WasteWater

